Organometallic manipulations of fluoroolefins mediated or catalyzed by low-coordinate nickel

Alexandre J. Sicard

A thesis submitted to the Faculty of Graduate and Postdoctoral Studies
in partial fulfillment of the requirements for the M.Sc degree in Chemistry

Department of Chemistry and Biomolecular Sciences
Faculty of Science
University of Ottawa

Contents

List of Figures & Tables

Abbreviations

Ad	1-adamantyl
AHF	anhydrous hydrogen fluoride
bipy	2,2'-bipyridyl
CFC	chlorofluorocarbon
COD	1,5-cyclooctadiene
Cp	cyclopentyl (esp. when referring to the phosphine PCp_3)
Cy	cyclohexyl
dcppe	1,2-bis(dicyclopentylphosphino)ethane
dibpe	1,2-bis(diisobutylphosphino)ethane
dibpp	1,3-bis(diisobutylphosphino)propane
dipp	2,6-diisopropylphenyl
dppf	1,1'-bis(diphenylphosphino)ferrocene
HCC	hydrochlorocarbon
HCFC	hydrochlorofluorocarbon
HCFO	hydrochlorofluoroolefin
HCO	hydrochloroolefin
HFC	hydrofluorocarbon
HFO	hydrofluoroolefin
HFP	hexafluoropropylene
Mes	mesityl
NHC	*N*-heterocyclic carbene
TFE	tetrafluoroethylene
TIPP	triisopropylphosphite
V_{bur}	buried volume
VDF	vinylidene difluoride
Xy	2,6-dimethylphenyl (also 2,6-xylyl)

Abstract

Fluoroolefins in general represent a valuable class of feedstock materials which have proven integral to a number of industries including (but not limited to) refrigeration, agrochemicals, pharmaceuticals, and propellants. As ligands for transition metals they are privileged in the relative inertness of the C–F bonds and their electrophilicity, which makes them ideal candidates for coordination chemistry with late, electron rich metals. The scope of this thesis encompasses work with TFE and VDF, two readily available fluoroolefins that are used most commonly in the polymer industry. Through the use of low-coordinate nickel systems, value-added derivatives of these two olefins have been prepared. With TFE, a T-shaped perfluoronickelacyclopentane was obtained upon coordination of the bulky SIPr ligand; this complex underwent hydrogenation to give *1H,4H*-octafluorobutane at as low as 5 psi of hydrogen, in addition to giving rise to new ring-opened derivatives and a rare perfluorocyclobutyl complex. In the case of VDF, the regioselective hydrodefluorodimerization to a potentially valuable new refrigerant 2,4,4-trifluorobut-1-ene (HFO-1363pyf) catalyzed by nickel is reported, as well as a dimeric 2,4,4-trifluorobut-1-enylnickel derivative which is proposed in this text to originate from the β-fluoride elimination of an unprecedented 5-membered *2H,2H,4H,4H*-tetrafluoronickelacycle.

Preface

The work presented herein was made possible by NSERC and the Canada Research Chairs program, as well as University of Ottawa, Foundation for Innovation and Ontario Ministry of Economic Development and Innovation.

The work with TFE presented in *Part 1* was done in collaboration with my good friend and colleague Mr. Nicholas O. Andrella. My specific responsibilities for the article were mainly based in starting material preparation, testing reactivity with TMSOTf, and manuscript composition. I acknowledge and am grateful to Mr. Andrella for having provided ideas, feedback, and invaluable counsel during the course of my research. Alongside him I wish to also acknowledge Ms. Kaitie Giffin, who has always been graciously willing to provide valuable insights into the Ni–fluoroalkyl project, with which she is the most experienced in our group. Alongside them, I wish to acknowledge the remainder of the membership of *Team Fluorine* at the Baker group for being an excellent group of collaborators.

Finally, I wish to thank Prof. Baker for being receptive and open-minded to my frequently sporadic ideas, sub-projects and sidebars; even if they didn't all work as expected, having these small side-projects was key to the development of intuition and instinct which are invaluable in the primary research field.

Introduction

Small Fluorinated Molecules: *Prior Art*

Small organic perhalogenates have been used since the early 20th century as propellants and refrigerants due to their high volatility and inherent oxidative inertness (demonstrated by their nonexistent flash point, and ability to rapidly extinguish flames). Access to small fluorinated chlorocarbons was granted by the invention of the Swarts reaction, which (in broad terms), comprises the reaction of a chlorocarbon (or hydrochlorocarbon) with anhydrous hydrofluoric acid in the presence of a pentavalent antimony catalyst (or a $Sb(III)/Cl_2$ couple). A collection of popular 1st-gen. CFC refrigerants is shown in Fig. 1. Antimony is not the only Lewis acid employed in such transformations; any sufficiently halophilic Lewis acid may be employed to the same end. US 2,439,299[1] (by Hovey & Carnell of Phillips Petroleum Co.) instructs on a method using titanium tetrafluoride (or a $TiCl_4$/HF couple *in situ*) as the Lewis acid catalyst, which is applied towards the preparation of CFC-12 from a variety of HCC precursors. Mixtures of products may be also be obtained by disproportionation of CFCs over an acid catalyst; US 2,478,201[2] (by Miller & Bratton of Allied Chem. and Dye Corp.) outlines a process wherein CFC-12 is heated to 600˚C in the presence of aluminum fluoride to produce CFC-11, CFC-13, CF_4, and CCl_4, mainly. Rather than using HF to fluorinate a chlorocarbon, it is also possible to chlorinate a HCC precursor, as illustrated in US 2,417,059[3] and 2,459,767[4] (by Calfee & Smith of Allied Chem. and Dye Corp.) wherein HFC-152a converted to CFC-12 using elemental chlorine at high temperatures (500-900˚C). This exit gas also contains HCl and CCl_4 which may be easily removed by distillation as described by US 2,450,415[5] (by Benning of Kinetic Chemicals Inc.).

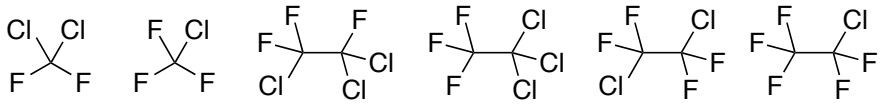

Fig. 1: Popular 1st-generation CFC-type refrigerants (currently phased out)

The ready availability of these inexpensive compounds allowed for the discovery of new applications in the aerosol industry, giving rise to the re-packaging of popular consumer products in aerosolized form. For example, a propellant mixture of 60% CFC-114 and 40% CFC-12 was applied in US 2,908,650[6] (by Fine of Colgate Palmolive Co.) as an aqueous solution with water-soluble alkali metal soaps, imparting "desired properties of stability, propellancy, ease of delivery, etc. to shaving cream compositions". Other notable examples of the time were by Edelstein[7] ("Aerosol apparatus for decorative coating"), La-Via[8] of Olefin Mathieson Chemical Co. ("Aerosol sun-screening composition"), Kerr[9] of Protective Coatings Corp. ("Self-spraying artificial snow composition"), and Mills[10] of Monsanto Chemicals ("Hair spray composition…"). The popular Silly-String® toy, invented by Cox and Fish[11] of Wham-O Mfg. Co. ("Foamable resinous composition") was also born during this aerosol revolution.

In response to suspicion of negative atmospheric effects brought upon by this expanded use of CFCs, the Montreal Protocol was drafted, commencing a legislatively forced phase-out of these first-generation refrigerants/propellants. The 2nd generation class, known collectively as HCFCs (hydrochlorofluorocarbons) possess fewer C-Cl bonds (the homolyses of which are responsible for the "ozone-depletion" phenomenon). Though their phase-out is now included in the Montreal protocol (due to their greenhouse-gas activity), they are still in wide use in developing countries as acceptable temporary alternatives to the more heavily regulated 1st-generation refrigerant and propellant formulations. The most popular entrant in this category is HCFC-22 (chlorodifluoromethane) which can be prepared easily by catalytic fluorination of chloroform by HF with a $SbCl_5/SbCl_3$ couple[12], or alternatively by high-temperature chlorination of HFC-32 in a Vycor® tube[13], by hydrochloro-fluorination of carbon black at

500˚C in a NiFeMo tube[14]. Similarly to the 1st-generation, many of the popular entrants in this category are based on ethane. For example, US 2,894,044[15] (by Prill of Monsanto Chemicals) describes a process wherein methyl chloroform is partially fluorinated under Swarts conditions (AHF/SnF_4) to give HCFC-141b. A catalyst-free route to the same compound is reported in US 3,833,676[16] (by Morioka & Ukaji of Daikin Kogyo Co.). A second fluorine can be added using a stronger acid combination (AHF/$SbCl_5$) as reported in US 2,146,354[17] (by Scherer of I. G. Farbenindustrie Aktiengsellschaft). The 1,2-dichloro isomer can be obtained starting from trichloroethylene without an acid catalyst as described in US 2,399,024[18] (by Harmon of du Pont). Though these are in the process of being phased out, they still have industrial uses as intermediates to other fluorochemicals – most famously the pyrolysis of HCFC-22 to tetrafluoroethylene (TFE) as described in US 2,406,794[19] (by Benning, Downing, & Park of Kinetic Chemicals Inc.). The same company is also responsible for the polymerization of TFE[20] to give PTFE, now marketed as Teflon®. Some popular HCFC refrigerants are shown in Figure 2.

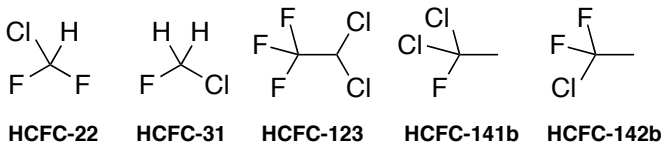

Fig. 2: Popular 2nd-generation HCFC-type refrigerants (gradually phasing out)

The 3rd generation of refrigerants is comprised of the HFC class, where there are no longer C-Cl bonds present in the compounds. Because of this, HFCs have no ozone-depleting potential, and are seen as valuable alternatives to HCFCs, which retain some of this property from their parent CFCs. Unfortunately, HFCs are not devoid of greenhouse gas activity, which means that the use of even these compounds is beginning to be discouraged. The most popular HFC in use today is 1,1,1,2-tetrafluoroethane (HFC-134a); this is because of its ability to directly replace CFC-12 in older refrigeration units. There are several preparative routes to this valuable compound; the original method in US 2,885,427[21] (by Ruh, Davis, and Broadworth of Dow Chemical Co.) involves the fluorination of trichloroethylene in the presence of CrF_3/

O_2, however this reaction also produces HFC-125, HCFC-133a, and HCFO-1121, in addition to unreacted starting material, all of which must be separated by distillation. A more selective method is outlined in US 4,311,863[22] (by Gumprecht of du Pont) where HCFC-133a is reacted with aqueous HF in the presence of alkali metal fluorides (typically KF), producing exclusively the target product. A less-fluorinated derivative HFC-152a has been used as an alternative to HCFC-134a, and can be prepared easily by addition of 2 equivalents of HF to acetylene under BF_3 catalysis as described in US 2,425,991[23] (by Burk, Coffman, & Kalb of du Pont). The more fluorinated derivative HFC-125 can be made by hydrofluorination of TFE using a chromium oxyfluoride catalyst as per CA 1,196,345[24] (by Von Halasz of Hoechst Ag). A popular propellant based on the propane framework is HFC-227ea, which can be made easily by hydrofluorination of cheaply available hexafluoropropylene (HFP) using chromium oxyfluoride catalysts as described in US 4,158,023[25] (by von Halasz of Hoechst Ag). The simplest HFCs in common use are HFC-32 – prepared by fluorination of methylene chloride under Swarts conditions as in US 2,062,743[26] (by Daudt & Youker of Kinetic Chemicals Inc.) – and HFC-23 – prepared by pyrolysis of HCFC-133a as in US 2,413,695[27] (by Benning, Downing, & McHarness of Kinetic Chemicals Inc.). Some C4 HFCs have become popular in recent years as well, with the most popular being HFC-365mfc, currently marketed under Solvay's Solkane® brand as a high temperature working fluid that can be easily handled as a liquid at room temperature. It can be prepared from HFC-141b (*via* 1,1,3-trichloro-1,3-difluorobutane) under Swarts conditions as described in US 6,518,467[28] (by Tung and Van Der Puy of Honeywell International Inc.). The most common HFCs and their azeotropic blends are shown in Figure 3.

HFCs have a lower greenhouse gas activity than HCFCs and CFCs, and are non ozone-depleting, which has earned them a market preference recently. However, a new 4th-generation of refrigerants has emerged which has neither greenhouse gas activity nor ozone-depleting potential. This generation contains compounds known as HFOs (hydrofluoroolefins) and HCFOs (hydrochlorofluoroolefins). The presence of the olefinic functionality ensures that the compounds do not survive transit to the stratosphere.

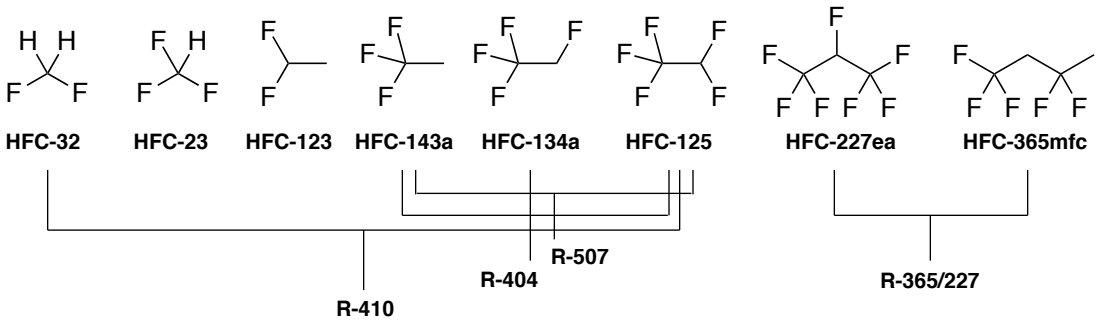

Fig. 3: Popular 3nd-generation HFC-type refrigerants and some popular blends (in current use)

HFOs are being marketed heavily by Arkema Inc. and Honeywell International Inc., accounting collectively for the vast majority of IP pertaining to the manufacture and design of HFOs for propellant/foaming/refrigerant applications. The most popular members of this class are HFO-1234yf and HFO-1234ze, of which there are many syntehses known in the art, from a plethora of different HCC, HCFC, or FC starting materials. The first commercialized preparation of HFO-1234yf is described in US 2,931,840[29] (by Marquis of du Pont) where methyl chloride and tetrafluoroethylene are pyrolyzed in a reactor held at 850-900˚C with a contact time of 0.8-1.45 seconds. Since then, more economical reaction conditions have been devised. For instance, 1234yf can be prepared by sequential hydrogenation and dehydrofluorination reactions of HFP (proceeding *via* HFC-236ea, HFO-1225ye, and HFC-245eb intermediates) as described in US App. 14,978,789[30] (by Pigamo, Devic, & Wendlinger of Arkema France); this 4-step process (shown in Figure 4) is rendered economical mainly by the low cost of the reagents used, in particular HFP, and the moderate temperatures of each step. US App. 13,695,807[31] (by Elsheikh *et al.* of Arkema Inc.) shows that HFC-245cb (the alternate isomer of 245eb) may be dehydrofluorinated to give

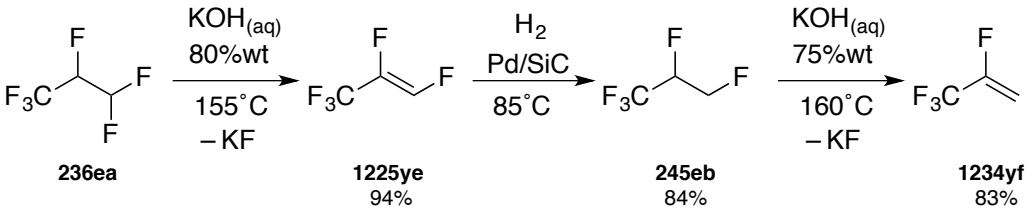

Fig. 4: Arkema's synthesis of HFO-1234yf from the HFP hydrogenation product

HFO-1234yf. Under their conditions, HF is liberated in the presence of a chromium oxyfluoride catalyst rather than directly removed using caustic alkali. In addition to dehydrofluorination of HFC-245eb as shown in Figure 4, HFC-245cb (1,1,1,2,2-pentafluoropropane) may be used as a substrate. The 2-chloro congener (HCFO-1233xf) may be prepared according to US App. 13,642,589[32] (Pigamo, Wendlinger, & Bonnet of Arkema France) by liquid-phase fluorination of either HCC-240db or HCC-240aa (or a mixture of the two) using a unique Swarts catalyst in imidazolium-based ionic liquid at 50-150˚C. US 9,278,895[33] (by Deur-Bert *et al.* of Arkema France) describes the same reaction in the gas phase using a Cr oxyfluoride catalyst. Similarly, US 9,302,961[34] (by Pigamo, Wendlinger, & Doucet) reveals that HCC-240aa, HCFC-243db, and HCO-1230xf can also be precursors for HFO-1234yf *via* fluorination using a heterogeneous Ni/Cr catalyst, demonstrating considerable substrate flexibility in these methodologies. A unique approach is reported by Fozzard[35] of Phillips Petroleum Co. involving the thermal cyclodimerization of HFP and ethylene at between

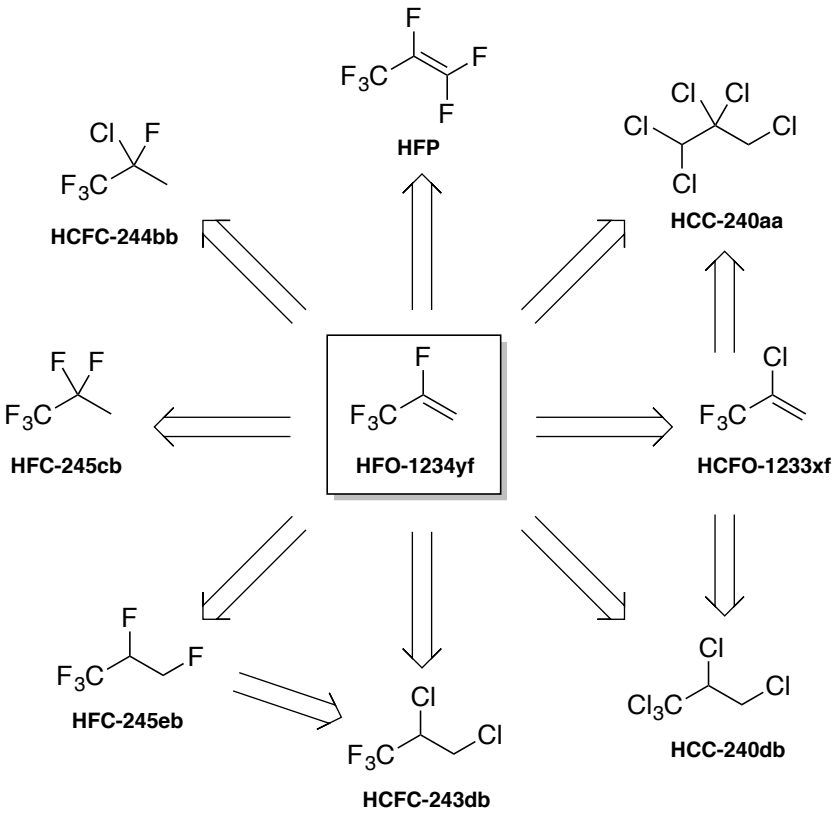

Fig. 5: Retrosynthetic pathways to HFO-1234yf from various HCC, HFC, and HCFO precursors

200-600˚C, producing 1-trifluoromethyl-1,2,2-trifluorocyclobutane. Cracking of the cyclobutane interimediate produces HFO-1234yf and vinylidene difluoride. The retrosynthetic analysis of 1234yf is shown in Figure 5. The Phillips methodology is depicted in Figure 6.

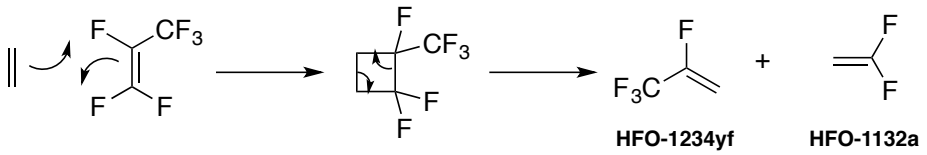

Fig. 6: Phillips' preparation of 1234yf via a mixed-olefin cyclobutane intermediate.

The other isomer, HFO-1234ze is similarly popular, and can be made by analogous pathways to the yf isomer. Its rise in popularity may be attributed to the work done by AlliedSignal Inc. in the late 1990s. HFC-245fa can be dehydrofluorinated to cis/trans HFO-1234ze over fluorinated alumina at 400˚C in 95% yield as described in US 5,986,151[36] (by Van Der Puy of AlliedSignal Inc.). The precursor HFC-245fa is easily available from HCC-240aa/db under Swarts conditions as described in US 5,763,706[37] (by Sung Tung *et al.* of AlliedSignal Inc.); this reaction also produces HFO-1234ze, HCFO-1233zd (the 1-chloro congener of 1234ze), and HCFO-122zb as byproducts. For instance, HFC-245fa can be dehydrofluorinated to cis/trans HFO-1234ze using Arkema's chromium oxyfluoride catalyst[38] mentioned previously. It can also be prepared from the HCFO-1233zd with HF in the gas phase according to US 6,472,573[39] (Yamamoto *et al.* of Daikin Industries Ltd.) or by dehydrohalogenation of either HCFC-244fa or HFC-245fa using caustic alkali as demonstrated in US 7,230,146[40] (Merkel, Singh, & Tung of Honeywell International Inc.). A unique approach has been taken by Mukhopadhyay *et al.* (also of Honeywell) in US 7,345,209[41] where trifluoromethyl iodide and vinyl fluoride (HFO-1141) react in an autoclave at 200˚C to produce 1-iodo-1,3,3,3-trifluoropropane as an intermediate, which is subsequently subjected to aqueous KOH, producing HFO-1234ze. The approach also works using trifluoromethyl bromide, proceeding *via* the 1-bromo-congener. Within this report is also mentioned the addition of CCl_4 to vinyl chloride, producing HCC-240db as an intermediate, which when subjected to HF in the presence of Cr_2O_3 at between 5-100

psi of pressure, yields HCFC-244fa, which may be dehydrochlorinated to HFO-1234ze. The dehydrobromination of 1,1,1,3-tetrafluoro-2-bromopropane (prepared by addition of Br2 to 3,3,3-trifluoropropylene in the presence of HF) gives the same product as described in US 7,189,884[42] by the same researchers at Honeywell. A retrosynthetic analysis for HFO-1234ze is shown in Figure 7.

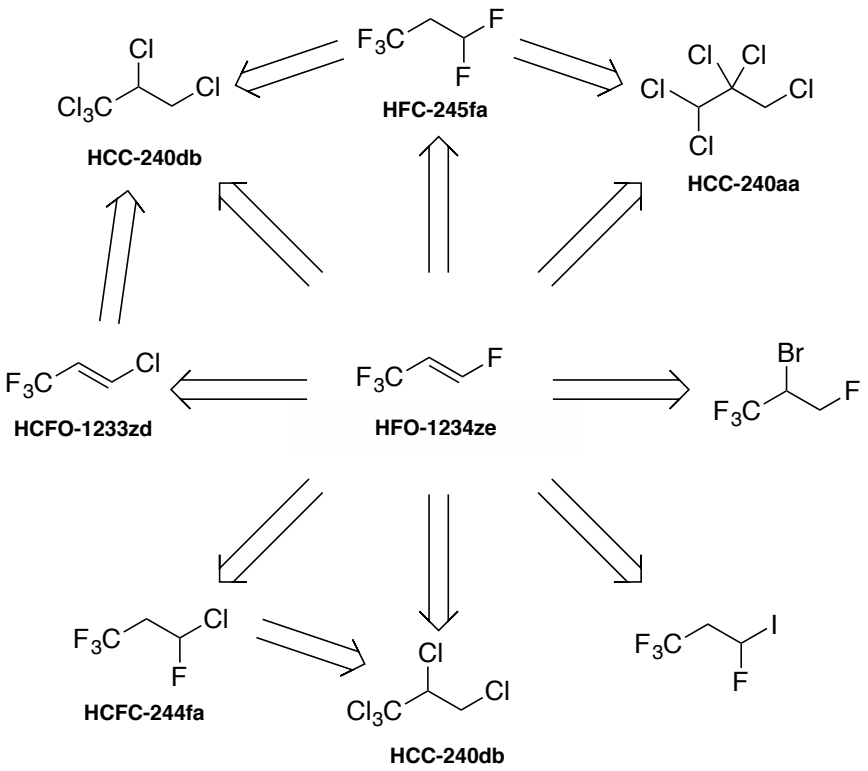

Fig. 7: Retrosynthetic pathways to HFO-1234ze from various HCC, HFC, and HCFO precursors

C_4 HFO compounds have only recently been emerging in the market, with the current leader – HFO-1336mzz – being marketed by DuPont Fluorochemicals (now Chemours) as Formacel® 1100 (as a blowing agent for urethane foams) and as Opteon® 1100 (as an alternative refrigerant). Chemours is currently building the world's first full-scale production facility for 1336mzz in Changshu, China, with expected completion in 2017[43]. Its preparation comprises the hydrodechlorination of HFCO-1316mxx *via* HCFO-1326mxz over a $Pd/BaCl_2/Al_2O_3$ catalyst as described in US 7,795,482[44] (by Nappa & Swearingen of du Pont). Several other heterogeneous catalysts (including Cu/C, Lindlar catalyst, $Pd/BaSO_4$, and Cu/CaF_2) are named in the patent, with other

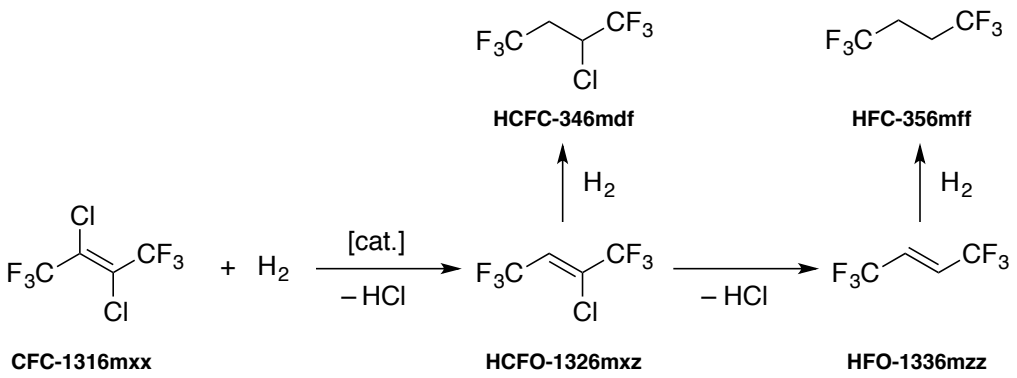

Fig. 8: DuPont's preparation of HFO-1336mzz

possible byproducts including HFC-356mff and HCFC-346mdf as shown in Figure 8. Though both isomers are observed, the *trans* is favored by most catalysts tested.

In US 8,901,360, Ross *et al.* of Honeywell describe a process wherein exclusively the *cis*-isomer of HFO-1336mzz can be produced from carbon tetrachloride and 1,2-dichloro-3,3,3-trifluoropropene in a 5-step process shown in Figure 9. Other butylene-

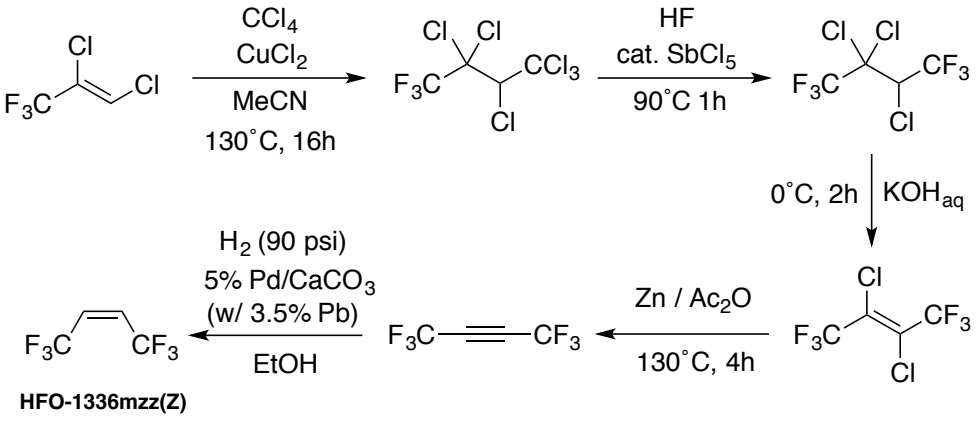

Fig. 9: Honeywell's preparation of *cis*-HFO-1336mzz

based HFO candidates have been investigated by Alty & Du Boisson of Central Glass Co. Ltd in US 7,482,499[45] – *viz.* 2,4,4,4-tetrafluoro-1-butylene and 1,1,1,3-tetrafluoro-2-butylene. The precursor is the readily available HFC-365mfc, and the reaction conditions for the thermal dehydrofluorination comprise heating in a metal-on-carbon-filled tube from 450-520˚C. The products of an example using only activated carbon

shown in Figure 10. The internal olefin (as well as some butadiene) is made as a side product, with no selectivity for the cis or trans isomer.

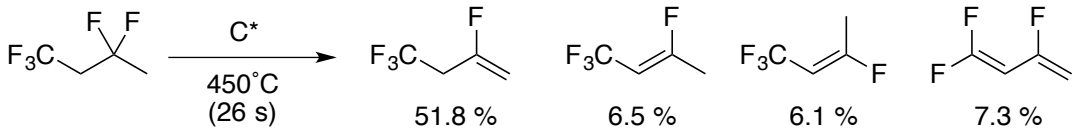

Fig. 10: Example of Central Glass' dehydrofluorination of HFC-365mfc to give hydrofluorobutylenes

It is worthwhile to note that all of the HFO candidates mentioned here are prepared by similar routes. The olefinic functionality is most commonly obtained by either thermal or base-assisted dehydrohalogenation, liberating one equivalent of HX (or MX + H_2O in the case of the base-assisted methods). The reactions producing HF as a byproduct are more desirable than the alkali hydroxide methods since HF can be re-used in upstream processes, whereas alkali fluoride salts are essentially useless waste. None of the processes mentioned herein make use of the much more atom-efficient catalytic "olefin upgrading" as is done with ethylene and its derivatives.

Fluoroolefin Coordination Chemistry: *Prior Art*

Carbon-fluorine bonds are among the strongest in all of organic chemistry, rendering them much more difficult to manipulate (*viz.* to install or remove) than their heavier congeners. In the case of fluoroolefins – compounds which (within this text) include only compounds containing at least one vinylic C–F bond – the high electronegativity of fluorine (coupled with the strength of the C–F bond) has a depletive effect on the electron density (and thus, the σ-donor ability) within the π-bond. A consequence is clearly shown in these olefins' preference for late, low-valent metals which are more favorably disposed towards π-backbonding as shown in Figure 11. In practice, this means that the coordination chemistry of fluoroolefins is almost exclusively studied on metals of group VIIB or later. There is a rich precedent for the coordination chemistry of tetrafluoroethylene (TFE) compared to the relatively sparse body of

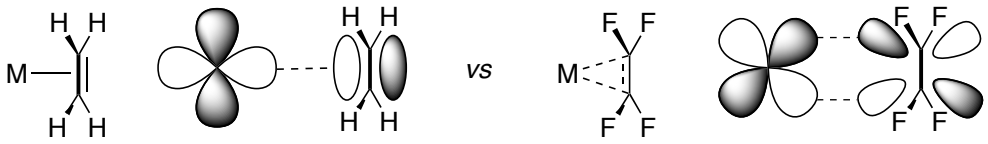

Fig. 11: Coordination chemistry of TFE vs ethylene

knowledge on hydrofluoroolefins; this is likely due to the greater availability of TFE in the early days of this research. Much of the early work in this field was pioneered by Wilkinson[46] on iron and Stone[47] on nickel (Figure 12). Owing to their high reducing power, these zerovalent late-metals are able to formally reduce tetrafluoroethylene to give the first reported perfluorinated metallacyclopentanes. This will be elaborated upon

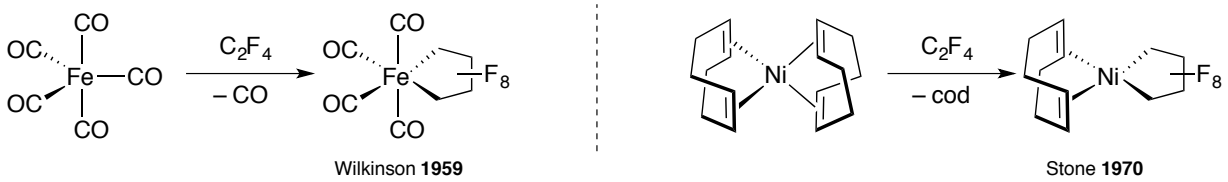

Fig. 12: The two first reports of perfluorometallacycles

later in both Parts 1 and 2. Simple fluoroolefin adducts have also been prepared as early as 1965 by Jones and coworkers on monovalent rhodium and iridium (Figure 13)[48]. Similar compounds based on cyclopentadienyl-systems were also prepared by Cramer[49]. Being inherent electrophiles, fluoroolefins are susceptible to nucleophilic attack; this can be exploited by inserting the fluoroolefin into a reactive metal hydride bond, an observation which was first reported by Stone on Mn[50], Mo, and W. For non-fluorinated olefins, this may have induced polymerization, but once inserted, the fluoroalkyl forms a stable covalent bond and does not insert again, as was also

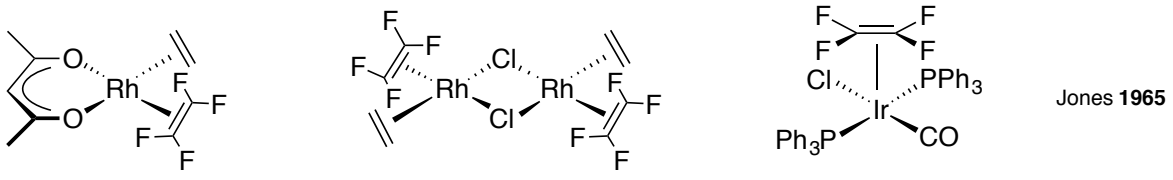

Fig. 13: TFE adducts of group VIIIB reported by Jones. *N.B.* no metallacycles are formed here.

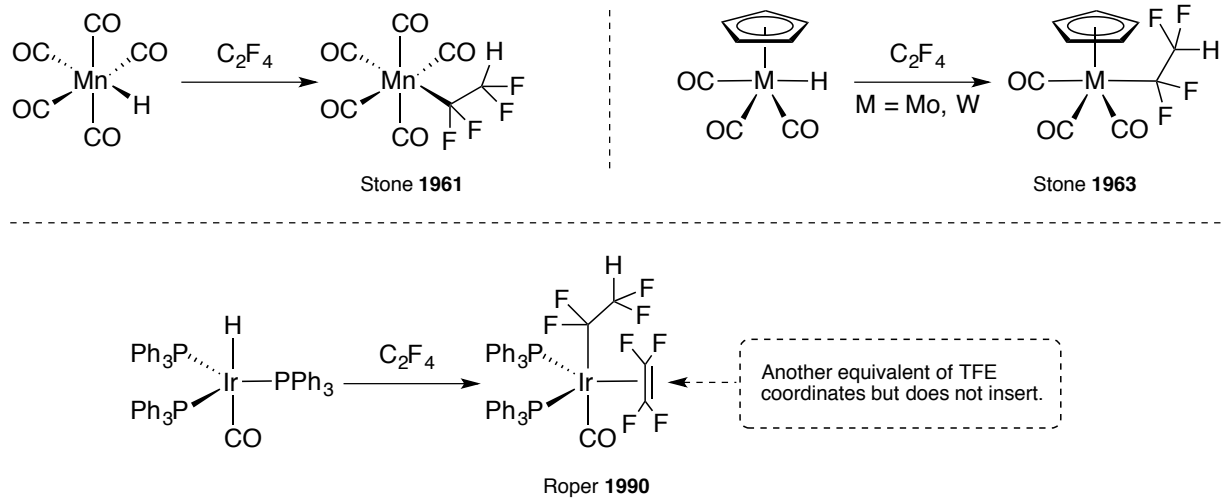

Fig. 14: Insertions of TFE into metal hydrides. *N.B.* only a single insertion ever occurs.

demonstrated later on by Roper on monovalent iridium[51] (Figure 14). Simple adducts of metals with fluoroolefins can be described as π-Lewis acid/base pairs in their simplest form, but it was first demonstrated by Wilkinson in 1967[52] (Figure 15) that the olefin adduct could be "functionalized" in oxidative conditions. In the absence of acid, Wilkinson's complex merely forms a π-adduct with TFE, but in the presence of HCl, the *2H*-tetrafluoroethyl fragment is obtained. However, the resulting complex remains

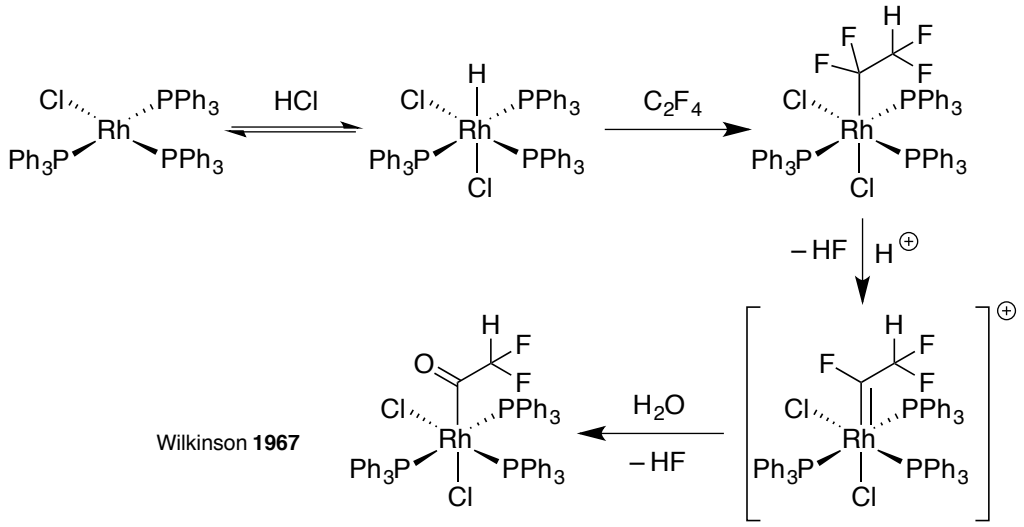

Fig. 15: Insertion of TFE into an *in-situ* generated Rh(III) hydride, C-F protonolysis, and hydrolysis.

unstable in the presence of excess acid, as the (normally highly resilient) C–F bonds are prone to protonation. This is a phenomenon that has been observed in the present research as well, and will be elaborated on later. The precedent in the literature for activation of C-F bonds at nickel will also be discussed in the introductory passages of *Part 1*.

NHC Ligands & Low-Coordinate Metal Complexes: *Prior Art*

N-heterocyclic carbenes (NHCs) have enjoyed a widespread adoption as ligands in organometallic chemistry and catalysis – most famously in Grubbs olefin metathesis catalysts (2nd generation or later)[53,54]. NHCs behave as spectator ligands, and are characterized as very effective σ-donors and negligible π-acceptors; this is usually quantified by the Tolman electronic parameter (the fundamental CO stretching frequency of $[Ni(CO)_3L]$ complexes)[55]. NHC ligands are often also used for their unique distribution of steric bulk; when the relative size of phosphine ligands are compared, it is common to use their cone angle, where the larger the substituent is, the larger the angle will be. Due to the pyramidalized nature of phosphine ligands, the cone angle is a natural measure of their size; NHCs on the other hand, can be irregularly shaped, and are usually wider than they are deep. At the origin, the Tolman steric parameter was extended by Nolan for NHC ligands to include a length parameter (A_L) and a height parameter (A_H), thus accounting for the irregular shapes[56]. The downside of this model is the loss of simplicity afforded by the cone-angle model, therefore an alternative was proposed later by Nolan and Cavallo which was known as the percent buried volume ($\%V_{bur}$) which describes the total volume occupied by the ligand within a sphere of defined radius from the metal center[57]. Because the buried volume is a spatial measure independent of geometry, it is a much more universal parameter and can be extended to phosphine ligands as well, allowing these two ligand classes to be more directly compared. A depiction of the two parameters is shown in Figure 16. A comprehensive review comparing various phosphine and NHC ligands per their steric parameters was published in 2010 by Clavier and Nolan[58]. The reference model for steric parameters is

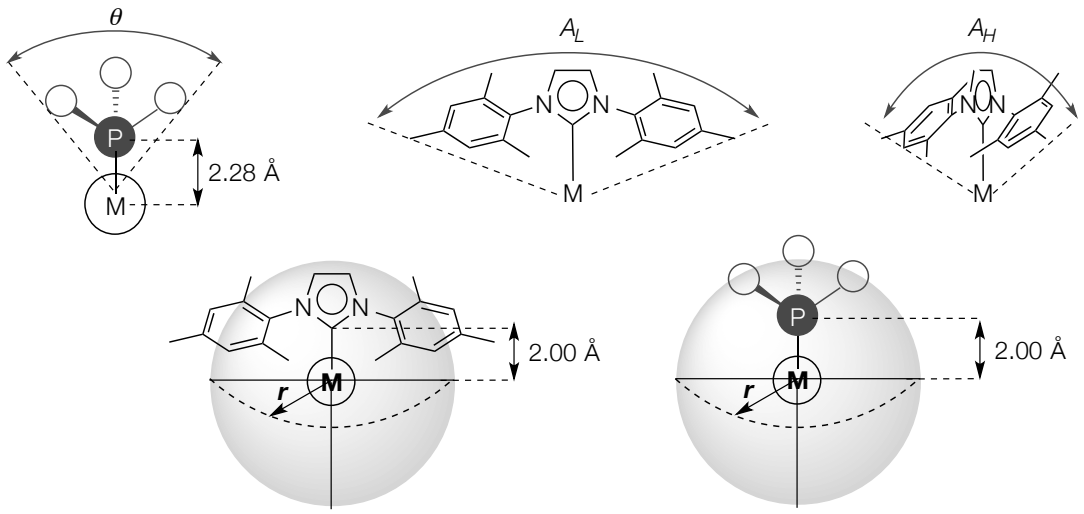

Fig. 16: Comparison of different methods of measuring steric bulk of phosphines and NHC ligands.

commonly aurous chloride; this is due to the remarkable ability of Au(I) to coordinate the largest of ligands, as well as the simple linear geometry that they adopt.

Owing to the large steric bulk attainable by NHC ligands, their use has enabled the isolation of unusually low-coordinate metal complexes. Of particular relevance to this work is the preparation of low-coordinate *low-valent* metal complexes bearing NHC ligands – especially nickel(0). The reactivity of such complexes arises from their coordinative unsaturation (giving plenty of room for the incoming substrate) and highly reducing character. For example, Braun, Radius, & coworkers have demonstrated that a 3-coordinate nickel(0) complex (Figure 17-I) featuring the I*i*Pr ligand can activate C-F bonds on hexafluorobenzene[59]. The same complex was used by Radius *et al.* to catalyze the addition of diphenylacetylene to biphenylene[60]. Matsubara *et al.* reported a facile synthetic pathway to 2-coordinate nickel(0) bis-NHC complexes (Figure 17-II) starting from the readily available $Ni(acac)_2$[61] and sodium hydride in the presence of the imidazolium salt precursor. A similar technique was used by Kuhl, Schneider, & Fort to generate a mono(NHC) nickel(0) precursor *in situ* for use as a transfer hydrogenation catalyst for imines[62]. The group of Belderrain & Nicasio have used an NHC-nickel(0) bis(styrene) (Figure 17-III) as a catalyst for C-N coupling of indoles and carbazoles[63]. A

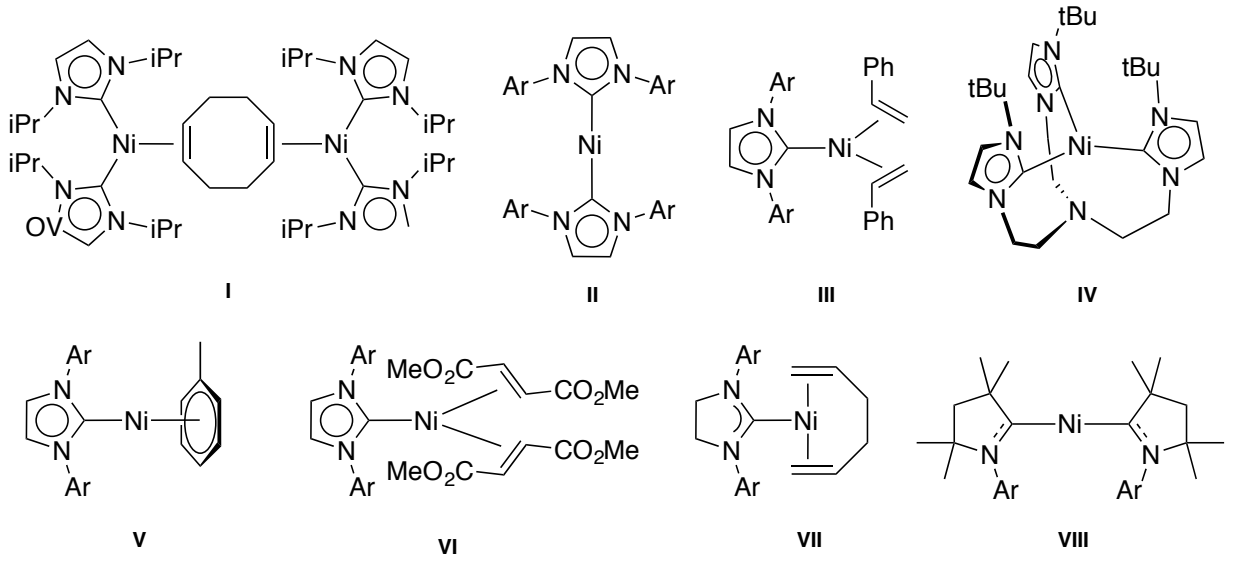

Fig. 17: Popular nickel(0)-NHC starting materials in the literature

tris(NHC) tripodal ligand was used by Meyer *et al.* to prepare an exceptionally electron-rich nickel(0) complex (Figure 17-IV)[64]. In a report by Ogoshi *et al.,* a mono-NHC nickel(0) containing an η^6-coordinated arene has been conveniently prepared by hydrogenating bis(1,5-cyclooctadiene)nickel(0) in aromatic solvent in the presence of one equivalent of either IPr, SIPr, or IPr*[65] (Figure 17-V). Stable 3-coordinate Ni(0)-NHC complexes (Figure 17-VI) can also be made from $Ni(COD)_2$ NHC ligand in the presence of dimethyl fumarate in THF at RT[66]. The addition of SIPr to bis(π-allyl)nickel conveniently produces a 3-coordinate 1,5-hexadiene adduct (Figure 17-VII) as reported by Hazari *et al*[67]*.* Finally a 2-coordinate bis(CAAC) nickel(0) complex (Figure 17-VIII) has been prepared by Roesky *et al.* and used as a catalyst for the coupling of aryl halides[68]. By using these bulky and electron-rich ligands, significant gains in reactivity have been observed in a variety of nickel-catalyzed and -mediated processes. For example, a 2-coordinate nickel-imido complex bearing the bulky IPr* ligand reacts with ethylene to produce a 3-coordinate metallacyclobutane, which β-hydride eliminates to give the enamine product[69] (Figure 18). In a report by Schneider *et al.*[70], bulkier NHC ligands (IPr, SIPr) were found to be superior for the coupling of aryl halides with arylmanganese reagents when compared to slightly smaller NHCs (IMes, ITol). Nickel(II) complexes bearing pyridine-functionalized NHC ligands have been used to

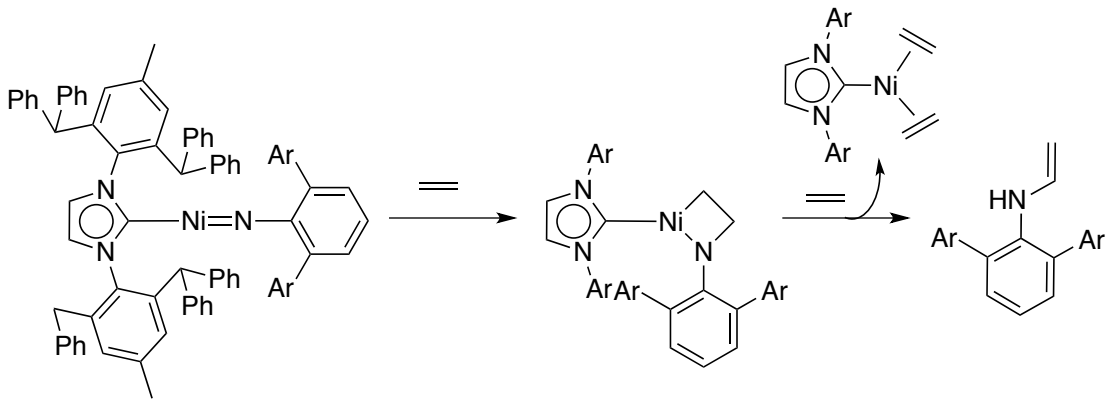

Fig. 18: A rare C-H amination of ethylene mediated by a 2-coordinate nickel imido complex

catalyze the Kumada coupling of unactivated aryl chlorides at room temperature[71]. A similar strategy has been applied by Organ *et al.* in the development of commercially available and air-stable NHC-palladium dichloride complexes (marketed as PEPPSI – for Pyridine Enhanced Precatalyst Preparation Stabilization and Initiation) suitable for carrying out difficult cross coupling reactions of ortho-substituted aryls under relatively mild conditions[72].

Part 1
Three-coordinate nickelacyclopentanes: Preparation and reactivity

Abstract

This chapter contains a transcribed publication[73] of some recent results with 3-coordinate nickelacyclopentanes derived from tetrafluoroethylene. Note that some of the figures may have been altered from their original form to better suit the layout of this text. My role in this publication was centered around the Brønsted acid reactivity, as well as in the preparation of the starting materials. The origin of this project rests on the work of Baker wherein tetrafluoroethylene was hydrodimerized *via* Ni-phosphite metallacycles. The success of this project came from the use of exceptionally bulky NHC ligands which (as mentioned in the introduction) bring unique properties that enhance the reactivity of the metallacycles. The complex in question exhibited new reactivity with Lewis and Brønsted acids, and was able to undergo ring-contraction to a rare Ni-heptafluorocyclobutyl complex. Furthermore, the hydrodimerization step *as per* Baker's previous report was able to proceed with the three-coordinate metallacycle at much lower pressure owing to increased ability of the Ni center to coordinate hydrogen. Overall, the NHC-Ni scaffold has opened the door to a host of new chemistry with perfluorometallacycles; this strategy has thus percolated throughout the nickel-fluoroalkene project and the motif will no doubt be featured prominently in results to come.

Introduction & Prior Art

Fluorocarbons and their derivatives are valuable as refrigerants, agrochemicals, unique solvents/surfactants and fluoropharmaceuticals, with annual sales of the latter alone in the billions of dollars.[74] As the demand for fluorinated chemicals has increased, so too have synthetic methods for introducing fluorine and fluorocarbon groups.[75, 76, 77] Despite recent advances, transition metal-mediated/-catalyzed routes are rare in comparison to the well-developed organometallic chemistry of hydrocarbons[78]. The challenge rests in the stability of metal– perfluoroalkyl (M–R^F) bonds, relative to metal–alkyl bonds[79]. M– C^F bonds are typically inert to processes such as insertion/alkyl migration reactions, vital to metal-mediated catalytic cycles.[7] Moreover, C–F bonds are stronger than C–H bonds[80], posing another obstacle to metal-based approaches.

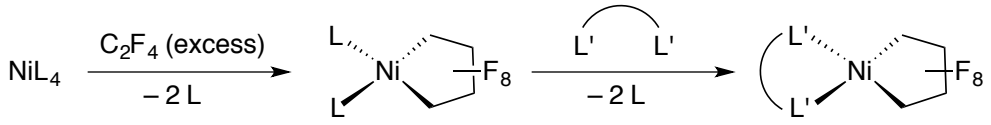

Fig. 19: Synthesis of perfluoronickelacyclopentanes *(L = PR_3, $P(OR)_3$; L' = 2,2'-bipy, dppe)*

We are investigating perfluoronickelacyclopentane complexes (PNCPs) as platforms for functionalized fluorocarbons with an initial focus on fundamental stoichiometric reactions. PNCPs have been synthesized previously by reaction of tetrafluoroethylene (TFE, CF_2=CF_2) with Ni^0 complexes. The displacement of P ligands by bidentate ligands has also been reported (Figure 19)[81]. To date, reports concerning the reactivity of PNCPs are sparse: Burch and co-workers found that Lewis acidic BF_3 effects fluoride abstraction from C_α and phosphine migration to the activated carbon (Figure 20-a)[82]. Extending this reaction to the unsymmetrical P^S chelate, we showed that treatment with excess isonitrile effected cleavage of the Ni–C^F bond (Figure 20-b)[83]. With

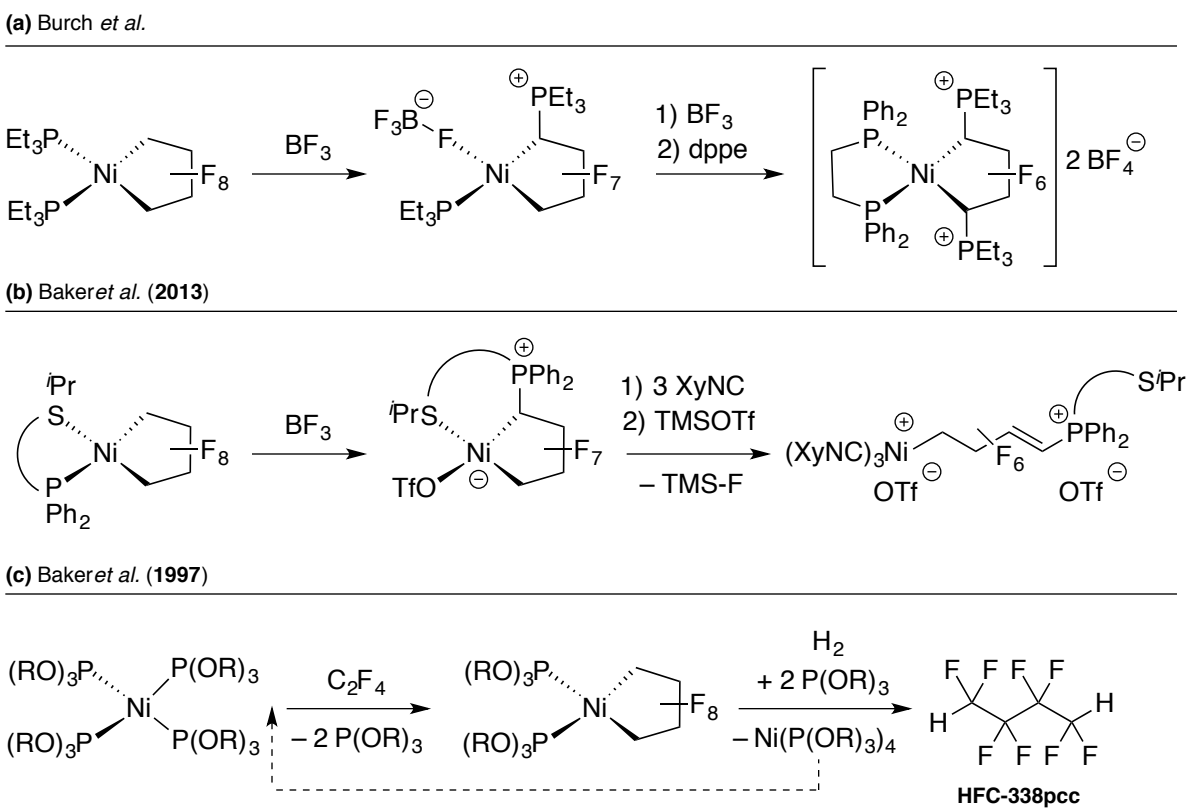

Fig. 20: Previously reported reactivity of perfluoronickelacyclopentanes

phosphite co-ligands, a remarkable hydrogenolysis reaction enables the selective catalytic hydrodimerization of TFE (Figure 20-c)[84]. As far as we know, this reaction is the only example of a perfluorometallacyclopentane participating in a catalytic cycle[85].

Our approach to metallacycle functionalization hinges on the reactivity of metal-activated C_α–F bonds[86] wherein we replace a C–F bond by C–Nu vs. the current paradigm C–L (Nu = nucleophile, L = ligand). Using N-heterocyclic carbenes (NHCs)[87], we aimed to access low-coordinate PNCPs wherein the strong M–CNHC bond may also prevent ligand migration to C_α. There is considerable precedent for such an approach to low- coordinate metal complexes[88]. Hillhouse and coworkers prepared a two-coordinate nickel–imido complex bearing the exceptionally bulky IPr* ligand (analog of IPr with 2,6-bis(di-phenyl-methyl)phenyl groups instead of 2,6-diisopropyl-phenyl)[89]. Similarly, Miyazaki and coworkers synthesized a T- shaped three-coordinate nickel(I) chloride

species [Ni(IPr)$_2$Cl] by treatment of two-coordinate [Ni(IPr)$_2$] with aryl chlorides[90]. Also, Hartwig et al. synthesized a low-valent, three-coordinate palladium(II) norbornyl species [Pd(SIPr)(NHAr)(Nor)], which underwent facile C–N bond reductive elimination when heated[91].

In this report we show that low-coordinate NHC Ni perfluorometallacycles undergo facile C_{sp3}–F and M–CF bond cleavage as well as C_α-functionalization[92]. We also demonstrate the first migration of a fluoroalkyl to a reactive carbon center. This is significantly different from the reactivity previously observed for phosphine Ni perfluorometallacycle complexes[93].

Results & Discussion

Starting from bis(phosphite) PNCP[94] (**1a** and **b**) we were able to cleanly synthesize coordinatively-saturated or -unsaturated nickel perfluorometallacycles. Thus, **1a** reacts smoothly with 1 equiv. of ItBu (ItBu = 1,3-di-tert-butylimidazol-2-ylidene) to afford the NHC/phosphite product **2** (Figure 21, top; X-ray structural characterization presented in ESI)[95]. Significantly, the reaction between the larger SIPr ligand [SIPr = 1,3-bis(2,6- diisopropylphenyl)imidazolin-2-ylidene] and a nickel metallacycle with sterically-demanding co-ligands (**1b**) results in displacement of both phosphite ligands, yielding the pseudo- three-coordinate/14e-Ni(II) metallacycle **3** (Figure 21, bottom). The molecular structure of complex **3**, as determined by single crystal X-ray diffraction, exhibits a T-shaped coordination about the Ni and features a weak agostic interaction with the isopropyl methyl group (Ni–C 1⁄4 2.757(1) A˚; compare Ni–CF bond distance trans to the NHC (1.934(1) Å) with that trans to the agostic interaction (1.875(1) Å) (Figure 22A). The ^{19}F NMR spectrum of **3** in C_6D_6 is consistent with ideal C_{2v} symmetry at room temperature, with only two distinct singlet resonances at 101.9 (F_a) and 138.6 ppm (F_b). While these resonances both broaden significantly at 213 K, it is apparent that the T-flip interconversion encounters only a small energy barrier[96]. To confirm this, we carried out DFT calculations (at the B3LYP/ TZVP level with and without the empirical

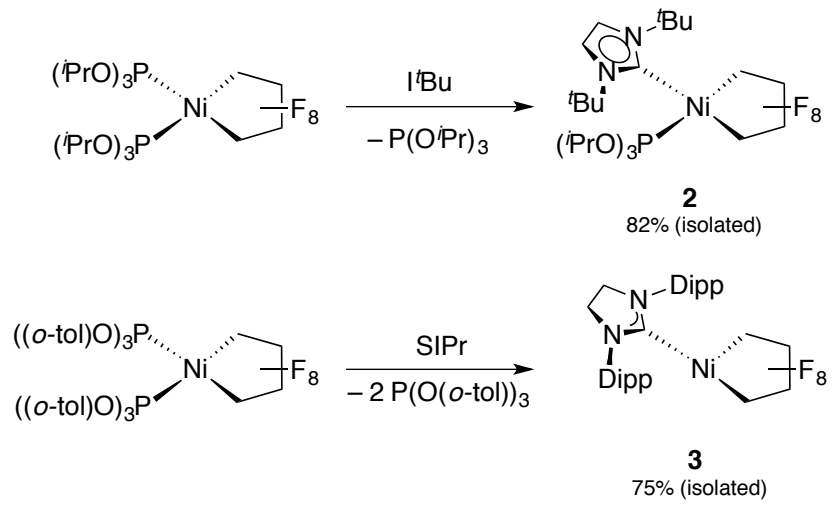

Fig. 21: Syntheses of NHC perfluoronickelacyclopentane complexes

dispersion correction of Grimme)[97]. Intriguingly, the calculations reveal two spin-singlet structures with a very small energy difference ($\Delta G_{298\,K}$ = 0.0–1.5 kcal mol^{-1}). The first computed structure coincides well with the observed solid-state structure of **3**; the 3-center bond order index between the Ni and the corresponding C–H bond of 0.05 is much less than 8/27 (~0.3), the maximum possible value for a 3-center 2-electron bond. As a result, the Mayer valence index for Ni in structure 3 is only 3.09. The second structure (**3**') features a weak η^3 interaction between the aryl group of the NHC ligand at the 4th coordination site of the Ni atom (Figure 22B). Mayer bond orders for the corresponding three Ni–C interactions are in the 0.02–0.05 range, with a total bond order of 0.09. This suggests a semi-bidentate binding mode for the class of NHC ligands possessing pendant aryl groups. From calculations with the dispersion correction, structure **3**' has the same Gibbs free energy as **3**. Without the dispersion correction, structure **3**' is actually 1.5 kcal mol^{-1} lower in energy than **3**. The 3-coordinate structure with trigonal coordination around Ni and symmetric binding of the C_4F_8 ligand is a transition state with a low energy ($\Delta G^{\ddagger}_{298\,K}$ = 2.1 kcal mol^{-1} relative to **3**). Thus, it is clear that cleavage of the weak agostic and/or η^3-aryl bond is facile and allows for rapid reorientation of the ligands around the Ni center. Attempts to obtain evidence for structure **3**' by low temperature NMR were frustrated by dynamic processes associated with the T-flip and hindered rotations about the M–C and perhaps N–C bonds.

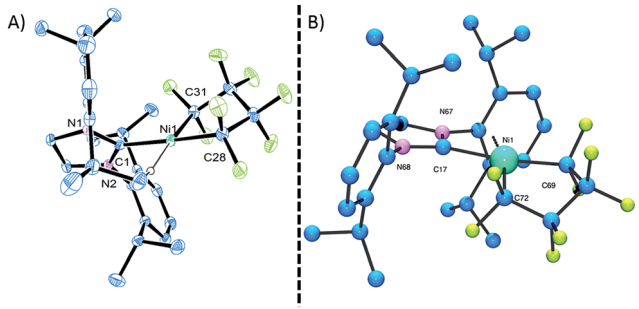

Fig. 22: (A) ORTEP representation of the molecular structure of **3**. Thermal-ellipsoid probabilities are set to 35% with hydrogen atoms omitted for clarity. The Ni–C(1) distance is 1.854(2) Å. (B) Optimized structure of low energy Ni–aryl isomer 30; Ni–C_{aryl} distances are = 2.818, 3.329, 3.379, 4.166, 4.204, 4.543 A˚. The Ni–C(17) distance is 1.989 Å.

The HOMO of **3** (ε = 6.01 eV; Figure 23, left) is localized on the Ni (87%), primarily from a d_{z2} orbital contribution (71%). Lower-laying orbitals display interactions between metal d_{xz}, d_{yz} orbitals and the π-system of the aryl group[98]. The LUMO (ε = 1.96 eV; Figure 23, right) is an anti-bonding combination of the metal d_{x2-y2} orbital (total Ni character of 45%) with the π-donor orbitals of the NHC and C_4F_8 ligands. Thus, reactivity of the M–C bond is likely under orbital control and arises from an interaction with the HOMO of **3**. In contrast, C–F bond activation is likely a combination of orbital and charge control with a slant towards the latter as the hardness of the Lewis acid increases[99].

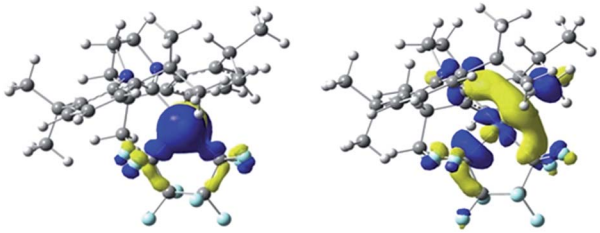

Fig. 23: The HOMO (left) and LUMO (right) of **3**. Isosurface values of 0.04 au are used.

Initial studies on the C–F bond activation reactions of **3** are promising in the context of synthesizing functionalized fluorocarbons by metal-mediated approaches. Firstly, when **3** is treated with the Lewis acid TMSOTf (TMS = Me_3Si, OTf = SO_3CF_3), α-fluoride-abstraction, accompanied by Ni–C^F bond cleavage and C^F–C^F bond formation,

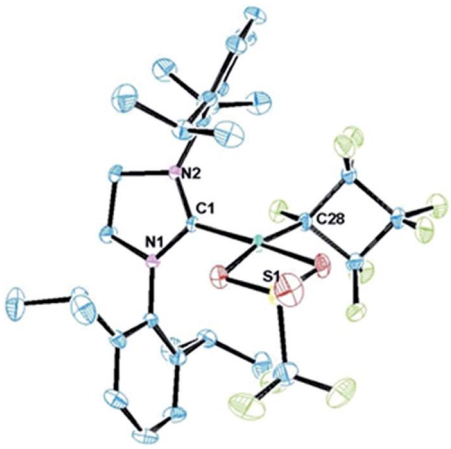

Fig. 24: ORTEP representation of the molecular structure of **4a** with thermal ellipsoid probabilities set to 30% and hydrogen atoms omitted for clarity. The Ni-C(1) distance is 1.854(2) Å

furnishes a rare per- fluorocyclobutyl complex **4a** (Figure 25, 75% isolated yield)[100]. The driving force behind this transformation is likely related to the triflate leaving group ability and the formation of a strong C–C bond[101]. Importantly, the NHC remains bound to the nickel atom (i.e., does not migrate to C_α), potentially opening new pathways to functionalized fluorocarbon derivatives. Upon heating complex **4a** (80ºC in C_6D_6, 24 h), perfluorocyclobutylene is produced, presumably via a β-fluoride elimination mechanism, although the metal-containing co-product(s) have not yet been identified[102]. Interestingly, a single OTf containing product can be discerned by ^{19}F NMR (93.37 ppm) but a Ni–F signal could not be located. The ^{1}H NMR shows that the NHC remains intact. Upon addition of PPh_3 to the reaction mixture, PPh_3F_2 was identified as a major product, suggesting formation of a Ni–F thermolysis co-product.

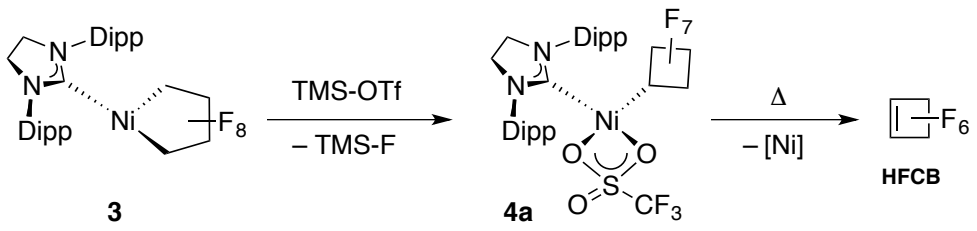

Fig. 25: Synthesis and decomposition of **4a**.

The distorted square planar structure of complex **4a** (Figure 24) features a bidentate triflate ligand which can also likely access the κ^1-mode in solution as evidenced by the simple ^{19}F NMR spectrum[103] and observed tendency to eliminate. The perfluorocyclobutyl ring is nearly planar, the Ni–C bond is short [1.890(2) Å] due to the weak s-trans influence ligand, and the C_α–F bond distance (1.384(3) Å) is considerably longer than the other C–F bonds (average of 1.33 Å).

The reactivity enhancement offered by low-coordinate **3** is evidenced by the sluggish reaction of 4-coordinate complex **2** with TMSOTf to give a mixture of unidentified products. Indeed, monitoring the reaction of **3** and TMSOTf at 25ºC allowed for the identification of a Ni–C_4F_7 intermediate **5a** apparently containing a C_α–OTf linkage (triflate CF_3 ^{19}F NMR resonance is coupled to C_α–F: $^5J_{FF}$ = 11 Hz). This is in contrast to previous suggestions of a metal fluorocarbene intermediate (Figure 26)[104].

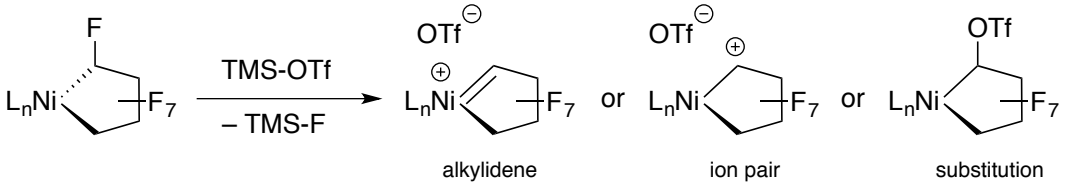

Fig. 26: Possible intermediates in the reaction of **3** with TMSOTf

Having established that the NHC ligand remains bound to the metal upon fluoride-abstraction from **3**, we shifted our focus to C–F bond functionalization using Brønsted acids. Treatment of **3** with trifluoroacetic acid [TFA; pK_a = 3.4 (DMSO)][105] gives HF and the more stable (vs. **5a**) trifluoroacetate-substituted metallacycle **5b** that could be characterized spectroscopically at room temperature (Figure 27). Nonetheless, accompanying formation of perfluorocyclobutylene, presumably formed via an analogous structure to **4a**, led us to move to weaker Brønsted acids. Remarkably, reaction of **3** with acetic acid [pK_a = 12 (DMSO)][106] (Fig. 27, bottom) yielded the stable ester metallacycle **5c** (30% isolated yield) as well as the Ni–C^F bond cleavage product **6a** in a 1:1 ratio. At a similar acidity [pK_a = 11 (DMSO)][107] but increased steric bulk,

2,4,6-trimethyl-benzoic acid gave a 10:1 mixture favouring the ring cleavage product, **6b**.

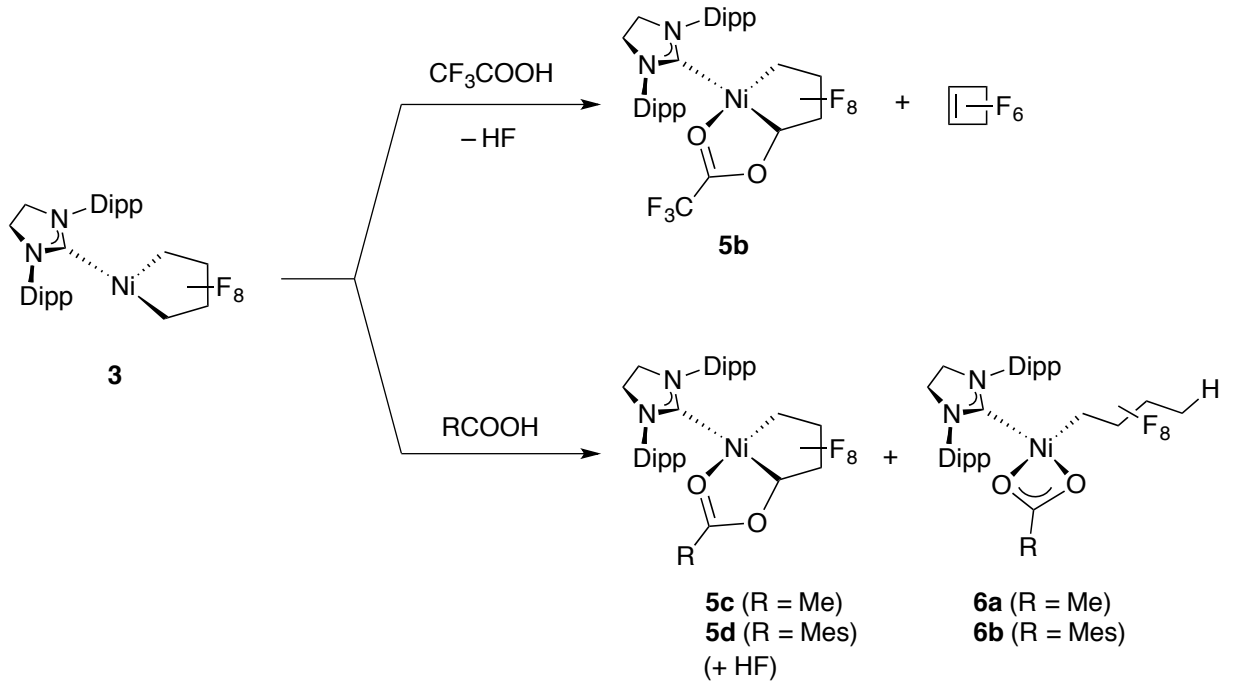

Fig. 27: Reaction of **3** with trifluoroacetic, acetic, and 2,4,6-trimethylbenzoic acids

The molecular structure of **5c** features similar Ni–C bond distances (1.895(7) vs. 1.896(6) Å) and a distorted square planar coordination (Figure 28). The functionalized heptafluoro-metallacyclopentane ring is puckered with the smallest C–C bond distance being C(32)α–C(39)β [1.49(1) Å]. The carbonyl oxygen completes the nickel coordination sphere (Ni–O1 = 1.969(4) Å).

The ^{19}F NMR spectra of **5a**–**d** are very similar and support our original proposal for the low temperature intermediate **5a** in the reaction of **3** with TMSOTf. The C_α–F ^{19}F chemical shifts of the functionalized carbon, (-117.2 and -119.2 ppm) can be compared with those of the phosphonium analogs (-115.6 and -117.8 ppm) shown in Figure 20.

As expected, the ring-opened products **6a** and **b** display nearly identical ^{19}F NMR chemical shift patterns with the Cγ– and Cδ–F resonances distinguished by F–H coupling of 6 and 52 Hz, respectively. These unique complexes have been identified as

their potassium cation adducts using ESI-MS (747.2 g mol^{-1} and 851.4 g mol^{-1} respectively) and are surprisingly inert to thermolysis at 80 C in C_6D_6 for 20 h.

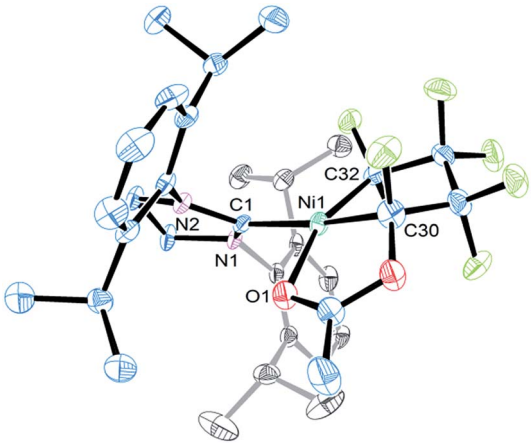

Fig. 28: ORTEP representation of the molecular structure of **5c** with thermal ellipsoid probabilities set to 30% and hydrogen atoms omitted for clarity. The Ni-C(1) distance is 1.928(2) Å.

Considering the importance of esters as synthons in organic transformations[108] this C–O bond-forming reaction **3** → **5** is very appealing from the standpoint of synthesizing functionalized fluorocarbons. As such, understanding competing pathways for M–C vs. C–F bond cleavage would be valuable[109]. Viable reaction pathways can be considered as proceeding via either 5- or 6- membered transition states (Figure 28). The selective HF elimination observed for TFA, is eroded as Ni–C bond protonolysis (orbital control) competes using acids of intermediate acidity (*e.g.* pKa ~11)[110]. With the bulkier trimethylbenzoic acid, kinetic acidity factors in the tighter 5-membered ring transition state could severely limit HF elimination[111].

Conclusions

In summary, we have prepared the first NHC–perfluorometallacyclopentane complexes and exploited the bulky SIPr ligand to stabilize a pseudo-three-coordinate nickelacycle, **3**. Importantly, **3** undergoes C_α–F abstraction reactions without migration

of the NHC ligand. Instead, we see an unprecedented migration of the fluoroalkyl to the reactive carbon center, giving rise to the novel perfluorocyclobutyl complex via Ni–C^F bond cleavage. More importantly, the low-coordinate nature of **3** allows for ring functionalization. Strong acids favour selective C_α functionalization, but the resulting products are unstable with respect to competing metallacycle ring contraction and elimination of perfluorocyclobutene. With less acidic reagents stable ring-functionalized products are formed but a competing Ni–C^F bond cleavage pathway comes into play and dominates for bulkier carboxylic acids. These are the first examples of selective functionalization of a PNCP and synthesis of thermally stable Ni–C_4F_8H complexes. These results are encouraging in the context of developing metallacycle-based routes to func- tionalized fluorocarbons.

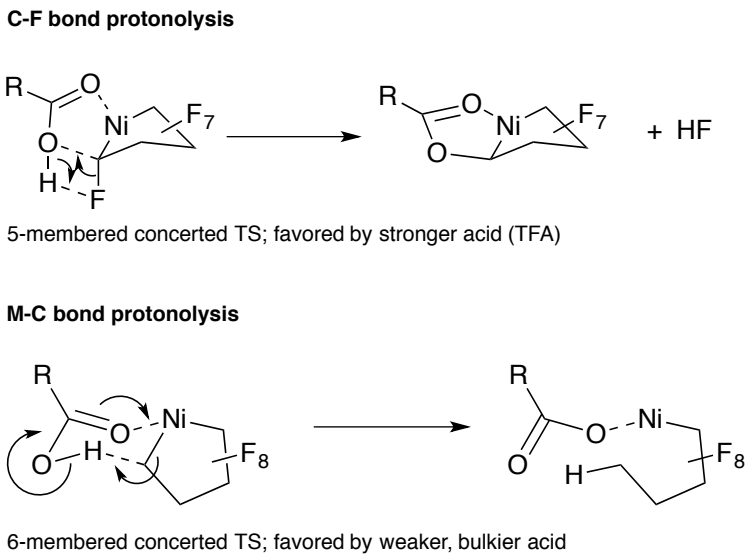

Fig. 29: Proposed reaction pathway for C-F activation vs. Ni-R^F protonolysis.

Ongoing work is focused on (a) expanding the scope of ring functionalization substrates suitable for reactions with **3** and (b) reductive and oxidative approaches for removing the functionalized fluorocarbon fragments from the metal. Preliminary results of the hydrogenolysis of compound **3** indicate enhanced reactivity towards H_2 (i.e., at 7 psig and 25ºC) vs. reported 4-coordinate phosphite variants[112]. However, loss of selectivity[113]

is observed with the synthesis of two distinct products. Full details of these results will be published in due time.

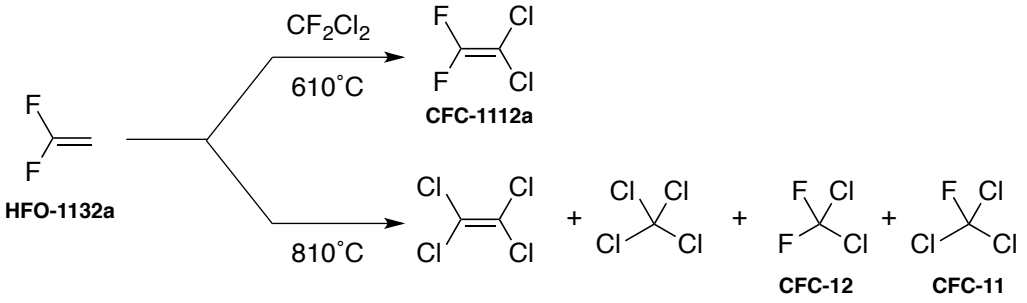

Fig. 30: Early uses of vinylidene fluoride included chlorination to give a wide array of industrially relevant chlorocarbons and CFCs.

Part 2
Vinylidene difluoride: Organometallic chemistry and catalysis

Introduction & Prior Art

In Vinylidene difluoride (HFO-1132a, $CF_2=CH_2$) is an industrially useful monomer which can be prepared by the reaction of Halon-1211 (CF_2ClBr) with methane in a 1:2 ratio at 900˚C[114], or by the dehydrochlorination of 1,1-difluoro-2-chloroethane at between 500–750˚C[115]. A recent patent reports its preparation starting from the readily available chlorodifluoromethane (HCFC-22) and methyl chloride at 800˚C[116]. This olefin has given rise to the polymer PVDF (poly(vinylidene difluoride)) – obtained via free-radical vinyl polymerization (FRVP) – which has found use as a chemically inert

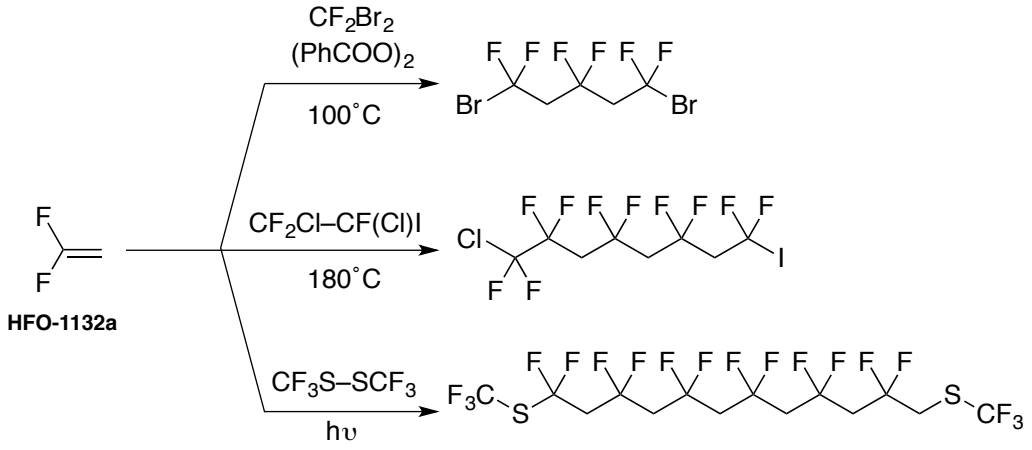

Fig. 31: Free-radical reactions predominated at the origin of VDF chemistry. The highest telomers for various free-radical systems are shown.

thermoplastic. Similarly, most of the chemistry derived from HFO-1132a is free-radical based. Some of the earliest industrial uses were patented by Allied Chemical and Dye Corporation, including chlorination at 810ºC to produce a variety of chloro- and chlorofluoro-carbon products[117], and the reaction with dichlorodifluoromethane to produce 1,1-difluoro-2,2-dichloroethylene[118] (Figure 30). HFO-1132a can also be hydrofluorinated with AHF in the presence of an aluminum fluoride catalyst to give 1,1,1-trifluoroethane (HFC-143a), a useful refrigerant[119]. The telomerization of this olefin has been carried out using a variety of free-radical initiators[120,121,122], three of which are outlined in Figure 31, obtaining as high as $n = 6$ additions.

Very little has been published in terms of the organometallic and coordination chemistry of vinylidene difluoride. The first report of a coordination compound thereof was by Stone and coworkers in 1969 on zerovalent nickel (Scheme 3"a). This work was built upon by Hoberg & Duhl in 1989 when analogous Ni compounds with bidentate ligands were prepared; the same report also contains a unique insertion of the VDF group into an organic isocyanate (Scheme 3"b). HFO-1132a has been reported to dehydrofluorinate in some cases; a strange example of this was observed by Keim & Fischer with a Fe(II) half-sandwich compound, resulting in a metallacyclopropene product[123] (Figure 32-a). Another strange example was observed with an Os(IV) hydride, which gave an alkylidyne upon dehydrofluorination[124] (Figure 32-b). The loss of C–F bonds is not unique, as it was also observed by reacting HFO-1132a with zirconocene dihydride[125] (Figure 32-c), giving two new Zr products (none of which being a fluoroalkyl), as well as by reacting the HFO with an Os(II) alkyl hydride, giving a metal vinylidene with the loss of methane[126] (Figure 32-d). VDF was also reacted with a cationic Ir dimer by Cowie and coworkers to give a bridging metallacyclobutane[127].

VDF has been recently employed by Honeywell International as an HFC precursor to generate the 4th generation refrigerant R-1234ze by coupling with other abundant feedstock gases such as HCFC-22, hexafluoropropylene oxide, and tetrafluoroethylene[128].

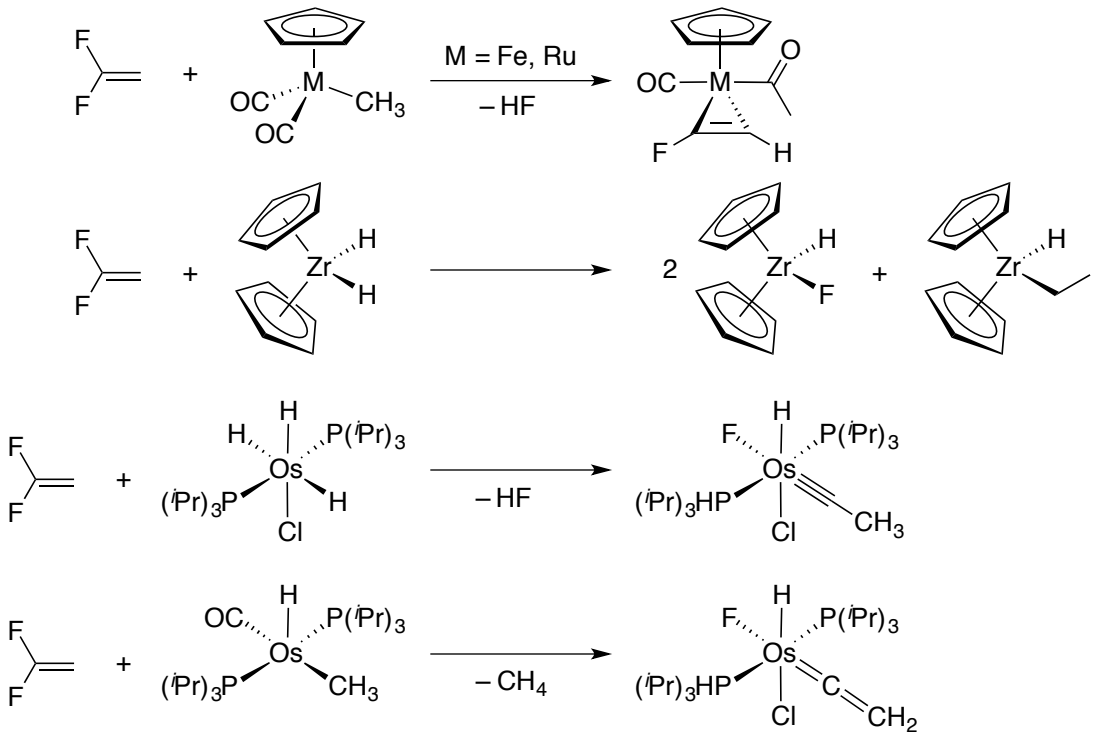

Fig. 32: Examples of defluorinative (or dehydrofluorinative) reactions of HFO-1132a mediated by transition metal complexes

Current Work

In light of the relatively narrow scope of published work in coordination chemistry of vinylidene difluoride (particularly on nickel), a project was undertaken to replicate with VDF the group's past successes with TFE. The original target was a metallacyclopentane whose enhanced reactivity (owing to the only partial fluorination) could be exploited to generate new strategically-fluorinated organic derivatives. It is important to note that because VDF is an unsymmetrical olefin, three different isomers of metallacyclopentane are possible: head-to-head, head-to-tail, or tail-to-tail (Figure 33). Owing to the extreme polarization of this olefin, selectivity for the head-to-tail is expected. The aim of this study is to examine the reactivity of the metallacyclopentanes that contain a higher hydrogen content. Firstly, HFOs (as 4th-generation refrigerants)

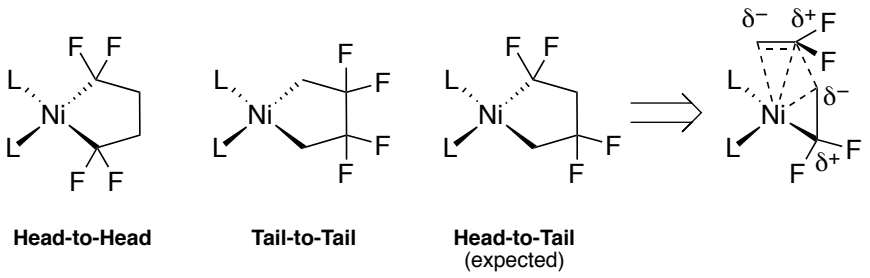

Fig. 33: Possible isomers of a VDF-derived nickelacyclopentane with the head-to-tail isomer as the expected result

are of current commercial interest, and so improved methods for their synthesis are in industrial demand. Secondly, the chemistry of metallacycles derived from trifluoroethylene has been shown by K. Giffin[129] (a fellow member of this research project) to deviate considerably from that of the perfluorinated metallacycles already discussed in Part 1. The presence of C-H bonds to the metallacycles appears to increase their propensity for β-fluoride elimination, a phenomenon never observed in studies of perfluorometallacycles. With the trifluoroethylene systems, the 5-membered metallacycles are isolable, but upon treatment with a Lewis acid (trimethylsilyl trifluoromethanesulfonate) the major isomer (head-to-tail) loses an α-fluoride, giving the ring-opened metallacycle which β-eliminates to the diene as shown (Figure 34). The minor isomer, upon loss of α-fluoride, undergoes phosphine migrations to both α-

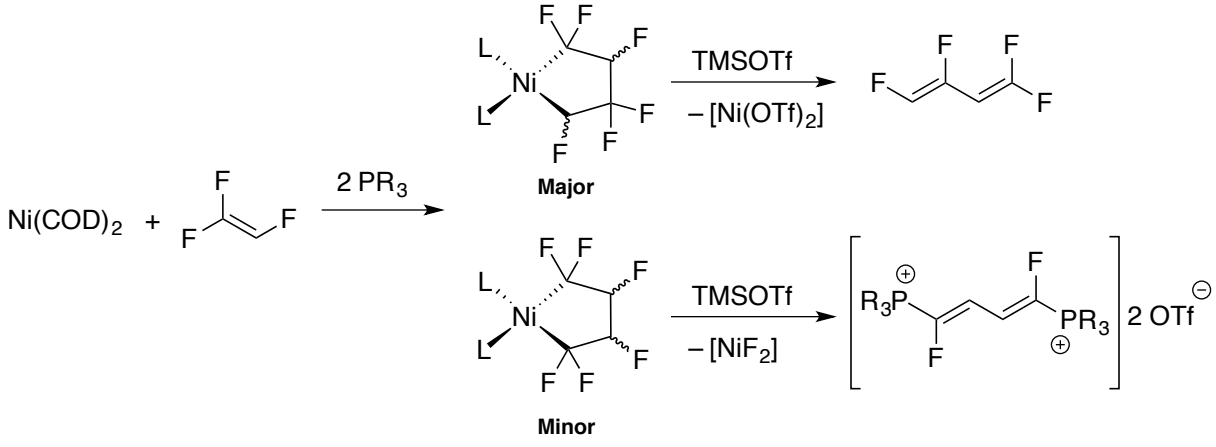

Fig. 34: Reactions of both isomers of trifluoroethylene-derived metallacyclopentanes with TMSOTf to give hydrofluorobutadiene products

carbons, followed by β-elimination to give a diphosphonium diene salt. It is clear that hydrofluoroolefin-derived metallacycles are subject to different reactivity trends than tetrafluoroethylene-derived metallacycles, and with this newfound reactivity in mind, parallel chemistry with vinylidene difluoride was pursued.

Previously, only three-membered metallacycles have been reported from HFO-1132a, and their ligand scope was limited to triphenylphosphine and tricyclohexylphosphine. In this work, a wider array of phosphine ligands were screened. The smaller phosphine ligands (tripropylphosphine, e.g.) give the three-membered metallacycle exclusively, with no observation of larger metallacycles even upon heating; their ^{19}F and ^{31}P NMR chemical shifts are reported in Table 1. Select diphosphine ligands are were also screened for reactivity and gave exclusively the three-membered metallacycle in all cases. The DPEphos derivative was fully worked up and isolated, while the rest were characterized by ^{19}F and ^{31}P NMR spectroscopy; their chemical shifts and coupling constants are reported in Table 2. The isolated DPEphos metallacycle was subjected to trimethylsilyl triflate and the resulting (and expected) vinyl triflate product was characterized by ^{19}F NMR. The three-membered metallacycle is extremely labile, with any attempt at ligand substitution resulting in extrusion of vinylidene difluoride. The complex is unstable in halogenated solvents, further demonstrating its tendency to behave as nickel(0) in solution.

TABLE 1: MONODENTATE PHOSPHINE 3-MEMB. VDF METALLACYCLES

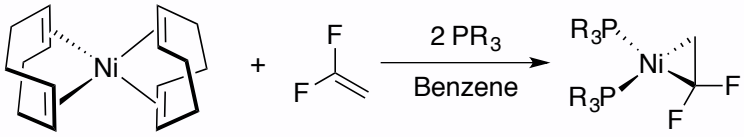

R	^{19}F Signal	^{31}P Signals
n-Pr	–96.4 ppm J_{F-H} = 14 Hz, J_{F-P} = 40, 27.5 Hz	7.5 ppm, 12.8 ppm J_{P-P} = 33 Hz
n-Bu	–96.4 ppm J_{F-H} = 13 Hz, J_{F-P} = 40, 27 Hz	8.7 ppm, 14.0 ppm J_{P-P} = 31 Hz
i-Bu	–95.3 ppm J_{F-H} = 14 Hz, J_{F-P} = 37, 24 Hz	8.0 ppm, 13.0 ppm J_{P-P} = 30 Hz

TABLE 2: BIDENTATE PHOSPHINE 3-MEMB. VDF METALLACYCLES

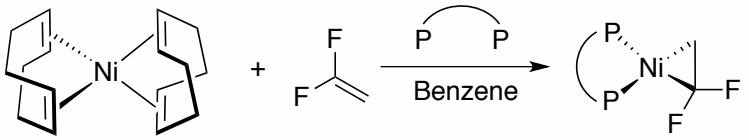

P^P	^{19}F Signal	^{31}P Signals
dcppe	–92.0 ppm *J_{F-H} = 14.5 Hz, J_{F-P} = 49.5, 39 Hz*	59.7 ppm, 63.1 ppm *J_{P-P} = 57 Hz*
dibpe	–92.6 ppm *J_{F-H} = 13.5 Hz, J_{F-P} = 50, 40.5 Hz*	31.9 ppm, 36.8 ppm *J_{P-P} = 65.5 Hz*
dibpp	–94.6 ppm *J_{F-H} = 14 Hz, J_{F-P} = 46, 36.5 Hz*	0.7 ppm, 4.9 ppm *J_{P-P} = 25 Hz*
dppf	–94.7 ppm *J_{F-H} = 12.5 Hz, J_{F-P} = 42.5, 28 Hz*	21.3 ppm, 24.5 ppm *J_{P-P} = 21.5 Hz*

The inability of any chelating phosphine ligands (even highly basic ones such as dcppe) to give products beyond three-membered metallacycles supports the notion that in order to proceed from a three-membered to a five-membered metallacycle, there must be a forced lowering of coordination number at nickel at some point. A similar issue is not encountered with TFE as the olefin is sufficiently reactive to compete effectively with other ligands for coordination at the nickel center. Unfortunately, as the number of fluorine atoms is removed from an olefin, it appears to become ever less competitive with phosphine or phosphite ligands at the electron-rich nickel(0) (i.e. less like TFE and more like ethylene). For this reason, all reactions attempted starting from NiL_4 (L = tri(o-tolyl)phosphite, triphenylphosphine, triethylphosphite (generated *in situ*) were unsuccessful. In light of the group's successes using NHC ligands, a similar strategy was employed here to enforce a low-coordinate intermediate. Unfortunately, conventional aryl NHC ligands (IPr, SIPr, IMes, SIMes) are unsuitable for this purpose as they react with the fluorinated olefin[130]. Only NHC ligands bearing tert-alkyl substituents on the nitrogens are sterically hindered enough so as to be inert to fluoroolefins; of those ligands, ItBu and IAd are the most common, and were selected for this study. Interestingly, the reaction of $Ni(COD)_2$/NHC with VDF gave exclusively the β-fluoride elimination product from a five-membered head-to-tail metallacycle, which appears as a *μ*–F dimer (Figure 36). The compound was characterized by NMR, MS,

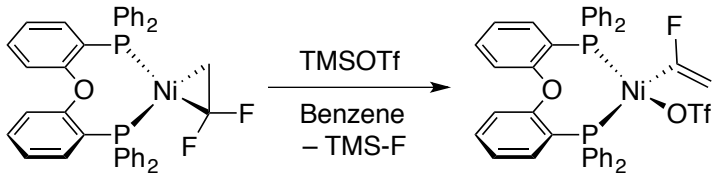

Fig. 35: Reaction of the DPEphos 3-memb. metallacycle with TMSOTf, giving the fluorovinyl product (characterized by NMR).

and X-ray crystallography. Similar complexes were prepared using tricyclopentylphosphine and di(tert-butyl)*n*-butylphosphine, however these products could not be easily isolated in bulk form, and so were characterized by NMR (Table 3) and X-Ray crystallography (for the tricyclopentylphosphine-adduct - Figure 38). In no case was the parent metallacycle observed. The formation of such a product diverges from the chemistry of the 3-coordinate TFE metallacycle, which exhibits no desire to β-eliminate, and in fact is normally activated at the α-fluorides as shown in *Part 1*. This stark difference can be due to a number of factors. Firstly, the β-fluoride elimination pathway is accompanied by an accumulation of positive charge at the β-carbon; on a perfluorometallacycle, that positive charge would presumably be highly destabilized by the neighboring difluoromethylene groups, whereas on a VDF-derived metallacycle, the β-carbon is flanked by CH_2 groups which can better stabilize a positively charged transition state. Furthermore, because of the forced orientation of the C–F bond, intramolecular β-elimination is highly unlikely for a five-membered metallacycle; there can be no agostic interaction even if there is an empty coordination site in the cis position. Thus, a dimeric transition state is proposed (Figure 37). If this mechanism is

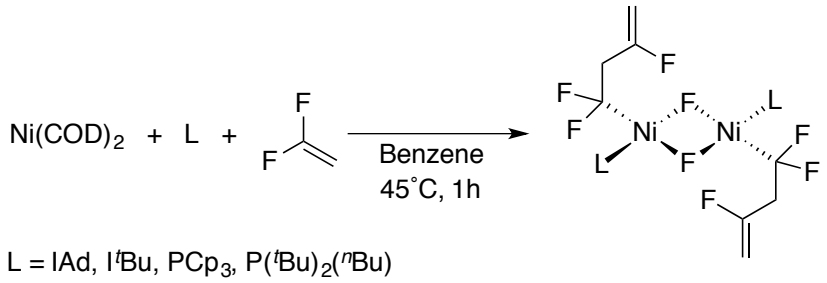

Fig. 36: Formation of nickel trifluorobutenyl μ-fluoride complexes from HFO-1132a and $Ni(cod)_2$ using bulky and highly electron-rich ligands

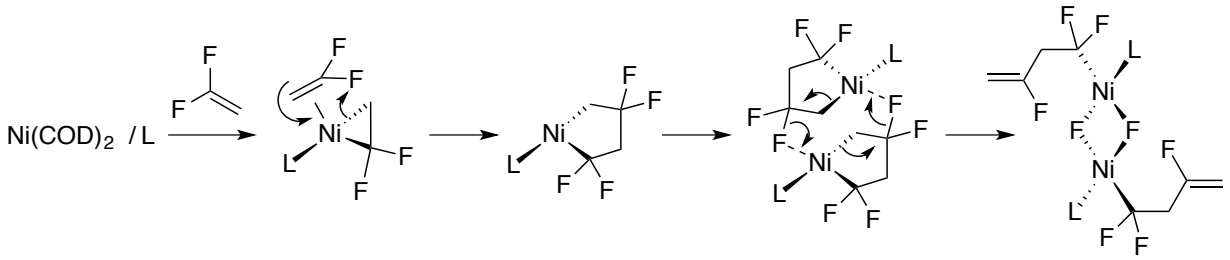

Fig. 37: Proposed mechanism for the μ-fluoro butenyl formation.

operant, then it is made possible here by the lower buried volume of the IAd and I*t*Bu NHC ligands (compared to the SIPr ligand used in Part 1), which allows enough space for the formation of such a dimer. When the reaction is carried out with a 1:1 ratio of NHC and a small phosphine ligand (such as PPr_3 or PBu_3), the three-membered metallacycle (a mixture of *cis*/*trans* [Ni(PR_3)(IAd)(η^2-VDF)]) predominates and only a small amount of butenyl product is observed. If the dimer is reacted with a strong acid (p-nitrobenzoic acid) the fluoride is protonated, forming the Ni-benzoate and leaving the fluoroalkyl unaffected. Attempts to couple the trifluorobutenyl fragment using Grignard reagents failed, giving unselective cleavage of C–F bonds. The butenyl complexes were unreactive towards tetraphenyltin, tetraallyltin, or allyltributyltin, suggesting a particularly strong Ni—F bond. Interestingly, when diphenylzinc was reacted with the IAd product in the presence of 1 equiv. of triethylphosphite, a new diene (1-phenyl-1,3-difluoro-1,3-butadiene) was found and characterized by NMR (Figure 39); both cis and trans isomers are present in a 1:1.5 ratio, respectively. The supposed intermediate [$(EtO)_3$P–

TABLE 3: CHARACTERIZATION OF F-BRIDGED BUTENYL DIMERS

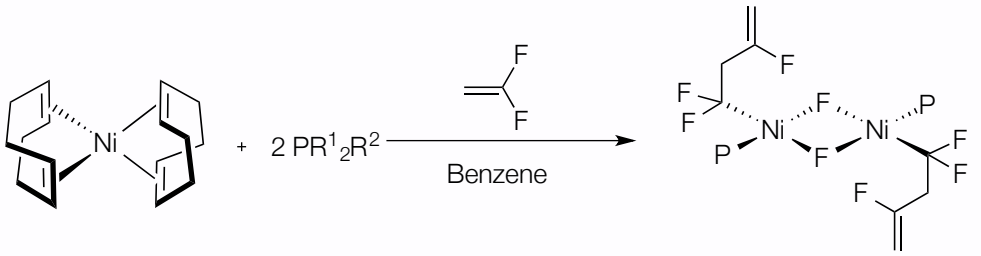

R^1, R^2	^{19}F Signals	^{31}P Signal
R^1 = R^2 = Cp	-68.8 ppm (α-F), -87.4 ppm (γ-F), -387 ppm (Ni-F)	38.2 ppm
R^1 = *t*-Bu, R^2 = *n*-Bu	–69.8 ppm (α-F), –87.6 ppm (γ-F), -380 ppm (Ni-F)	56.0 ppm

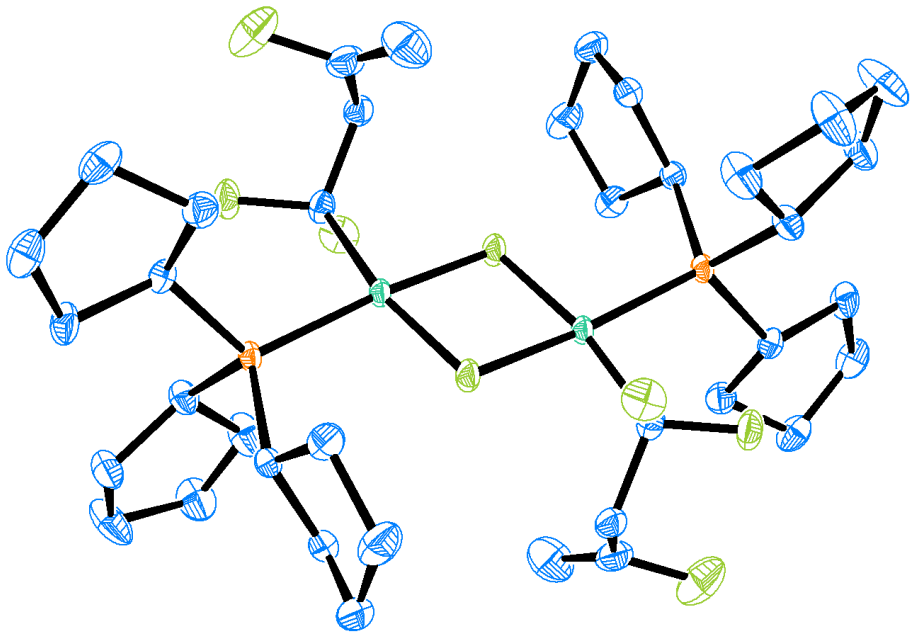

Fig. 38: ORTEP representation of the tricyclopentylphosphine-μ-F-trifluorobutenyl adduct (H-atoms omitted)

Ni–Ph] complex can also be observed. It is noteworthy that the reaction does not proceed unless the triethylphosphite is present. If a small *phosphine* ligand (tri-*n*-propylphosphine, e.g.) is used instead, no reaction is observed. The exact mechanism for this reaction is unknown at this time, but it has been found to require a superstoichiometric amount of the organozinc to proceed to completion, suggesting a more complex mechanism perhaps worth studying at a later date.

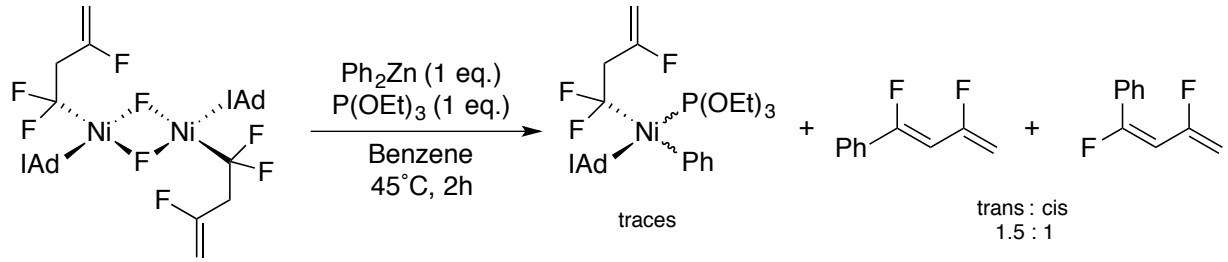

Fig. 39: Reaction of the butenyl product with diphenylzinc to produce new dienes

In the landmark finding for this project, 2,4,4-trifluorobut-1-ene (HFO-1363pyf) was obtained cleanly upon reaction of the same butenyl with either triethylsilane or triphenylsilane at 40-60˚C. The organic product was characterized by ^{19}F NMR but could not be isolated at that scale due to its volatility. Furthermore, this olefin can be produced catalytically from HFO-1132a using as little as 1 mol% of $Ni(COD)_2$ and ligand with stoichiometric silane (Figure 40). This result is particularly significant in its selectivity during the defluorinative step; only one fluorine atom is removed, giving a single isomer. There is precedent in the literature for the use of silane reagents to hydrodefluorinate organic compounds, such as the early example by Milstein[131] & coworkers, however this is the first report that combines the hydrodefluorination with olefin dimerization to give a new, higher-value product. This catalyzed reaction is also

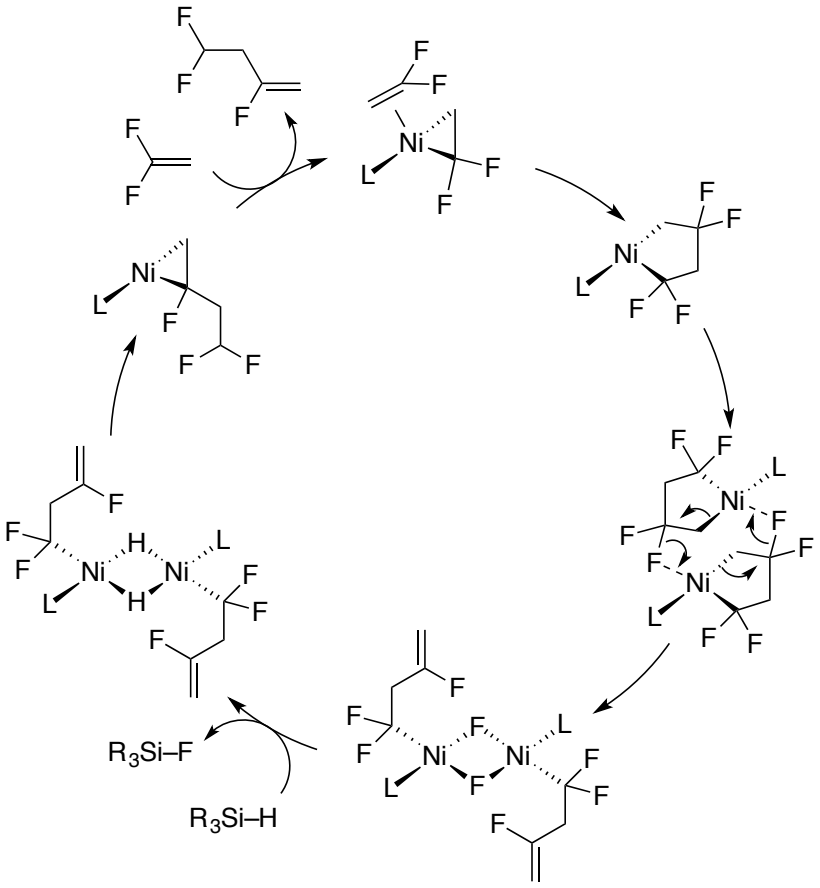

Fig. 40: The catalytic hydrodefluorodimerization cycle to produce HFO-1363pyf

unique in its avoidance of the hydrosilylation mechanism, implying that the oxidative addition of the Si-H bond at Ni(0) is too slow to compete with the olefin addition/β-elimination steps. The reaction may be done using NHC ligands or the aforementioned phosphine ligands. A survey of catalytic conditions was carried out and the results are shown in Table 4.Reactions were carried out on a scale of 0.2 ml of silane with 20 ml of HFO-1132a injected into a septum-capped vial.

TABLE 4: CATALYTIC CONVERSION OF HFO-1132A TO HFO-1363PYF

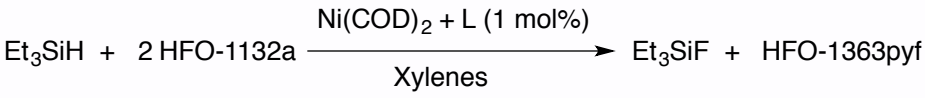

Ligand	Temp. (˚C)	Time (h)	Conversion (%)
IAd	***45***	***18***	***98***
ItBu	*45*	*18*	*50*
ItBu	*80*	*4*	*70*
ItBu	*110*	*1.5*	*85*
PCp_3	*45*	*18*	*90*

Future Work

With the current interest in HFOs in mind, it is desirable to design a process wherein 1363pyf may be prepared at least at a 100 gram scale, with an eventual 1 kg batch size as the ultimate goal. If such a venture is to be successful, a much less expensive catalyst is required. First, this means moving exclusively to phosphine ligands, as they are generally much more cheaply available, and their preparative methods (especially hydrophosphination) are generally higher yielding and more atom-efficient than NHC preparations. Second, an alternative source of nickel(0) must be devised, as $Ni(COD)_2$ is both too expensive and too unstable to be considered at scale (a 1 kg preparation of 1363pyf would demand > 20 grams of $Ni(COD)_2$). The current favorite candidate is bis(π-cinnamyl)nickel which (similarly to bis(π-allyl)nickel)) reductively couples upon addition of a ligand to give a 3-coordinate nickel(0) product.

Third, it is more desirable to carry out the reaction at a slightly higher temperature so as to complete the reaction faster as shown in Table 4; unfortunately, in medium highly concentrated in silane, the catalyst failure rate is high, possibly arising from the formation of Ni(II) hydrides which subsequently decompose to nickel black. To increase the lifetime of the nickel catalyst under these conditions, a system will be put into place to introduce the silane reagent gradually (*e.g.* a metering pressure pump). It is also hoped that through the rational design of phosphine ligands, a more rugged catalyst can be prepared. Finally, it is hoped that this chemistry can be extended to other C2-hydrofluoroolefins, and possibly C3-hydrofluoroolefins currently known in the literature.

Conclusions

In conclusion, the results presented in this text demonstrate that by using sterically hindered ligands and enforcing a low-coordination number at nickel, completely different reactivity can be exposed. This was exploited with the goal of advancing the organometallic chemistry of TFE and VDF, paving the way to higher-value products derived from said feedstocks beyond simple polymers and telomers. With TFE-derived metallacyclopentanes, going from a 4-coordinate system to a 3-coordinate system gave rise to a new ring-contraction and ring-opening; furthermore, the hydrogenation step originally devised for the 4-coordinate system was optimized to a much lower pressure of hydrogen. With vinylidene difluoride, the first metal-catalyzed hydrodefluorodimerization was developed based on a low-coordinate nickel species containing a bulky NHC ligand. The identity of the dimeric isolated product hints at a parent metallacycle, but also shows that if such an intermediate is operant, it is highly unstable and has yet to be observed. The findings in Part 2 demonstrate also the vast difference in reactivity between fully- and partially-fluorinated olefins, as such β-eliminations have yet to be observed for fully-fluorinated metallacycles. Vinylidene difluoride has been shown to follow a similar trend to trifluoroethylene, with β-elimination occurring spontaneously in the absence of exogenous Lewis acid. It differs from the former olefin mainly in that even in the presence of excess olefin and two equivalents of

phosphine, the 5-membered metallacycle fails to form, likely due to the lower coordination ability of the olefin. The trend thus demonstrates that through sequential removal of fluorine from the olefinic precursor, β-elimination becomes ever more favorable, and contrasts the reactivity of fully-fluorinated nickelacyclopentanes with the same Lewis acid as mentioned in Part 1.

Supplement A (Part 1)

Contents

General Procedures. Experiments were conducted under nitrogen, using Schlenk techniques or an MBraun glove box. All solvents were deoxygenated by purging with nitrogen. Toluene, hexanes, diethyl ether (DEE) and tetrahydrofuran (THF) were dried on columns of activated alumina using a J. C. Meyer (formerly Glass Contour®) solvent purification system. Benzene-d_6 (C_6D_6) was dried by stirring over activated alumina (ca. 10 wt. %) overnight, followed by filtration. Acetonitrile-d_3 (CD_3CN) was dried by refluxing over calcium hydride under nitrogen. After distillation, CD_3CN was further dried by stirring over activated alumina (ca. 5 wt. %) overnight, followed by filtration. All solvents were stored over activated (heated at ca. 250^{o}C for >10 h under vacuum) 4 Å molecular sieves. Glassware was oven-dried at 120 ^{o}C for >2 h. The following chemicals were obtained commercially, as indicated: trimethylsilyl trifluoromethanesulfonate (Me_3SiOTf, Aldrich, 99%), bis(1,5- cyclooctadiene)nickel (0) ($Ni(cod)_2$, Strem, 98+%), triisopropyl phosphite ($P(O^iPr)_3$, Aldrich, 95%), tri-ortho-tolyl phosphite (P(O-o-tolyl)3), Alfa Aesar, 97%), 1,3-bis(2,6-diisopropylphenyl)imidazolidin-2-ylidene (SIPr, Sigma- Aldrich) and 1,3-di-tert-butylimidazol-2-ylidene (ItBu, Sigma-Aldrich). Tetrafluoroethylene (TFE) was purchased from ABCR (99%) or made by pyrolysis of polytetrafluoroethylene (Scientific Polymer Products, powdered) under vacuum, using a slightly modified literature procedure [10-20 mTorr, 650 ^{o}C, 30 g scale, product stabilized with R(+)-limonene (Aldrich, 97%), giving TFE of ca. 97% purity][132]. Compound $Ni[P(O^iPr)_3]_2(C_4F_8)$ was made by oxidative addition of tetrafluoroethylene to $Ni[P(O^iPr)_3]_4$ using slightly modified literature procedures[133].

$Ni[P(O^iPr)_3]_4$ complex was prepared from $Ni(COD)_2$ following reported methods. Metallacycle $Ni(C_4F_8)[P(O\text{-}o\text{-}tolyl)_3]_2$ was prepared by addition of TFE to $Ni[P(O\text{-}o\text{-}tolyl)_3]_3$ using slightly modified literature procedures[134]. $Ni[P(O\text{-}^iPr)_3]_4$ complex was prepared from $Ni(COD)_2$ following reported methods. ^{1}H, ^{19}F, $^{31}P\{^{1}H\}$, and $^{13}C\{^{1}H\}$

NMR spectra were recorded on a 300 MHz Bruker Avance instrument at room-temperature (21-23 ^{o}C) unless stated otherwise. ^{1}H NMR spectra were referenced to residual proton peaks associated with the deuterated solvents (C_6D_6: 7.16 ppm; CD_3CN: 1.94 ppm). ^{19}F NMR spectra were referenced to internal 1,3-bis(trifluoromethyl)benzene (BTB) [unless stated otherwise] (Aldrich, 99%, deoxygenated by purging with nitrogen, stored over activated 4 Å molecular sieves), set to –63.5 ppm. $^{31}P\{^{1}H\}$ NMR data were referenced to external H_3PO_4 (85 % aqueous solution), set to 0.0 ppm. Electrospray ionization mass spectral data were collected using an Applied Biosystem API2000 triple quadrupole mass spectrometer. UV-vis spectra were recorded on a Cary 100 instrument, using sealable quartz cuvettes (1.0 cm pathlength). Elemental analyses were performed by Laboratoire d'analyse élémentaire, Université de Montréal. (Montreal, Quebec, Canada). Note that the NMR spectra (^{1}H, ^{19}F, $^{19}F\{^{1}H\}$, and $^{31}P\{^{1}H\}$ for the title compounds are displayed at the end of the Supporting Information (Figures S7-27).

X-ray Crystallography. Data collection results for complexes **2**, **3**, **3**•H_2O, **4a** and **5c** represent the best data sets obtained in several trials for each sample (Table S1 and Table S11). The crystals were mounted on thin glass fibers using paraffin oil. Prior to data collection crystals were cooled to 200 K. Data were collected on a Bruker AXS KAPPA single crystal diffractometer equipped with a sealed Mo tube source (wavelength 0.71073 Å) APEX II CCD detector. Raw data collection and processing were performed with APEX II software package from BRUKER AXS[135]. Diffraction data for all the samples were collected with a sequence of 0.5° ω scans at 0, 120, and 240° in ϕ. Initial unit cell parameters were determined from 60 data frames with 0.3° ω scan each, collected at the different sections of the Ewald sphere. Semi-empirical absorption corrections based on equivalent reflections were applied[136]. Systematic absences in the diffraction data set and unit-cell parameters were consistent with monoclinic $P2_1/c$ (No. 14) for complexes 2, 4a and 5c, and orthorhombic $P2_12_12_1$ (No. 19) for **3**. Solutions in the centrosymmetric space groups for complexes **2**, **4a** and **5c** yielded chemically

reasonable and computationally stable results of refinement. Data for the complex 3 suggested a non-centrosymmetric space group for the model refinement. The structures were solved by direct methods, completed with difference Fourier synthesis, and refined with full-matrix least-squares procedures based on F^2.

Refinement of the structural model for 2 revealed one target molecule located in general position. Similarly, the structure of 3 displayed only one molecule of interest located in the general position. In this case, however, final refinement numbers suggested the presence of racemic twinning in the crystal. In order to take twinning into consideration the default TWIN instruction was employed. After additional refinement cycles the BASF parameter was refined to 0.14413.

The structural model for complex 4a contains one target molecule and one fully occupied hexane solvent molecule in the lattice. The complex molecule is located in the general position and the hexane solvent molecule is located on the inversion center of the space group.

Diffraction data for the crystal of complex 5c were collected to 0.75Å resolution; however, due to small crystal size and weak diffraction it was discovered that both R(int) and R(sigma) exceeded 35% for the data below 1.00Å resolution. Based on R(sigma) value, data were truncated to 0.95Å resolution for refinement. The asymmetric unit for this crystallographic model of **5c** consists of one target complex molecule located in the general position. Refinement results for the compound 5c suggested the presence of two non-merohedrally twinned domains. Careful examination of the original data frames and reciprocal space diffraction pictures confirmed the initial twinning assumption. In order to find independent orientation matrices 3258 reflections were collected from 4 sets of 40 frames each in different sections of the Ewald sphere. Collected reflection data were processed with CELL_NOW software[137] and produced two independent orientation matrices. 2636 reflections out of the original array were assigned exclusively to the first domain and 1521 (330 exclusively) reflections were assigned to the second domain. The data set was re-integrated with two independent orientation matrices,

treated for twinning absorption corrections and consecutive model refinement was performed using HKLF5 reflection data file. Twinning domain ratio coefficient (BASF) was refined to 0.1115.

For all the compounds hydrogen atoms positions were calculated based on the geometry of related non-hydrogen atoms. All hydrogen atoms were treated as idealized contributions during the refinement. All scattering factors are contained in several versions of the SHELXTL program library, with the latest version used being v.6.12.[138] Metrical data for **2**, **3**, **3**•H_2O, **4a** and **5c** are presented in Table S1and S11, and the CCDC files 968465 (2), 968466 (3), S6 968467 (**4a**), 1028645 (**5c**) and 1412522 (**3**•H_2O) contain the supplementary crystallographic data. These can be obtained free of charge from the Cambridge Crystallographic Data Centre via www.ccdc.cam.ac.uk/data_request/cif.

Computational Methods. Density Functional Theory (DFT) calculations were performed for each structure using the Gaussian 09 package. Geometry optimization at the B3LYP/TZVP level of theory (with and without the empirical dispersion correction GD3 of Grimme) was performed using the molecular structure of 3 from the X-ray diffraction experiment as a starting point. Harmonic frequency calculations were used to characterize the stationary points obtained during the geometry optimization. Tight SCF convergence was used in each calculation. Mulliken population analysis (MPA)-compositions of molecular orbitals, and 2- and 3-center Mayer bond orders were calculated using the AOMix package (www.sg-chem.net). Optimized structure coordinates are presented in Tables S7-10.

Computational Methods. Density Functional Theory (DFT) calculations were performed for each structure using the Gaussian 09 package. Geometry optimization at the B3LYP/TZVP level of theory (with and without the empirical dispersion correction GD3 of Grimme) was performed using the molecular structure of 3 from the X-ray diffraction experiment as a starting point. Harmonic frequency calculations were used to

characterize the stationary points obtained during the geometry optimization. Tight SCF convergence was used in each calculation. Mulliken population analysis (MPA)-compositions of molecular orbitals, and 2- and 3-center Mayer bond orders were calculated using the AOMix package (www.sg-chem.net). Optimized structure coordinates are presented in Tables S7-10.

Experimental

Synthesis of Ni[κ²-(CF₂)$-](ItBu)[P(OⁱPr)₃] (2). Yellow complex Ni[κ²-$(CF_2)_4$-][$P(O^iPr)_3$]₂ (**1a**) (0.100 g, 0.15 mmol) was placed in a 15 mL scintillation vial and dissolved in ~7 mL of toluene. Colorless [ItBu] (29 mg, 0.16 mmol) was then added to the mixture and left to sit at 25 °C for ~24 hours. Large yellow block crystals suitable for X-ray analysis formed. They were filtered off (30 mL medium pore fritted funnel), washed with pre-cooled hexanes (4 °C, 3 x 3 mL), and dried in vacuo to yield 85 mg of 2 (0.13 mmol, 89 % based on Ni[κ²-$(CF_2)_4$-][$P(O^iPr)_3$]₂). The isolated material was stored at room temperature under nitrogen. UV-vis (1.0 mM in THF): $\lambda_{max}(\varepsilon)$ = 322(341). ^{1}H NMR (300 MHz, CD_3CN) δ 1.19 (d, J ≈ 6 Hz, 18H, MeiPr) 1.94 (s, 18H, MetBu), 4.65 (sept, m, J ≈ 6 Hz, 3H, iPr H) 7.34 (s, 2H, CHIm). 19F NMR (282 MHz, CD3CN) δ -100.50 (d ‘quint’, 3JFP = 31, 3JFF ≈ 4JFF = 6 Hz, 2Fα), -102.93 (d ‘quint’, 3JFP = 33, 3JFF ≈ 4JFF = 4 Hz, 2Fα), -137.03, -138.54 (mult, 2Fβ). 31P{1H} NMR (121 MHz, CD3CN) 115.8 ppm (‘quint’ ‘tr’, 3JPF ≈ 32, 4JPF ≈ 7 Hz). Anal. Calc. for C24H41F8N2NiO3P: C, 44.54, H, 6.39, N, 4.33. Found: C, 44.54, H, 6.53, N, 4.28. See Figures S7-9 for 1H, 19F, 31P{1H} NMR spectra.

Synthesis of Ni[κ²-$(CF_2)_4$-](SIPr) (3). Yellow complex Ni[κ²-$(CF_2)_4$-][$P((O\text{-}o\text{-}tol)]_3$]₂ (**1b**) (1.00 g, 1.04 mmol) was placed in a 20 mL scintillation vial and dissolved in ~ 10 mL of benzene. Colorless [SIPr] (446 mg, 1.14 mmol) then added to the stirred mixture and the mixture heated at 35 °C for ~24 hours. The resulting deep red solution was concentrated in vacuo to a thick paste with some red precipitate. Hexanes (15 mL) were

then added to precipitate the product which was subsequently filtered (30 mL medium pore fritted funnel), washed with pre-cooled hexanes (4 °C, 3 x 5 mL), and dried in vacuo, affording 3 as a light red powder. Yield: 506 mg (0.78 mmol, 75 % based on Ni[κ^2-$(CF_2)_4$-][$P(O\text{-}o\text{-}tol)_3]_2$. The isolated material was stored at room temperature under nitrogen. UV-vis (1.5 mM in benzene): $\lambda_{max}(\varepsilon)$ = 486(461). 1H NMR (300 MHz, C6D6) δ 1.09 (d, J ≈ 6 Hz, 12H, 4 Me), 1.68 (d, J ≈ 6 Hz, 12H, 4 Me), 3.04 (sept, J ≈ 6 Hz, 4H, 4 iPr H), 3.13 (s, 4H, 2 CH2Im), 7.00-7.30 (mult, 6H, 6 Ar-H). 13C{1H} NMR (75 MHz, C6D6) δ 24.78, 24.96, 29.40, 53.50, 125.63, 127-129, 129.57, 131.26, 147.67. 19F NMR (282 MHz, C6D6, 25 °C) δ -101.90 (s, 4Fα), -138.63 (s, 4Fβ). 19F NMR (282 MHz, CD2Cl2, -50 °C) δ -99.32 (s, 2F'α), -103.07 (br s, 4Fα), -119.17 (s, 2F'α), -138.37 (s, 2F'β), -139.64 (br s, 4Fβ), -141.21 (s, 2F'β). Anal. Calc. for C31H38F8N2Ni: C, 57.34, H, 5.90, N, 4.31. Found: C, 56.22, H, 6.18, N, 4.17 (These values reflect those expected for the water adduct **3**•H2O Anal. Calc. for C31H40F8N2NiO: C, 55.79, H, 6.04, N, 4.20. See below: Figure 34, Table S11- 12) See Figures S10-12 for the 1H, 13C{1H} and 19F NMR spectra.

Synthesis of Ni[κ^1-(cyclo-C_4F_7)](SIPr)(OTf) (4a). Red complex Ni[κ^2-$(CF_2)_4$-](SIPr) (**3**) (0.100 g, 0.15 mmol) was placed in a 15 mL scintillation vial and dissolved in ~ 7 mL of benzene. Me3SiOTf (42 µL, 0.23 mmol) was added to the stirred mixture and left to stir at room temperature for ~24 hours. (N.B. Product 4 is unstable under these reaction conditions for prolonged periods of time, reaction times longer than 24 hours will lead to the formation of perfluorocyclobutene in the reaction medium). The deep pink solution was concentrated in vacuo and the resulting pink powder **4a** was washed with pre-cooled hexanes (4 °C, 3 x 5 mL) and dried in vacuo. Yield: 0.108 g, 0.14 mmol, 90 % based on Ni[κ^2-$(CF_2)_4$-](SIPr). The isolated material was stored at room temperature under nitrogen. UV-vis (1.0 mM in benzene): $\lambda_{max}(\varepsilon)$ = 503(218), 332(312). 1H NMR (300 MHz, C6D6) δ 1.04 (d, J = 7 Hz, 12H, 4 Me), 1.60 (br d, J ≈ 5 Hz, 6H, 2 Me), 1.71 (br, 6H, 2 Me) 3.2 (br ov mult, 6H, 4 iPr H + 2 CH2Im), 3.4 (br mult, 2H, CH2Im), 6.5-7.8 (mult, 6H, 6 Ar-H). 13C{1H} NMR (75 MHz, C6D6) δ 24.78, 24.96, 28.53, 28.87, 53.37, 124.3-125, 130.02, 133.96, 146.89.19F NMR (282 MHz, C6D6) δ -77.60 (s,

CF3), -110.01 (br d, $^2J_{FF}$ ≈ 228 Hz, 2Fβ), -123.75 (d, $^2J_{FF}$ = 229 Hz, 1Fβ), -123.79 (d, 2JFF = 229 Hz, 1Fβ) -129.80 (d mult, ^{2}JFF = 222 Hz, Fγ), -131.59 (d, $^2J_{FF}$ = 222 Hz, Fγ), -197.74 (br s, Fα). 19F NMR (282 MHz, CD2Cl2, -50 °C) δ -78.93 (s, CF3), -109.27 (d mult, $^2J_{FF}$ ≈ 227 Hz, 1Fβ), -112.22 (d mult, ^{2}JFF ≈ 231 Hz, 1Fβ), -124.18 (d, $^2J_{FF}$ = 227 Hz, 1Fβ), -124.26 (d, $^2J_{FF}$ = 231 Hz, 1Fβ) -129.80 (d mult, $^2J_{FF}$ = 222 Hz, Fγ), -131.59 (d, $^2J_{FF}$ = 222 Hz, Fγ), -197.74 (br s, Fα). Anal. Calc. for $C_{32}H_{38}F_{10}N_2NiO_3S$: C, 49.31, H, 4.91, N, 3.59, S, 4.11. (These values reflect those expected for the water adduct Anal. Calc. for C32H40F10N2NiO4S: C, 48.20, H, 5.06, N, 3.51, S, 4.02.) Found: C, 47.53, H, 5.05, N, 2.76, S, 4.21. See Figures S13-15 for the 1H, 13C{1H} and 19F NMR spectra.

^{19}F NMR spectrum of intermediate leading to 4a, Ni[κ^3-$(CF_2)_3$CF(OTf)-](SIPr) (**5a**): ^{19}F NMR (282 MHz, Tol- d_8, -35 °C) δ -73.27 (d, $^5J_{FF}$ = 11 Hz, CF_3[OTf]), -83.98 (d mult, $^2J_{FF}$ = 225 Hz, Fα), -99.73 (d mult, $^2J_{FF}$ = 225 Hz, Fα), -106.29 (br mult, Fα), -127.11 (d mult, $^2J_{FF}$ = 246 Hz, Fβ), -129.23 (d mult, 2JFF = 246, Fβ), -137.07 (d mult, $^2J_{FF}$ = 246 Hz, Fβ), -144.71 (d mult, $^2J_{FF}$ = 246, Fβ).

Synthesis of Ni[κ^3-$(CF_2)_3$CF(O_2CCF_3)-](SIPr) (5b). Red complex Ni[$κ_2$-$(CF_2)_4$-](SIPr) (**3**) (50 mg, 0.08 mmol) was placed in a 20 mL scintillation vial and dissolved in ~ 7 mL of benzene. Trifluoroacetic acid (7 µL, 0.085 mmol) was added to the stirred mixture (reaction should not be attempted in toluene) and left to stir at 25 °C for 10 minutes. The fluorescent yellow solution was concentrated in vacuo until a thick paste with some light yellow precipitate was remaining. Cold hexanes (4 °C, 3 x 5 mL) were added and decanted off to wash. The resulting product was dried in vacuo, affording 5b as a light yellow powder. Yield: 47 mg (0.06 mmol, 82 % based on Ni[κ^2- $(CF_2)_4$-](SIPr). The isolated material was stored at room temperature under nitrogen. UV-vis (1.5 mM in benzene): λmax(ε) = 486(461). ^{1}H NMR (300 MHz, C6D6) δ 1.05 (ov d, J ≈ 6 Hz, 12H, 4 Me), 1.36 (d, J ≈ 6 Hz, 6H, 2 Me), 1.47 (br, 6H, 2 Me), 3.19 (br, ov mult, 3H, 3 iPr H),

3.37 (br, ov mult, 5H, i-Pr H + 2 CH2Im), 6.80-7.06 (mult, 6H, 6 Ar-H). $^{13}C\{^{1}H\}$ NMR (75 MHz, C6D6) δ 22.66, 22.82, 26.17, 26.28, 28.41, 53.89, 124.20, 124.39, 127-129, 129.33, 146.57. 19F NMR (282 MHz, C6D6, 25 °C) δ -72.97 (s, CF3), -90.06 (d mult, ^{3}JFF = 245 Hz, 1Fα), -99.09 (d mult, $^{3}J_{FF}$ = 245 Hz, 1Fα), -116.17 (d d, $^{3}J_{FF}$ = 22, 11 Hz, 1Fα), -126.14 (d mult, $^{3}J_{FF}$ = 248 Hz, 1F, 1 CβF2), -130.76 (d d mult, $^{3}J_{FF}$ = 248, 22 Hz, 1Fβ), -134.17 (d mult, 3J_{FF} = 248 Hz, 1Fβ), -142.71 (d d mult, $^{3}J_{FF}$ = 248, 11 Hz, 1Fβ). Anal. Calc. for C33H38F10N2NiO2: C, 53.32, H, 5.15, N, 3.77. Found: C, 53.15, H, 6.01, N, 3.87. See Figures S16-18 for the 1H, 13C{1H} and 19F NMR spectra.

Synthesis of Ni[κ3-(CF2)3CF(O2CCH3)-](SIPr) (5c). Red complex Ni[κ^2-$(CF_2)_4$-](SIPr) (**3**) (50 mg, 0.08 mmol) was placed in a 20 mL scintillation vial and dissolved in ~ 7 mL of toluene. Acetic acid (5 µL, 0.085 mmol) was added to the stirred mixture and left to stir at 25 °C for 24 hours. The deep yellow solution was concentrated in vacuo (~ 1 mL). 5 mL of hexanes was added and the product was crystallized (-20 °C). The supernatant was decanted and the yellow crystals of 5c were washed with hexanes (2 x 5 mL) and dried in vacuo. Yield: 20 mg, 0.063 mmol, 38 % based on Ni[κ^2-$(CF_2)_4$-](SIPr). The isolated material was stored at room temperature under nitrogen. UV-vis (1.0 mM in benzene): $\lambda_{max}(\varepsilon)$ = 632 (361); 103 (485). ^{1}H NMR (300 MHz, C6D6) δ 1.05 (ov d, J ≈ 6 Hz, 12H, 4 Me), 1.36 (d, J ≈ 6 Hz, 6H, 2 Me), 1.47 (br, 6H, 2 Me), 3.19 (br, 4H, 4 iPr H), 3.37 (br, 4H, 2 CH2Im), 6.80-7.06 (m, 6H, 6 Ar-H). $^{13}C\{^{1}H\}$ NMR (75 MHz, C6D6) δ 22.66, 22.82, 26.17, 26.28, 28.41, 53.89, 124.20, 124.39, 27-129, 129.33, 146.57. 19F NMR (282 MHz, C6D6, 25 °C) δ -91.23(d mult, $^{2}J_{FF}$ = 253 Hz, Fα) , -101.86 (d mult, $^{2}J_{FF}$ = 253 Hz, Fα), -119.78 (d d, $^{3}J_{FF}$ = 17, 15 Hz, Fα), -126.35 (d mult, $^{2}J_{FF}$ = 247 Hz, Fβ), -130.90 (d d mult, $^{2}J_{FF}$ = 247, $^{3}J_{FF}$ = 15 Hz, Fβ), -135.10 (d mult, $^{2}J_{FF}$ = 248 Hz, Fβ), -143.33 (d d, $^{2}J_{FF}$ = 248, $^{3}J_{FF}$ = 17 Hz, Fβ), Anal. Calc. for $C_{34}H_{43}F_7N_2NiO_2$: C, 57.49, H, 6.16, N, 3.98. Found: C, 57.05, H, 6.21, N, 4.11. See Figures S19-21 for the 1H, 13C{1H} and 19F NMR spectra.

Synthesis of Ni[κ¹-(C_4F_8H)](SIPr)(OAc) (6a). Red complex Ni[κ²-(CF_2)$_4$-](SIPr) (**3**) (50 mg, 0.08 mmol) was placed in a 20 mL scintillation vial and dissolved in ~ 7 mL of toluene. Acetic acid (5 µL, 0.085 mmol) was added to the mixture and left to stir at 25 °C for 24 hours. The deep yellow solution was concentrated in vacuo to ca. 1 mL, 5 mL of hexanes were added and the product allowed to crystallize at -20 °C. The supernatant was decanted, concentrated and filtered through a short silica column (eluent: benzene), the first yellow band was collected. The volatiles were removed in vacuo. Yield of 6c: 25 mg (0.035 mmol, 45 % based on Ni[κ²-(CF_2)$_4$-](SIPr). UV-vis (1.0 mM in benzene): λmax(ε) = 296(343) ;427(494). 1H NMR (300 MHz, C6D6) δ 1.01 (s, 3H, 1 Me), 1.05 (d, J ≈ 7 Hz, 6H, 2 Me), 1.07 (d, J ≈ 7 Hz, 6H, 2 Me), 1.55 (d, J ≈ 7 Hz, 6H, 2 Me), 1.55 (d, J ≈ 7Hz, 6H, 2 Me), 3.13 (sept, J ≈ 7 Hz, 1H, 1 iPr H), 3.20 (sept, J ≈ 7 Hz, 1H, 1 iPr H), 3.21 (s, 2H, 1 CH2Im), 3.42 (sept, J ≈ 7 Hz, 1H, 1 iPr H), 3.45 (sept, J ≈ 7 Hz, 1H, iPr H), 3.48 (s, 2H, 1 CH2Im), 5.65 (tr tr, 2JFH = 53 Hz, $^3J_{FH}$ = 6 Hz, 1H, CF2H), 6.90-7.75 (mult, 6H, 6 Ar-H). 13C{1H} NMR (75 MHz, C6D6) δ 21.73, 22.73, 23.04, 26.43, 26.66, 28.33, 28.63, 53.57, 124.22, 124.64, 129.53, 135.29, 147.06, 147.56, 191.30; 19F NMR (282 MHz, C6D6) δ -95.90 (br tr, $^3J_{FF}$ = 9 Hz, Fα), -120.47 (br tr, $^3J_{FF}$ = 7 Hz, 2Fβ), -130.98 (br d mult, $^3J_{FH}$ = 6 Hz, 2Fγ), -137.99 (br d mult, $^2J_{FH}$ = 52 Hz, 2Fδ); m/z calcd for {Ni[κ¹-(C_4F_7H)](SIPr)(OAc)]}K+ (% intensity), 747.2 (100), 748.2 (36), 749.2 (46), 749.2(6.8) 751.2 (20), 752.2(3), 753.2 (2); m/z found, 747.3 (100), 748.3 (36), 749.2 (50), 751.2 (19), 752.2(3), 753.2 (1); See Figures S22- 24 for the 1H, 13C{1H} and 19F NMR spectra.

Synthesis of Ni[κ¹-(C_4F_8H)](SIPr)(O_2Cmes)] (6b). Red complex Ni[κ²-(CF_2)$_4$-](SIPr) (**3**) (50 mg, 0.08 mmol) was placed in a 20 mL scintillation vial and dissolved in ~ 7 mL of toluene. 2,4,6-trimethylbenzoic acid (14 mg, 0.085 mmol) was added to the stirred mixture and left to stir at 25 °C for 24 hours. The deep yellow solution was concentrated in vacuo to 1 mL, 5 mL of hexanes were added and the product allowed to crystallize at -20 °C. The supernatant was decanted and the crystals were washed with hexanes (2 x 5 mL). Yield of 6d: 48 mg (0.06 mmol, 77 % based on Ni[κ2-(CF2)4-](SIPr). UV-vis (1.5 mM in benzene): λmax(ε) = 486(461). 1H NMR (300 MHz, C6D6) δ 0.95 (d, J ≈ 7 Hz,

6H, 2Me), 1.04 (d, J ≈ 7 Hz, 6H, 2 Me), 1.07 (d, J ≈ 7 Hz, 6H, 2 Me), 1.51 (d, J ≈ 7Hz, 6H, 2 Me), 1.56 (d, J ≈ 7 Hz, 6H, 2 Me), 1.78 (s, 3H, MeAr), 1.94 (s, 6H, 2 MeAr), 3.09 (s, 2H, CH2Im), 3.12 (sept, J ≈ 7 Hz, 2H, 1 iPr H), 3. (sept, J ≈ 7 Hz, 1H, iPr H), 3.40 (s, 2H, 1 CH2Im), 3.54 (sept, J ≈ 7 Hz, 1H, 1 iPr H), 5.65 (tr tr, 2JFH ≈ 52 Hz, 3JFH ≈ 6 Hz, 1H, CF2H), 6.34 (mult, 2H, Ar H), 7-7.20 (mult, 6H, 6 Ar-H). 13C{1H} NMR (75 MHz, C6D6) δ 19.52, 20.62, 23.05, 23.44, 26.15, 26.56, 28.39, 28.80, 53.85, 124.52, 124.70, 129.38, 134.94, 135.62, 138.55, 146.61, 147.46, 189.86. 19F NMR (282 MHz, C6D6) δ -95.90 (br tr, 3JFF = 8 Hz, 2Fα), -120.80 (br tr, 3JFF = 8 Hz, 2Fβ), -130.99 (d mult, $^{3}J_{FH}$ = 6 Hz, 2Fγ), -138.68 (br mult, $^{2}J_{FH}$ ≈ 52 Hz, 2Fδ); m/z calcd for {[Ni[κ^{1}- (C_4F_7H)](SIPr)(OAr)]}K+ (% intensity), 851.3 (100), 852.3 (45), 853.3 (46), 853.3(10), 854.3(22), 855.3 (9), 856.3(4), 857.3 (2); m/z found, 851.4 (100), 852.3 (46), 853.4(49), 854.3 (22), 855.41(10), 856.3 (4), 857.3 (2); See Figures S25-27 for the 1H, 13C{1H} and 19F NMR spectra.

^{19}F NMR spectrum of minor product, Ni[κ^{3}-(CF_2)$_3$CF(O_2Cmes)-](SIPr) (**5d**): ^{19}F NMR (282 MHz, C6D6, 25 °C) δ -91.22 (d mult, $^{2}J_{FF}$ = 254 Hz, Fα), -101.86 (d mult, $^{2}J_{FF}$ = 254 Hz, Fα), -119.74 (d d, $^{3}J_{FF}$ = 17, 15 Hz, Fα), -126.25 (d mult, $^{2}J_{FF}$ = 245 Hz, Fβ), -130.80 (d d mult, $^{2}J_{FF}$ = 245, $^{3}J_{FF}$ = 17 Hz, Fβ), -135.05 (d mult, 2JFF = 248 Hz, Fβ), -143.27 (d d, $^{2}J_{FF}$ = 248, $^{3}J_{FF}$ = 15 Hz, Fβ).

Variable-temperature 19F NMR spectra of reaction intermediates leading to 4a:

Red complex Ni[κ^{2}-(CF_2)$_4$-](SIPr) (**3**) (10 mg, 0.015 mmol) was dissolved in 0.5 mL of CD_2Cl_2 in a screw cap NMR tube. The solution was precooled to 193 K and then placed in the NMR probe cooled to 223 K and a ^{19}F NMR spectrum was obtained (Figure S3) after 5 minutes to allow for temperature equilibration. The low temperature 19F NMR, clearly indicates no decoalescence of signals associated with 3, this indicates the presence of low energy processes which are consistent with our calculations. However, four new signals develop at this temperature, which may indicate interference and the

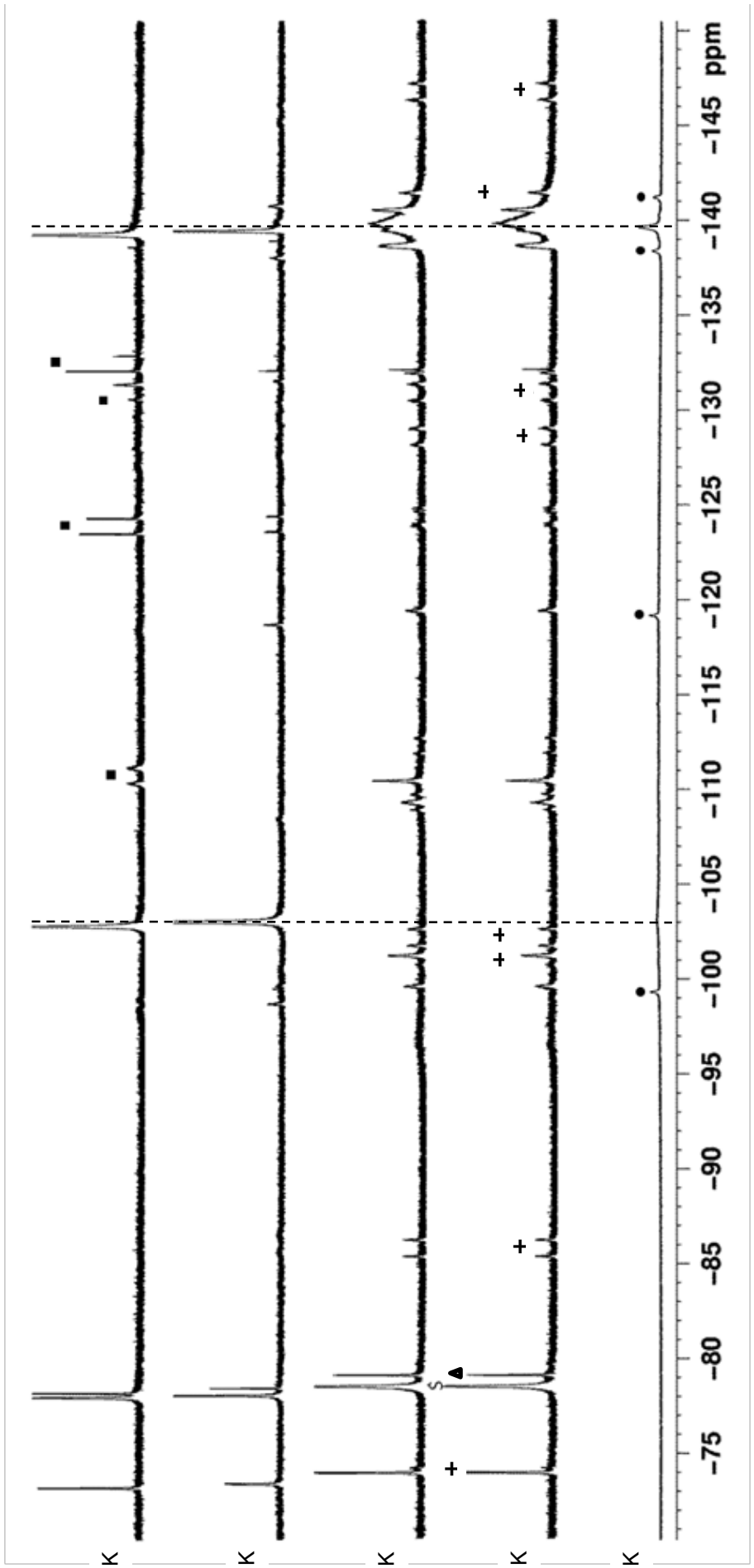

Figure S1. Low-temperature ^{19}F NMR spectra (282 MHz, CD_2Cl_2) of intermediate **5a** generation leading to product **4a**. Addition time is 0 (**a**), 30 min (**b**), 2 hours (**c**) and 3hours (**d**). Spectrum **e** was recorded after one hour additional reaction time at room temperature. The dashed line represents the trace of **3** across all reactions [223 K ^{19}F NMR spectra (282, CD_2Cl_2), provided below]. "$" is TMSOTf, " ▲ " is impurity present in TMSOTf, "●" is impurity at low temperature, "+" is **5a** and "■" is **4a** [223 K 19F NMR spectra (282 MHz, CD_2Cl_2), provided below]. Due to experimental limitations, the impurities are most likely due to water contamination.

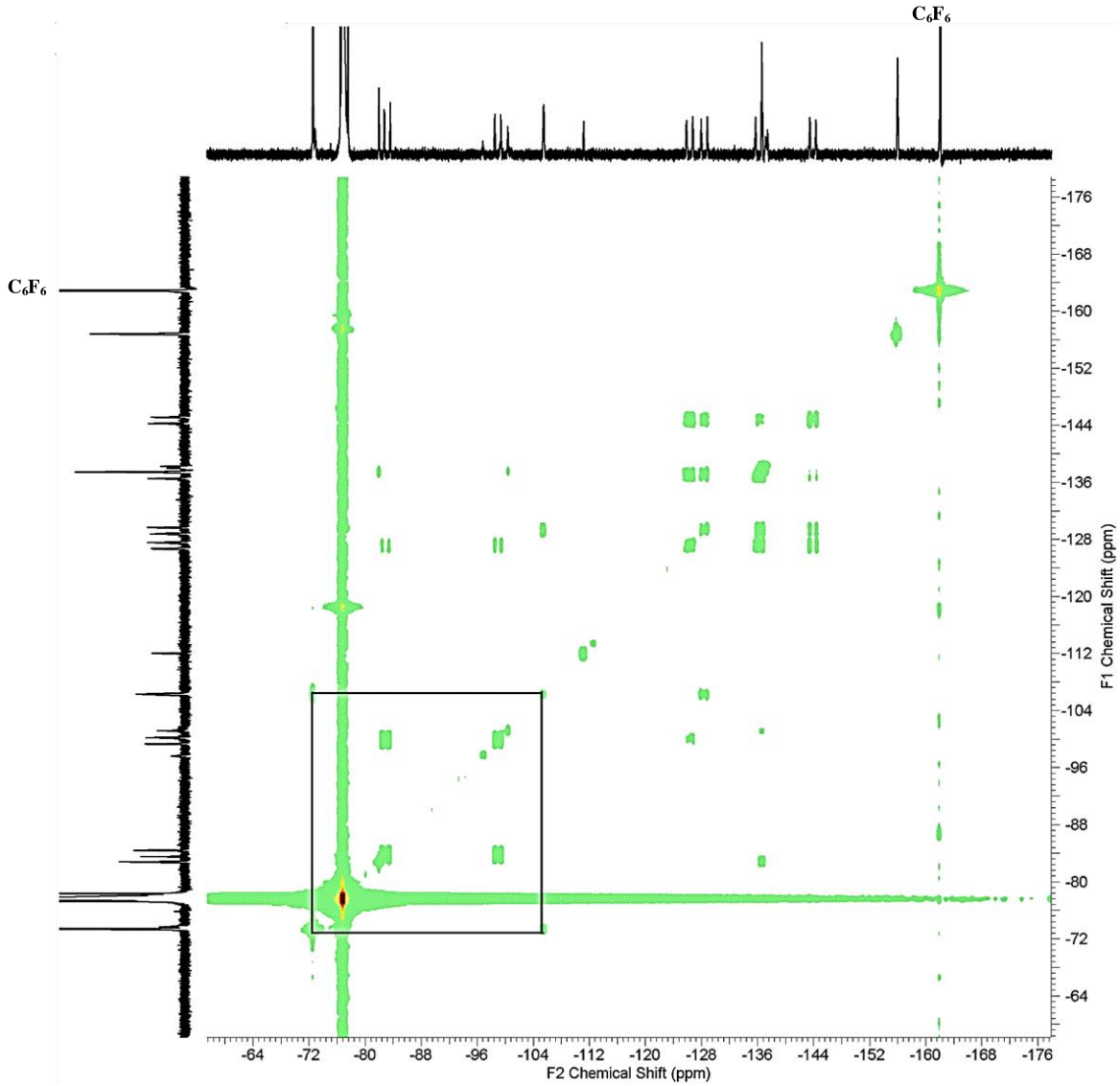

Figure S2. ^{19}F-^{19}F COSY NMR (282 MHz, Tol-d_8, 223 K) data for **5a**. Black box denotes through bond correlation of F (OTf) and F (C_α), $^5J_{FF}$ = 11 Hz Hexafluorobenzene (C_6F_6) was used as an internal NMR standard

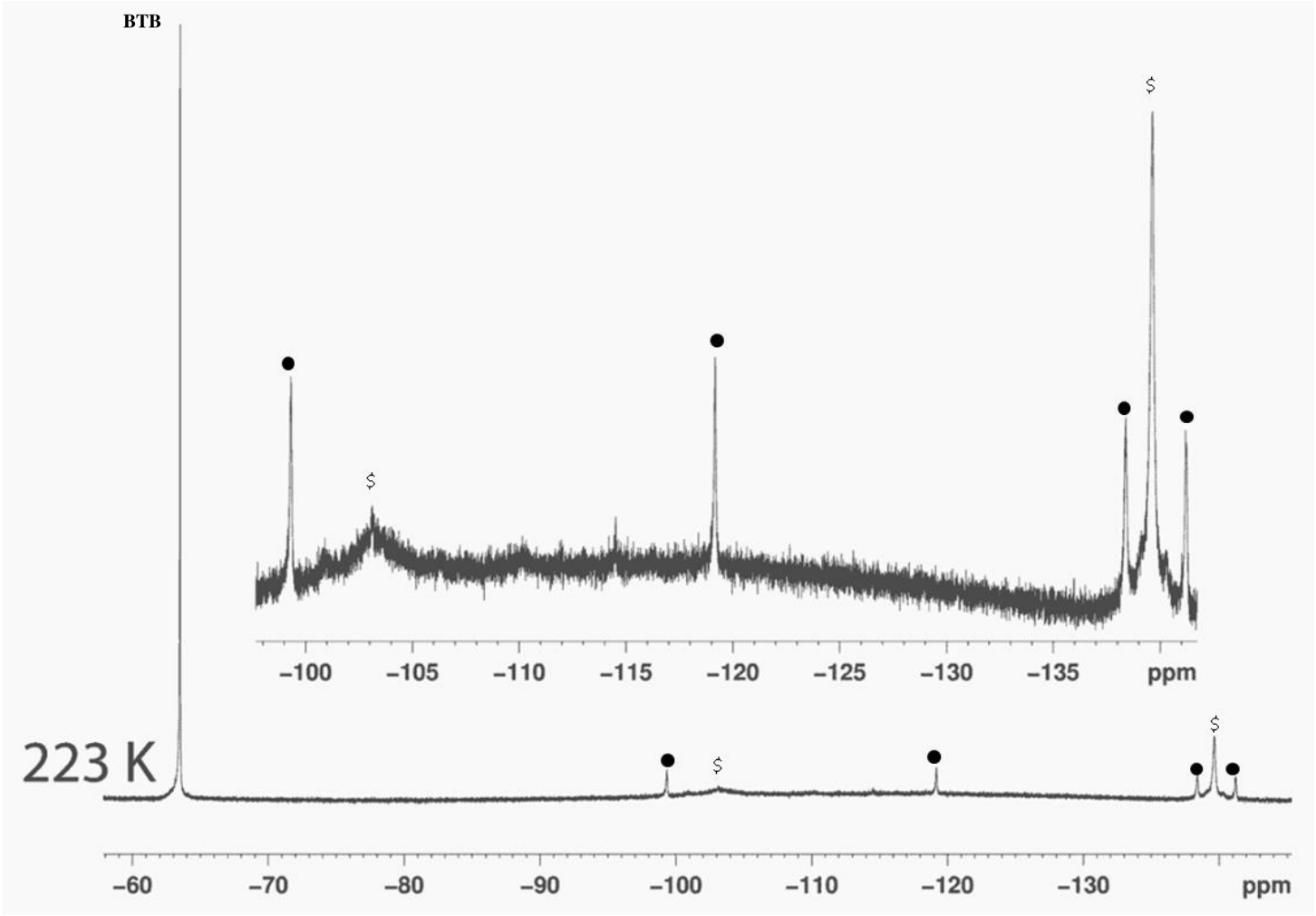

9

Figure S3. Low-temperature ^{19}F NMR spectrum (282 MHz, CD_2Cl_2, 223 K) of **3**. 1,3-Bis(trifluoromethyl)benzene (BTB) was used as an internal NMR standard. "$" = **3**, "●" = impurity.

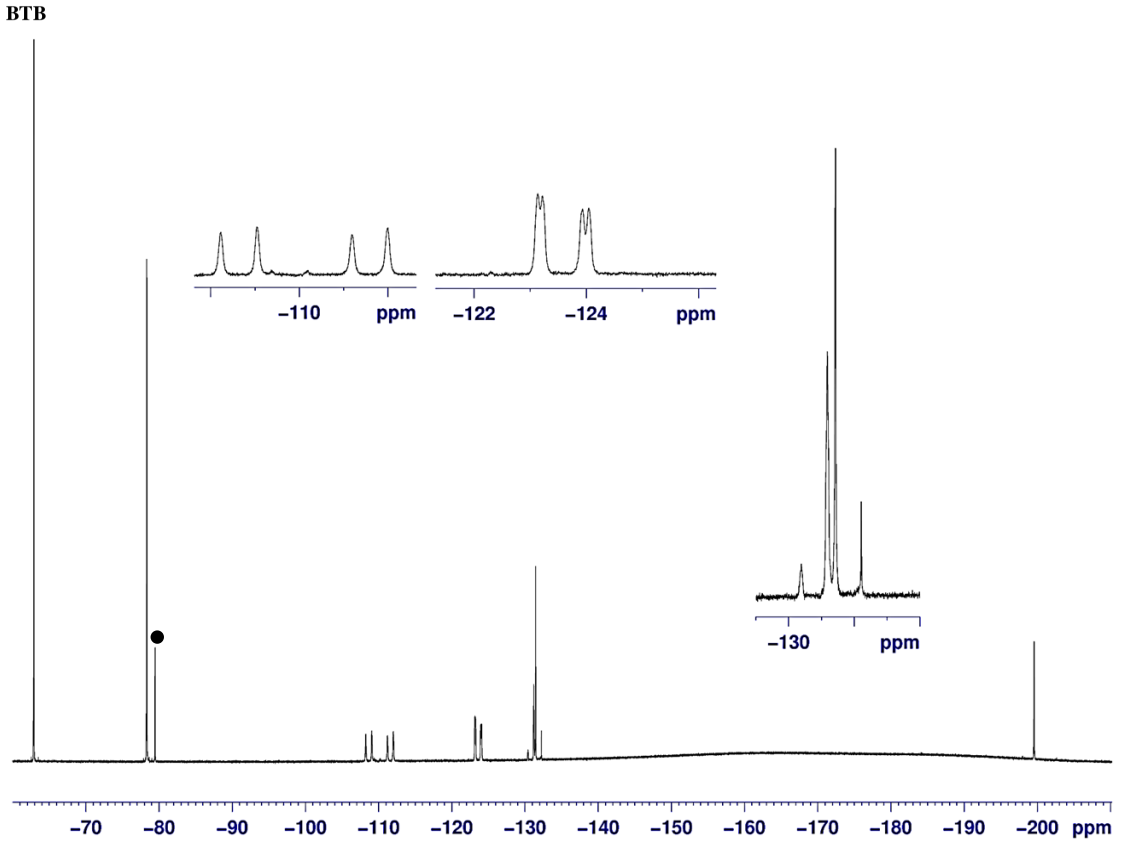

Figure S4. Low temperature ^{19}F NMR spectra (282 MHz, CD_2Cl_2) of **4**. 1,3-Bis(trifluoromethyl)benzene (BTB) was used as an internal NMR standard. "●" = OTf impurity.

formation of a new product possibly involving trace water coordination. The sample was removed from the probe and recooled to 193K. A pre-prepared solution of TMSOTf (4 μL, 0.023 mmol) in 0.5 mL of CD_2Cl_2 was injected into the NMR tube. The NMR tube was then placed in the NMR probe. The probe was cooled to 223 K and the 19F NMR spectrum was obtained (Figure S1) after 5 minutes to allow for temperature equilibration. The sample was warmed to 253 K and low temperature 19F NMR spectra were acquired at 30 min, 2 hours and 3 hours corresponding to Figures S1 a-d respectively. It is noted that a distinct intermediate possessing 19F NMR signals similar to those observed for **5b**, **c** is present in solution already after 5 minutes. However, the intermediate quickly dissipates even at low temperature after only 2 hours. After warming to room temperature, the intermediate is no longer present.

Decomposition of 4a:

Pink complex Ni[κ^1-(*cyclo*-C_4F_7)](SIPr)(OTf) (**4a**) (15 mg, 0.02 mmol) was dissolved in 0.5 ml of C_6D_6 in a J. Young NMR tube. The solvent-containing part of the tube was heated to 80˚C for 24 hours. ^{19}F NMR Yield of PFCB: 21%. We expect the discrepancy arises from the volatility of the PFCB. **Note: upon addition of PPh_3 to the reaction mixture [after heating], PPh_3F_2 was identified as a major product, suggesting formation of a Ni-F thermolysis byproduct.**

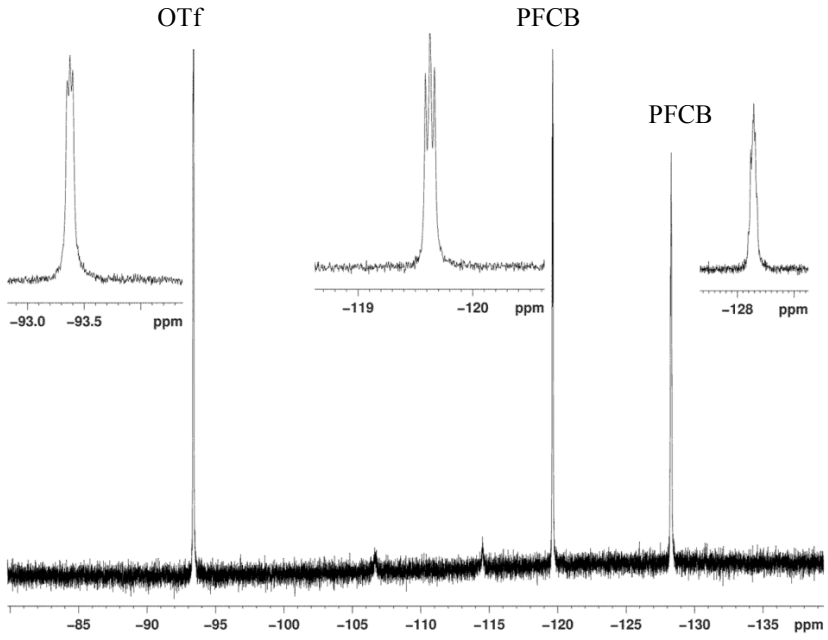

Figure S5. ^{19}F NMR spectrum (282 MHz, C_6D_6) after decomposition of **4a** to give perfluorocyclobutene (PFCB).

Product distributions of reactions with Brønsted Acids:

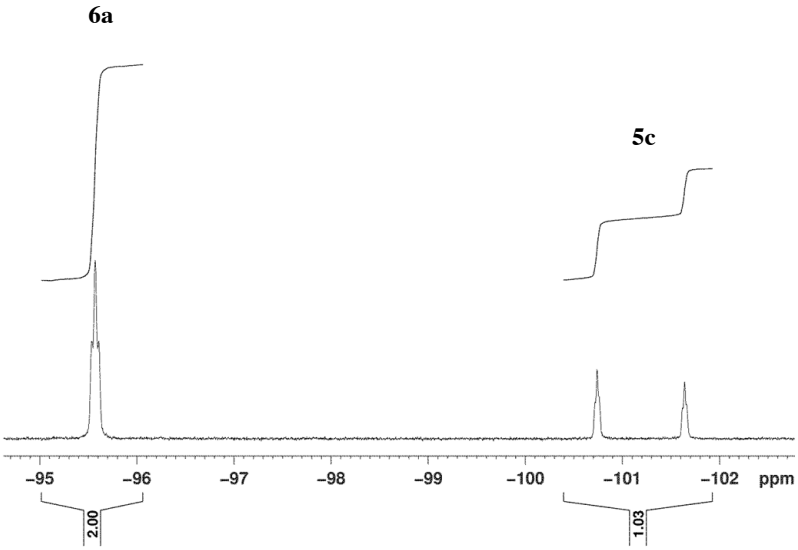

Figure S6. F_α region of ^{19}F NMR spectrum (282 MHz, C_6D_6) of reaction of **3** with acetic acid showing formation o **5c** and **6a** in a 1:1 ratio.

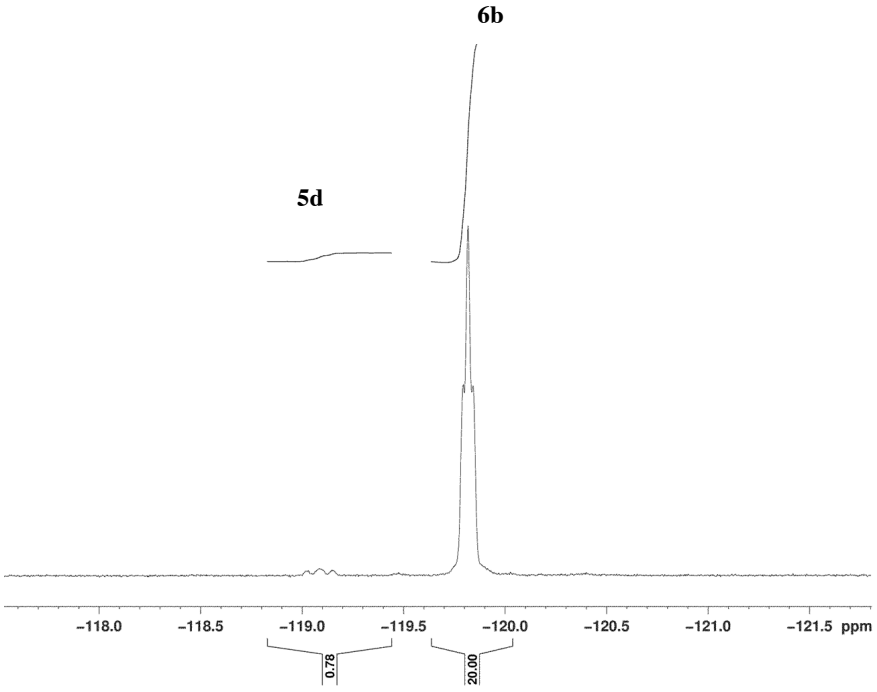

Figure S7. F_α region of ^{19}F NMR spectrum (282 MHz, C_6D_6) of reaction of **3** with 2,4,6–trimethylbenzoic acid t yield **5d** and **6b** in a 1:10 ratio.

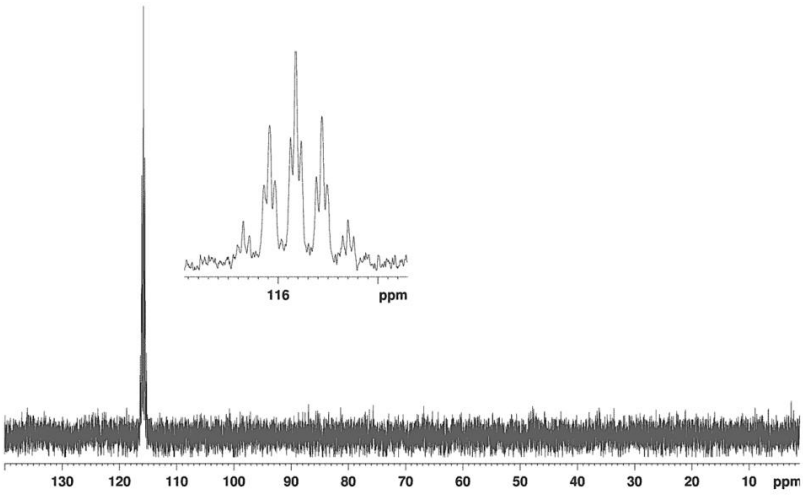

Figure S10. $^{31}P\{^{1}H\}$ NMR spectrum (121 MHz, C_6D_6) of **2**. The inset shows the expanded (horizontal scale) signal.

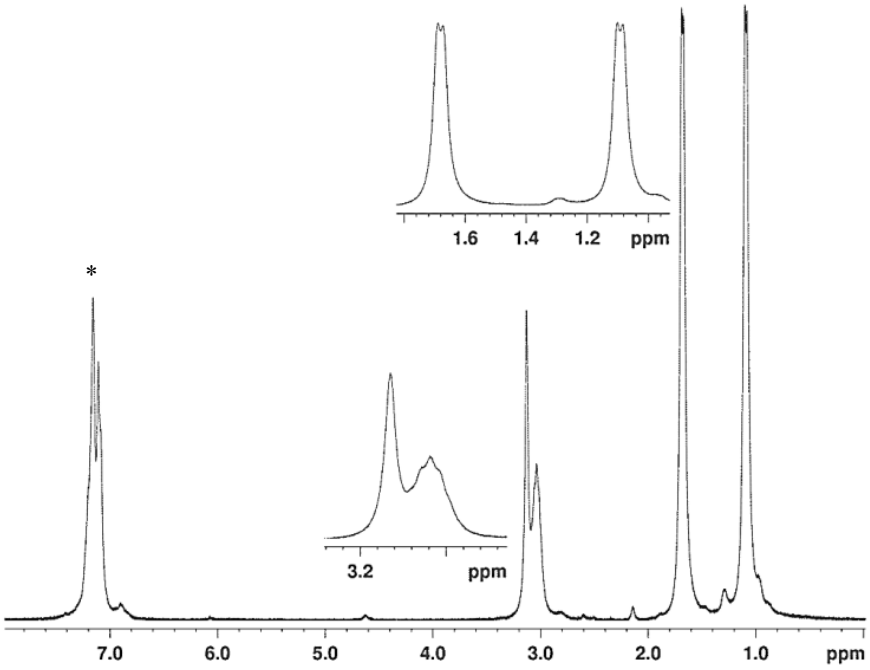

Figure S11. ^{1}H NMR spectrum (300 MHz, C_6D_6) of **3**. The residual protio-solvent peak is labeled '*'. The inset shows the expanded (horizontal scale) signal.

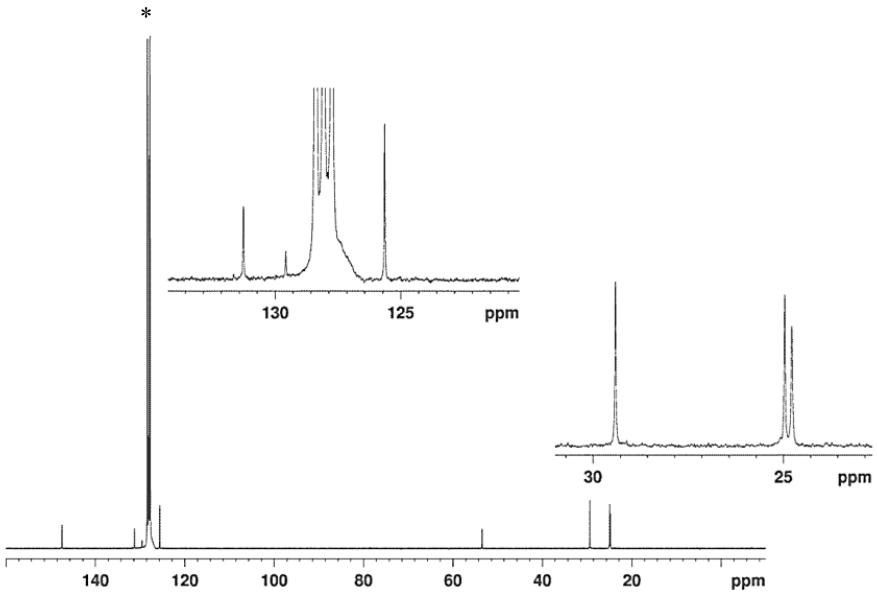

Figure S12. $^{13}C\{^{1}H\}$ NMR spectrum (75 MHz, C_6D_6) of **3.** The residual solvent peak is labeled '*'. The inset shows the expanded (horizontal scale) signal.

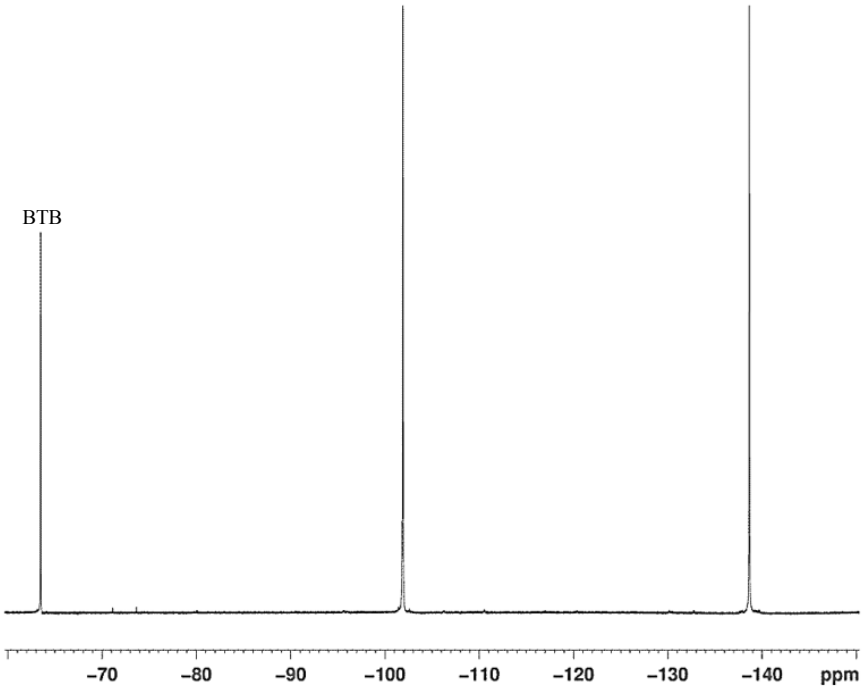

Figure S13. ^{19}F NMR spectrum (282 MHz, C_6D_6) of **3**. 1,3-Bis(trifluoromethyl)benzene (BTB) was used as an internal NMR standard.

NMR Spectra for the Title Compounds

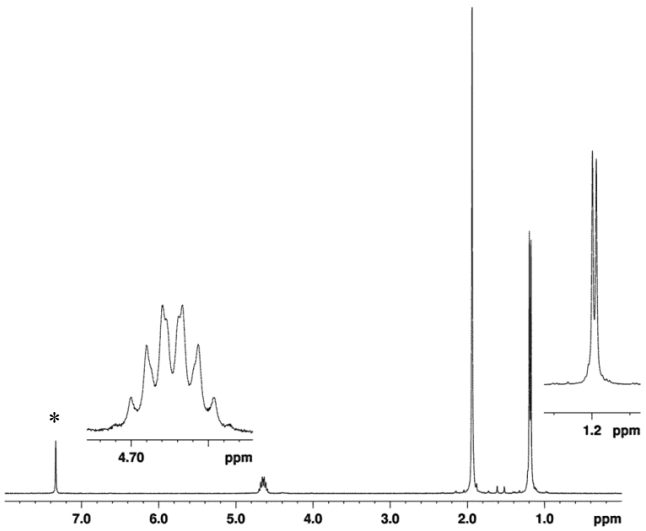

Figure S8. ^{1}H NMR spectrum (300 MHz, C_6D_6) of **2**. The insets show the expanded (horizontal scale) signals.

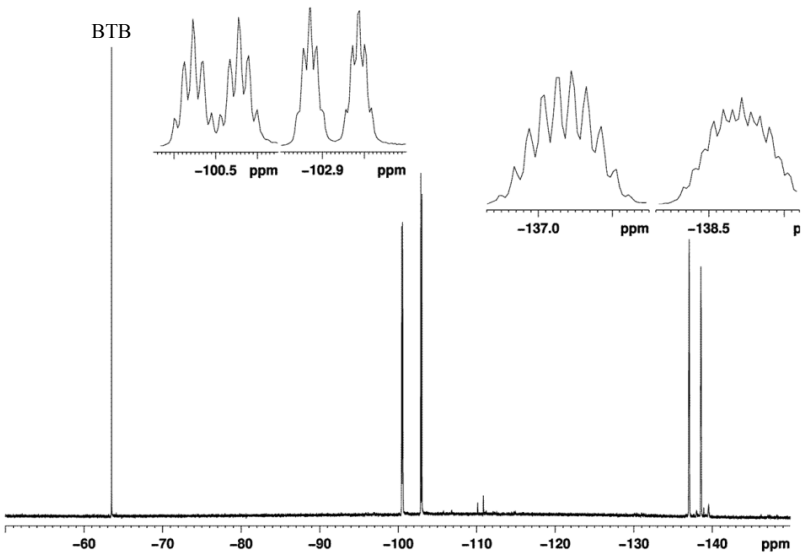

Figure S9. ^{19}F NMR spectrum (282 MHz, C_6D_6) of **2**. 1,3-Bis(trifluoromethyl)benzene (BTB) was used as an internal NMR standard. The insets show the expanded (horizontal scale) signals.

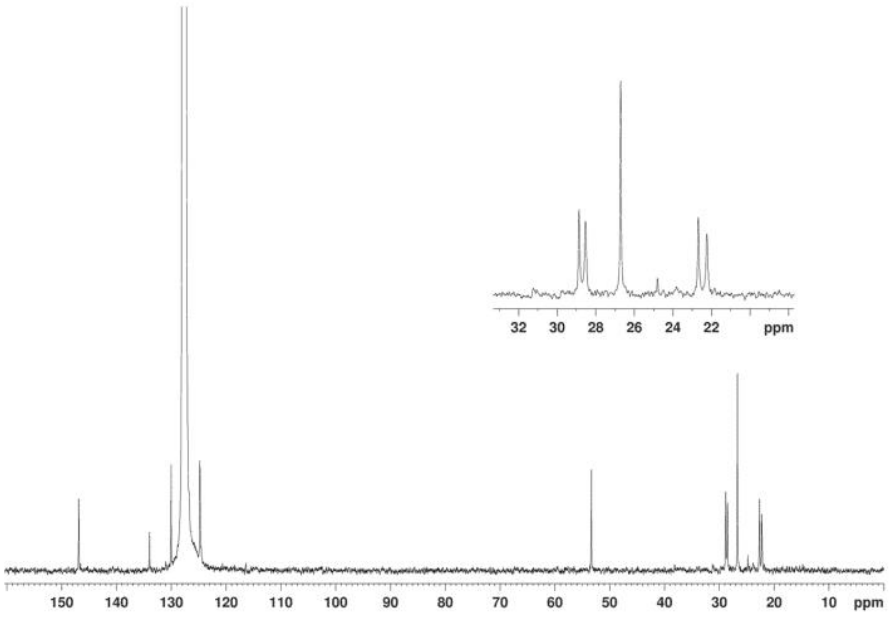

Figure S16. $^{13}C\{^{1}H\}$ NMR spectrum (75 MHz, C_6D_6) of **4a**. The inset shows the expanded (horizontal scale) signal.

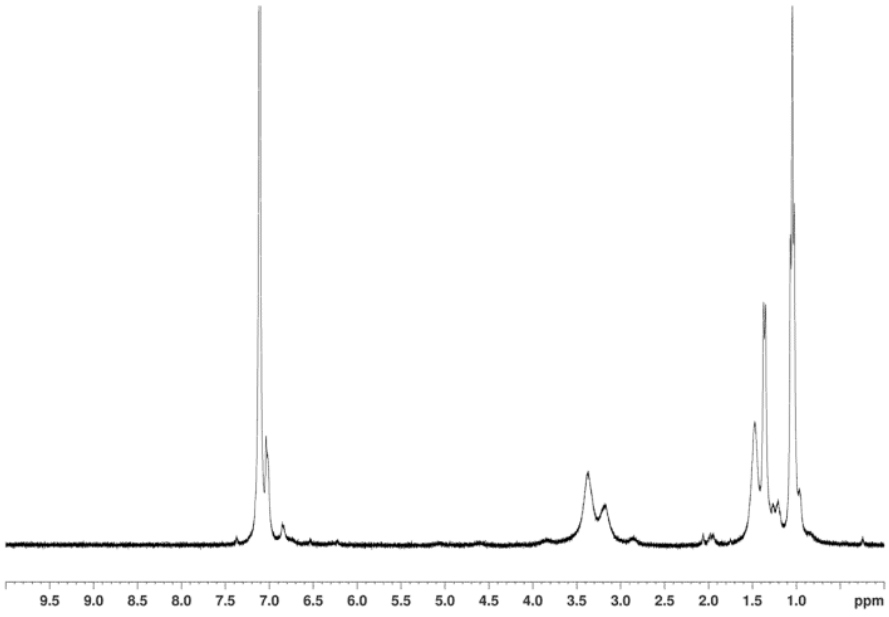

Figure S17. ^{1}H NMR spectrum (300 MHz, C_6D_6) of **5b**.

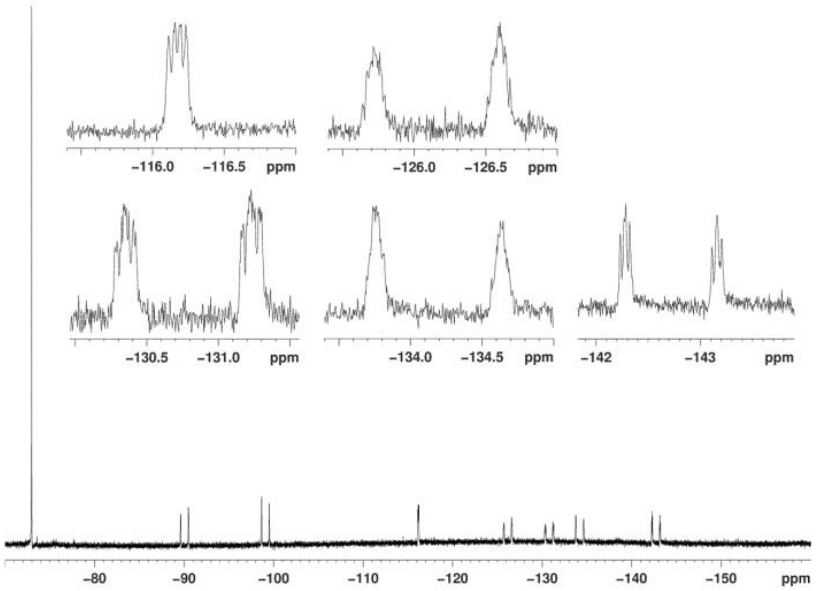

Figure S18. ^{19}F NMR spectrum (282 MHz, C_6D_6) of **5b**. 1,3-Bis(trifluoromethyl)benzene (BTB) was used as an internal NMR standard.

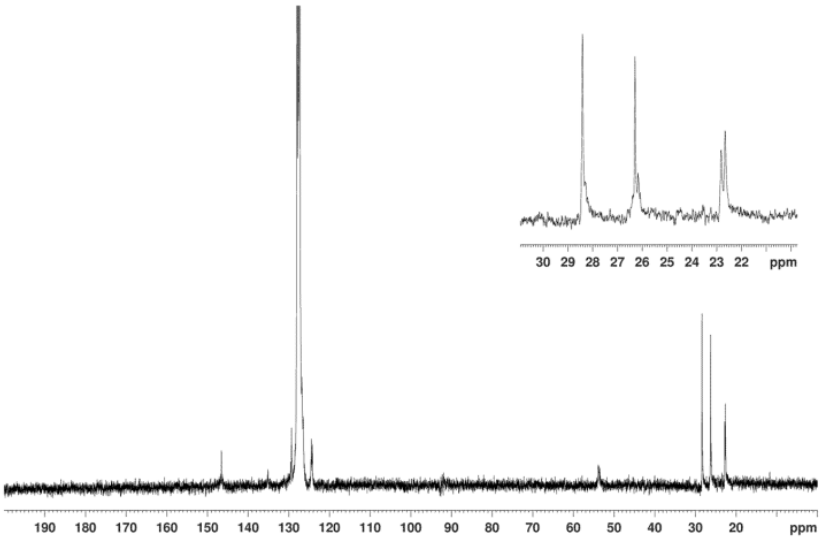

Figure S19. $^{13}C\{^1H\}$ NMR spectrum (75 MHz, C_6D_6) of **5b**. The inset shows the expanded (horizontal scale) signal.

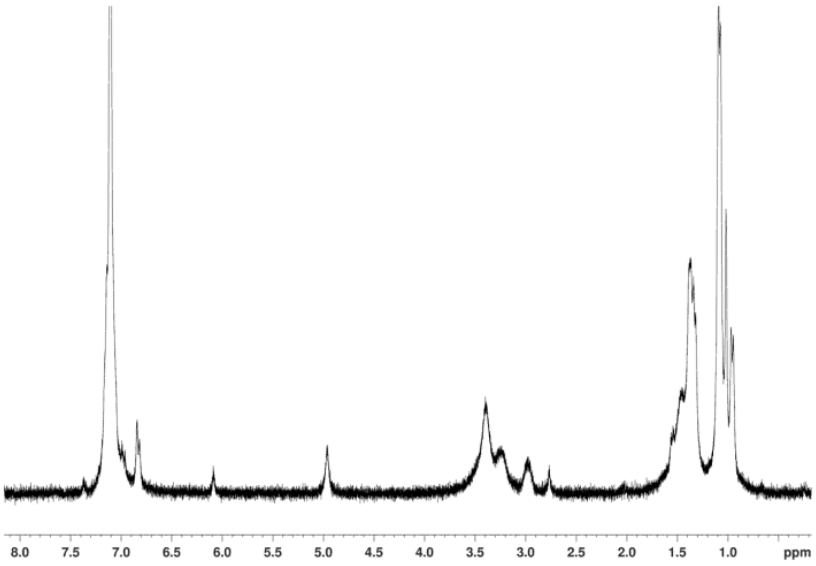

Figure S20. ^{1}H NMR spectrum (300 MHz, C_6D_6) of **5c.**

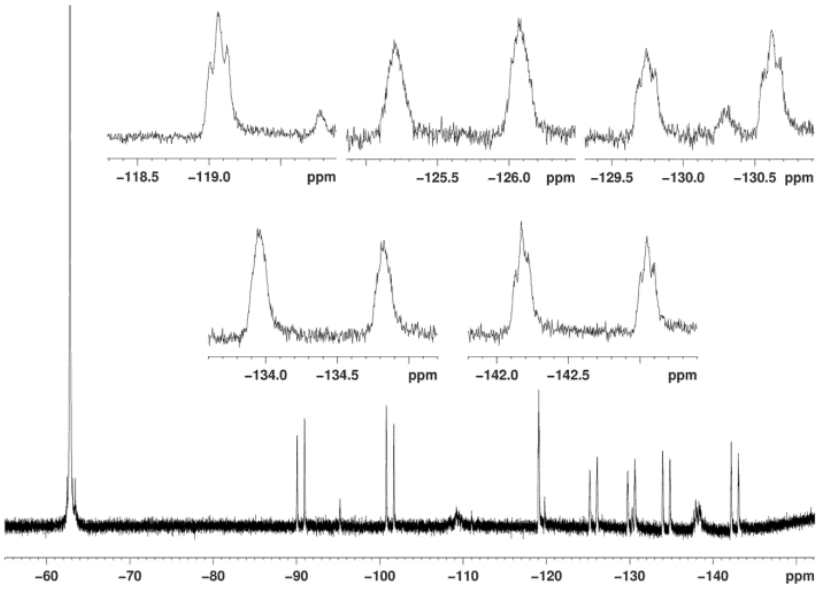

Figure S21. ^{19}F NMR spectrum (282 MHz, C_6D_6) of **5c**. 1,3-Bis(trifluoromethyl)benzene (BTB) was used as an internal NMR standard.

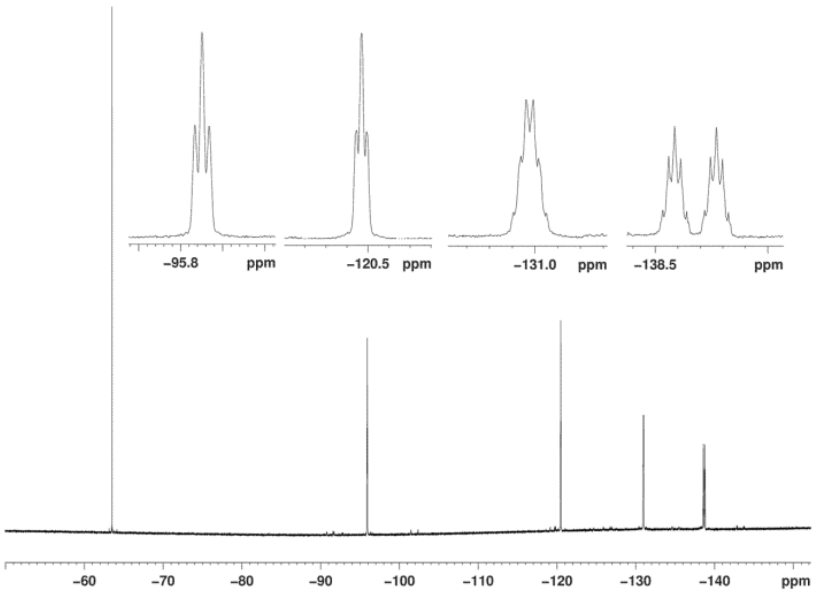

Figure S24. ^{19}F NMR spectrum (282 MHz, C_6D_6) of **6a**. 1,3-Bis(trifluoromethyl)benzene (BTB) was used as an internal NMR standard.

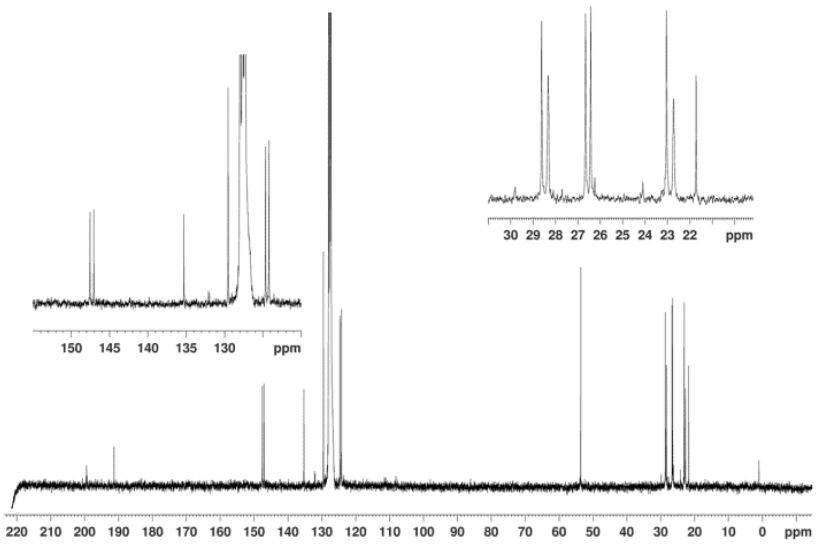

Figure S25. $^{13}C\{^1H\}$ NMR spectrum (75 MHz, C_6D_6) of **6a**. The inset shows the expanded (horizontal scale) signal.

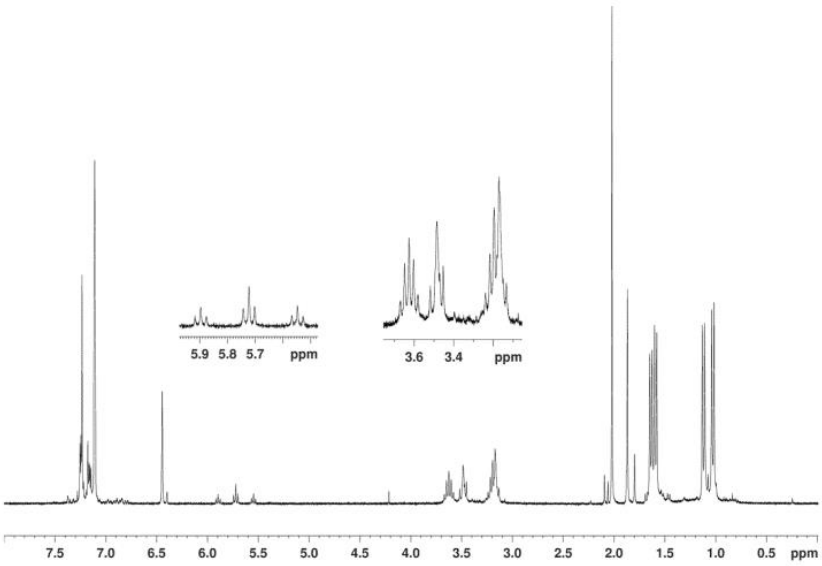

Figure S26. [1]H NMR spectrum (300 MHz, C_6D_6) of **6b**. The residual protio-solvent peak is labeled '*'. The inset shows the expanded (horizontal scale) signal.

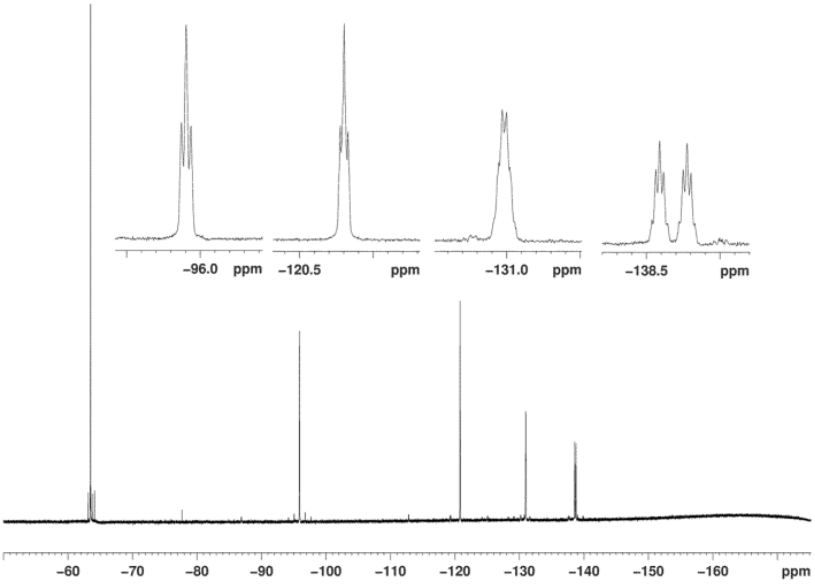

Figure S27. [19]F NMR spectrum (282 MHz, C_6D_6) of **6b.** 1,3-Bis(trifluoromethyl)benzene (BTB) was used as an internal NMR standard

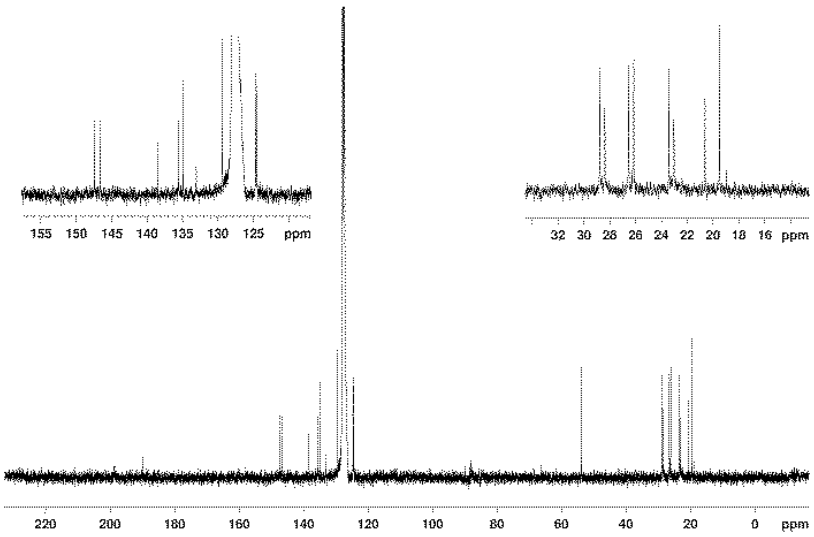

Figure S28. $^{13}C\{^{1}H\}$ NMR spectrum (75 MHz, C_6D_6) of **6b**. The inset shows the expanded (horizontal scale) signal.

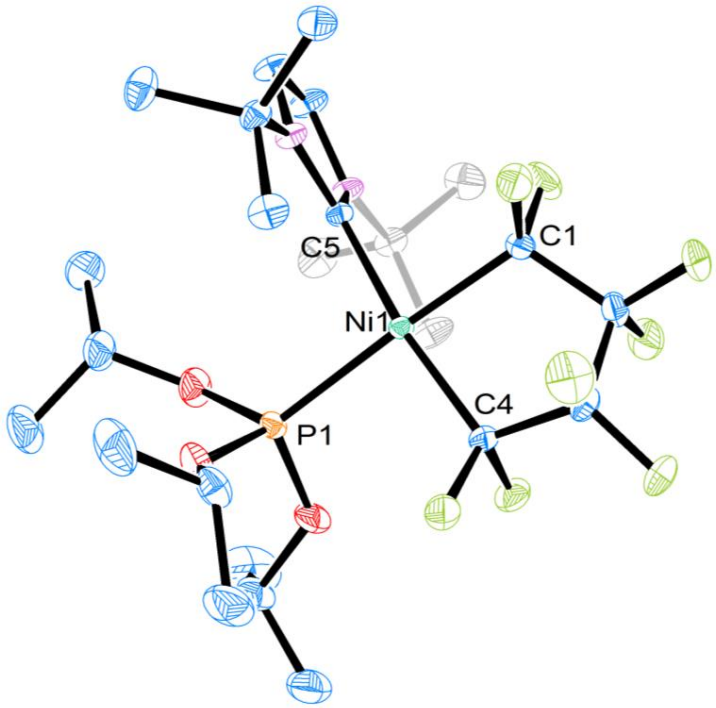

Figure S29. ORTEP representation of the molecular structure of 2 with thermal ellipsoid probability set to 30 % and hydrogen atoms omitted for clarity.

The HOMO of **3** (ε = -6.01 eV; Figure 2, left;) is localized on the Ni (87 %), primarily from a d_{z^2} orbital contribution (71 %). Lower-lying orbitals display interactions between metal d_{xz}, d_{yz} orbitals and the π-system of the aryl group.[22] The LUMO (ε = -1.96 eV; Figure 3, right) is an anti-bonding combination of the metal d_{x2-y2} orbital (total Ni character of 45%) with the □-donor orbitals of the NHC and C_4F_8 ligands.

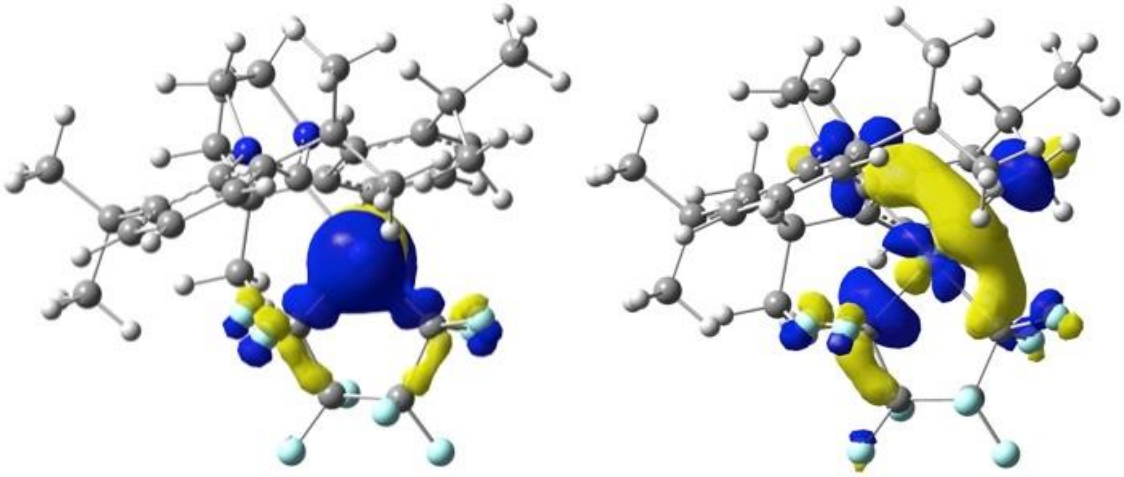

Figure S30. The HOMO (left) and LUMO (right) of **3**. Isosurface values of 0.04 au are used.

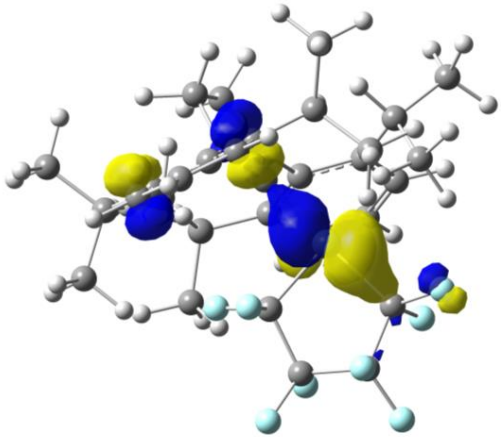

Figure S31: HOMO-1 of **3**. Isosurface values of 0.04 au are used.

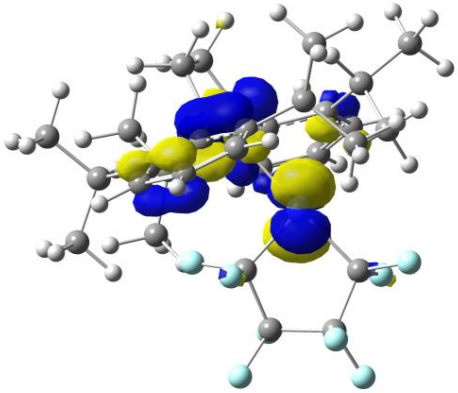

Figure S32: HOMO-4 of **3**. Isosurface values of 0.04 au are used.

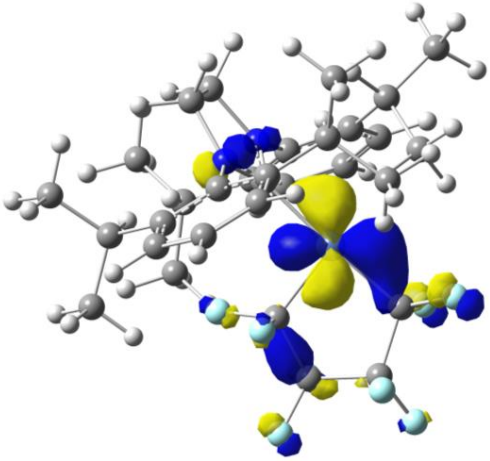

Figure S33: HOMO-9 of **3**. Isosurface values of 0.04 au are used.

Table S1. Crystal data and structure refinement

Complex	**2**	**3**	**4a**	**5c**
ID code	tb060	tb065	tb070	tb132_5
Formula	$C_{24}H_{41}F_8N_2NiO_3P$	$C_{31}H_{38}F_8N_2Ni$	$C_{35}H_{45}F_{10}N_2NiO_3S$	$C_{33}H_{41}F_7N_2NiO_2$
Mw	647.27	649.34	822.50	689.39
Color	yellow	Light red	pink	yellow
Temp (K)	200(2)	200(2)	200(2)	200(2)
Crystal system Space group	Monoclinic P2(1)/c	Orthorhombic P2(1)2(1)2(1)	Monoclinic P2(1)/c	Monoclinic P2(1)/c
a/Å	15.5474(12)	10.8851(4)	10.2361(5)	9.7181(4)
b/ Å	9.9548(8)	15.5440(6)	16.5042(8)	18.2160(7)
c/ Å	19.6379(15)	18.9208(7)	22.6115(11)	19.2228(7)
α/°	90.00	90	90	90
β/°	92.862(4)	90	90.960(2)	92.180(2)
γ/°	90.00	90	90	90
V/Å^3	3035.6(4)	3201.4(2)	3819.4(3)	3400.5(2)
Z	4	4	4	4
Dc/g cm^{-1}	1.416	1.347	1.430	1.347
μ/mm^{-1}	0.768	0.675	0.648	0.640
F(000)	1352	1352	1708	1440
Crystal size/mm	0.17x0.12x0.10	0.21x0.11x0.07	0.19x0.11x0.07	0.14x0.11x0.09
2θ range/°	2.08-28.47	2.15-28.32	1.53-28.36	1.54-23.43
Index range	-20<h<20 -13<k<13 -25<l<26	-14<h<14 -20<k<20 -25<l<25	-13<h<13 -21<k<21 -30<l<28	-10<h<10 0<k<20 0<l<21
Indep. reflns collected/unique	29150/7565	45918/7927	65889/9440	11781/6216
Max. and min. transmission	0.9271 and 0.8805	0.9543 and 0.8713	0.9561 and 0.8868	0.7449 and 0.5352
(Rint)	0.0226	0.0281	0.0396	?
R1, wR2 (I>2θ(I))	0.0326, 0.0838	0.0266, 0.0643	0.0580, 0.1410	0.0687, 0.1292
R1, wR2(all data)	0.0399, 0.0880	0.0318, 0.0663	0.0727, 0.1513	0.1053, 0.1475
Goodness of fit, F^2	1.011	1.035	1.046	1.062
Data/restraints/para	7565/0/352	7927/0/380	9440/0/469	9216/0/407
Largest diff. peak,	0.944, -0.261	0.327, -0.224	0.944, -0.717	0.871, -0.423

Table S2. Comparison of ^{19}F NMR δ (ppm) of Cα-substituted fluoronickelacycles (**5a**, **5b**, **5c**, **5d**).

Complex **5a**	Complex **5b**	Complex **5c**	Complex **5d**
-73.27	-72.97	---	---
-83.98	-90.06	-91.23	-91.22
-99.73	-99.09	-101.86	-101.86
-106.29	-116.17	-119.78	-119.74
-127.11	-126.14	-126.35	-126.25
-129.23	-130.76	-130.90	-130.80
-137.07	-134.17	-135.10	-135.05
-144.71	-142.71	-143.33	-143.27

Table S3. Bond lengths [Å] and angles [°] for complex **2**.

Ni(1)-C(5)	1.9454(14)
Ni(1)-C(4)	1.9447(15)
Ni(1)-C(1)	1.9555(16)
Ni(1)-P(1)	2.2150(5)
P(1)-O(2)	1.5818(14)
P(1)-O(3)	1.5926(13)
P(1)-O(1)	1.5943(13)
O(1)-C(16)	1.437(3)
O(2)-C(19)	1.459(2)
O(3)-C(22)	1.439(2)
N(1)-C(5)	1.3647(19)
N(1)-C(6)	1.383(2)
N(1)-C(8)	1.500(2)
N(2)-C(5)	1.3654(19)
N(2)-C(7)	1.388(2)
N(2)-C(12)	1.496(2)
C(1)-F(1)	1.3798(19)
C(1)-F(2)	1.392(2)
C(1)-C(2)	1.530(2)
C(2)-F(3)	1.356(2)
C(2)-F(4)	1.358(2)
C(2)-C(3)	1.509(2)
C(3)-F(5)	1.3509(19)
C(3)-F(6)	1.367(2)
C(3)-C(4)	1.525(2)
C(4)-F(8)	1.3871(18)
C(4)-F(7)	1.3904(19)
C(6)-C(7)	1.329(3)
C(8)-C(11)	1.506(2)
C(8)-C(9)	1.526(3)
C(8)-C(10)	1.537(3)
C(12)-C(15)	1.514(2)
C(12)-C(13)	1.531(2)
C(12)-C(14)	1.535(2)
C(16)-C(17)	1.511(3)
C(16)-C(18)	1.504(3)
C(19)-C(20)	1.507(3)
C(19)-C(21)	1.504(4)
C(22)-C(23)	1.511(3)
C(22)-C(24)	1.511(3)
C(5)-Ni(1)-C(4)	171.33(6)
C(5)-Ni(1)-C(1)	88.21(6)
C(4)-Ni(1)-C(1)	85.19(7)
C(5)-Ni(1)-P(1)	94.69(4)
C(4)-Ni(1)-P(1)	91.89(5)
C(1)-Ni(1)-P(1)	177.09(5)
O(2)-P(1)-O(3)	106.95(8)
O(2)-P(1)-O(1)	101.38(8)

O(3)-P(1)-O(1)	98.41(7)
O(2)-P(1)-Ni(1)	107.63(5)
O(3)-P(1)-Ni(1)	122.62(5)
O(1)-P(1)-Ni(1)	117.52(6)
C(16)-O(1)-P(1)	127.70(14)
C(19)-O(2)-P(1)	127.05(13)
C(22)-O(3)-P(1)	129.83(11)
C(5)-N(1)-C(6)	110.74(13)
C(5)-N(1)-C(8)	130.13(12)
C(6)-N(1)-C(8)	119.12(13)
C(5)-N(2)-C(7)	110.57(13)
C(5)-N(2)-C(12)	129.98(12)
C(7)-N(2)-C(12)	119.45(13)
F(1)-C(1)-F(2)	103.24(13)
F(1)-C(1)-C(2)	105.80(14)
F(2)-C(1)-C(2)	104.81(13)
F(1)-C(1)-Ni(1)	118.00(11)
F(2)-C(1)-Ni(1)	111.83(11)
C(2)-C(1)-Ni(1)	112.00(11)
F(3)-C(2)-F(4)	106.18(14)
F(3)-C(2)-C(3)	107.96(15)
F(4)-C(2)-C(3)	111.81(15)
F(3)-C(2)-C(1)	109.24(15)
F(4)-C(2)-C(1)	114.68(14)
C(3)-C(2)-C(1)	106.80(13)
F(5)-C(3)-F(6)	105.63(14)
F(5)-C(3)-C(2)	112.03(15)
F(6)-C(3)-C(2)	107.77(15)
F(5)-C(3)-C(4)	115.02(15)
F(6)-C(3)-C(4)	108.42(14)
C(2)-C(3)-C(4)	107.69(13)
F(8)-C(4)-F(7)	103.15(12)
F(8)-C(4)-C(3)	106.04(13)
F(7)-C(4)-C(3)	104.25(13)
F(8)-C(4)-Ni(1)	119.13(11)
F(7)-C(4)-Ni(1)	110.84(10)
C(3)-C(4)-Ni(1)	112.09(10)
N(1)-C(5)-N(2)	104.10(12)
N(1)-C(5)-Ni(1)	126.14(11)
N(2)-C(5)-Ni(1)	129.23(11)
C(7)-C(6)-N(1)	107.34(14)
C(6)-C(7)-N(2)	107.25(14)
N(1)-C(8)-C(11)	112.67(13)
N(1)-C(8)-C(9)	108.14(15)
C(11)-C(8)-C(9)	108.68(17)
N(1)-C(8)-C(10)	107.49(15)
C(11)-C(8)-C(10)	109.72(17)
C(9)-C(8)-C(10)	110.11(17)
N(2)-C(12)-C(15)	111.22(13)
N(2)-C(12)-C(13)	108.62(14)
C(15)-C(12)-C(13)	110.57(15)
N(2)-C(12)-C(14)	107.68(13)
C(15)-C(12)-C(14)	108.47(15)
C(13)-C(12)-C(14)	110.25(15)
O(1)-C(16)-C(17)	107.99(19)
O(1)-C(16)-C(18)	110.9(2)
C(17)-C(16)-C(18)	113.14(19)
O(2)-C(19)-C(20)	105.71(19)
O(2)-C(19)-C(21)	108.6(2)
C(20)-C(19)-C(21)	112.7(2)
O(3)-C(22)-C(23)	106.23(18)
O(3)-C(22)-C(24)	109.22(18)
C(23)-C(22)-C(24)	112.0(2)

Table S4. Bond lengths [Å] and angles [°] for complex **3**

Ni(1)-C(31)	1.8746(15)
Ni(1)-C(28)	1.9341(14)
Ni(1)-C(1)	1.9408(12)
N(1)-C(1)	1.3360(17)
N(1)-C(4)	1.4363(18)
N(1)-C(2)	1.4811(17)
N(2)-C(1)	1.3362(17)
N(2)-C(16)	1.4322(18)
N(2)-C(3)	1.4810(17)
F(1)-C(28)	1.3857(19)
F(2)-C(28)	1.3876(18)
F(3)-C(29)	1.3541(17)
F(4)-C(29)	1.355(2)
F(5)-C(30)	1.349(2)
F(6)-C(30)	1.3510(18)
F(7)-C(31)	1.3629(17)
F(8)-C(31)	1.3680(17)
C(2)-C(3)	1.521(2)
C(4)-C(9)	1.393(2)

C(4)-C(5)	1.402(2)
C(5)-C(6)	1.387(3)
C(5)-C(10)	1.513(3)
C(6)-C(7)	1.372(3)
C(7)-C(8)	1.362(3)
C(8)-C(9)	1.401(2)
C(9)-C(13)	1.511(2)
C(10)-C(11)	1.531(3)
C(10)-C(12)	1.531(2)
C(13)-C(14)	1.534(2)
C(13)-C(15)	1.536(2)
C(16)-C(17)	1.396(2)
C(16)-C(21)	1.408(2)
C(17)-C(18)	1.397(2)
C(17)-C(22)	1.524(2)
C(18)-C(19)	1.374(3)
C(19)-C(20)	1.382(3)
C(20)-C(21)	1.392(2)
C(21)-C(25)	1.520(2)
C(22)-C(23)	1.530(2)
C(22)-C(24)	1.532(2)
C(25)-C(26)	1.534(2)
C(25)-C(27)	1.536(2)
C(28)-C(29)	1.520(2)
C(29)-C(30)	1.521(2)
C(30)-C(31)	1.539(2)

C(31)-Ni(1)-C(28)	86.95(6)
C(31)-Ni(1)-C(1)	96.64(6)
C(28)-Ni(1)-C(1)	174.63(6)
C(1)-N(1)-C(4)	124.12(11)
C(1)-N(1)-C(2)	113.42(11)
C(4)-N(1)-C(2)	122.33(11)
C(1)-N(2)-C(16)	127.41(11)
C(1)-N(2)-C(3)	112.75(11)
C(16)-N(2)-C(3)	119.47(11)
N(1)-C(1)-N(2)	108.40(11)
N(1)-C(1)-Ni(1)	118.59(10)
N(2)-C(1)-Ni(1)	132.60(10)
N(1)-C(2)-C(3)	102.14(12)
N(2)-C(3)-C(2)	102.93(12)
C(9)-C(4)-C(5)	122.67(14)
C(9)-C(4)-N(1)	118.72(13)
C(5)-C(4)-N(1)	118.57(13)
C(6)-C(5)-C(4)	117.34(17)
C(6)-C(5)-C(10)	122.02(17)
C(4)-C(5)-C(10)	120.63(14)
C(7)-C(6)-C(5)	121.01(18)
C(6)-C(7)-C(8)	120.83(17)
C(7)-C(8)-C(9)	121.26(19)
C(4)-C(9)-C(8)	116.88(16)
C(4)-C(9)-C(13)	122.78(14)
C(8)-C(9)-C(13)	120.32(16)
C(5)-C(10)-C(11)	113.00(18)
C(5)-C(10)-C(12)	110.36(15)
C(11)-C(10)-C(12)	109.83(17)
C(9)-C(13)-C(14)	110.52(14)
C(9)-C(13)-C(15)	111.70(15)
C(14)-C(13)-C(15)	110.26(14)
C(17)-C(16)-C(21)	122.21(13)
C(17)-C(16)-N(2)	118.81(13)
C(21)-C(16)-N(2)	118.90(13)
C(16)-C(17)-C(18)	117.81(16)
C(16)-C(17)-C(22)	122.49(14)
C(18)-C(17)-C(22)	119.69(15)
C(19)-C(18)-C(17)	120.89(17)
C(18)-C(19)-C(20)	120.57(15)
C(19)-C(20)-C(21)	121.03(17)
C(20)-C(21)-C(16)	117.46(16)
C(20)-C(21)-C(25)	119.69(15)
C(16)-C(21)-C(25)	122.85(13)
C(17)-C(22)-C(23)	112.42(14)
C(17)-C(22)-C(24)	110.15(14)
C(23)-C(22)-C(24)	109.99(14)
C(21)-C(25)-C(26)	110.53(13)
C(21)-C(25)-C(27)	112.03(14)
C(26)-C(25)-C(27)	110.41(15)
F(1)-C(28)-F(2)	103.56(13)
F(1)-C(28)-C(29)	106.05(13)
F(2)-C(28)-C(29)	107.44(12)
F(1)-C(28)-Ni(1)	110.56(10)
F(2)-C(28)-Ni(1)	116.38(11)
C(29)-C(28)-Ni(1)	112.05(10)
F(4)-C(29)-F(3)	106.32(13)
F(4)-C(29)-C(30)	108.15(14)
F(3)-C(29)-C(30)	111.25(13)

F(4)-C(29)-C(28)	109.70(13)
F(3)-C(29)-C(28)	115.48(14)
C(30)-C(29)-C(28)	105.79(11)
F(5)-C(30)-F(6)	107.37(13)
F(5)-C(30)-C(29)	108.31(14)
F(6)-C(30)-C(29)	111.98(13)
F(5)-C(30)-C(31)	108.91(13)
F(6)-C(30)-C(31)	113.32(13)
C(29)-C(30)-C(31)	106.84(12)
F(7)-C(31)-F(8)	105.13(11)
F(7)-C(31)-C(30)	106.98(12)
F(8)-C(31)-C(30)	107.48(12)
F(7)-C(31)-Ni(1)	111.18(10)
F(8)-C(31)-Ni(1)	115.03(10)
C(30)-C(31)-Ni(1)	110.60(10)

Table S5. Bond lengths [Å] and angles [°] for complex **4a.**

Ni(1)-C(1)	1.854(2)
Ni(1)-C(28)	1.890(2)
Ni(1)-O(1)	2.0020(18)
Ni(1)-O(2)	2.0204(18)
Ni(1)-S(1)	2.5148(7)
S(1)-O(3)	1.419(2)
S(1)-O(1)	1.467(2)
S(1)-O(2)	1.471(2)
S(1)-C(32)	1.829(4)
F(1)-C(28)	1.384(3)
F(2)-C(29)	1.343(3)
F(3)-C(29)	1.338(4)
F(4)-C(30)	1.346(5)
F(5)-C(30)	1.325(4)
F(6)-C(31)	1.336(4)
F(7)-C(31)	1.331(4)
F(8)-C(32)	1.313(5)
F(9)-C(32)	1.320(4)
F(10)-C(32)	1.315(4)
N(1)-C(1)	1.340(3)
N(1)-C(4)	1.438(3)
N(1)-C(2)	1.489(3)
N(2)-C(1)	1.344(3)
N(2)-C(16)	1.440(3)
N(2)-C(3)	1.489(3)
C(2)-C(3)	1.507(4)
C(4)-C(9)	1.404(3)
C(4)-C(5)	1.411(3)
C(5)-C(6)	1.385(4)
C(5)-C(10)	1.522(4)
C(6)-C(7)	1.380(4)
C(7)-C(8)	1.385(4)
C(8)-C(9)	1.392(4)
C(9)-C(13)	1.522(4)
C(10)-C(11)	1.530(4)
C(10)-C(12)	1.530(4)
C(13)-C(14)	1.528(4)
C(13)-C(15)	1.538(4)
C(16)-C(21)	1.404(3)
C(16)-C(17)	1.403(4)
C(17)-C(18)	1.405(4)
C(17)-C(22)	1.520(4)
C(18)-C(19)	1.370(5)
C(19)-C(20)	1.377(4)
C(20)-C(21)	1.397(4)
C(21)-C(25)	1.518(4)
C(22)-C(23)	1.537(4)
C(22)-C(24)	1.538(5)
C(25)-C(26)	1.524(5)
C(25)-C(27)	1.538(4)
C(28)-C(31)	1.558(4)
C(28)-C(29)	1.563(3)
C(29)-C(30)	1.557(5)
C(30)-C(31)	1.555(4)
C(33)-C(34)	1.514(9)
C(34)-C(35)	1.434(9)
C(35)-C(35)#1	1.505(11)

C(1)-Ni(1)-C(28)	93.27(10)
C(1)-Ni(1)-O(1)	168.00(9)
C(28)-Ni(1)-O(1)	98.34(10)
C(1)-Ni(1)-O(2)	97.58(8)
C(28)-Ni(1)-O(2)	168.58(9)
O(1)-Ni(1)-O(2)	71.04(8)
C(1)-Ni(1)-S(1)	133.31(7)
C(28)-Ni(1)-S(1)	133.10(8)
O(1)-Ni(1)-S(1)	35.66(6)

O(2)-Ni(1)-S(1)	35.79(6)
O(3)-S(1)-O(1)	118.03(14)
O(3)-S(1)-O(2)	117.65(15)
O(1)-S(1)-O(2)	105.42(11)
O(3)-S(1)-C(32)	105.23(17)
O(1)-S(1)-C(32)	103.98(16)
O(2)-S(1)-C(32)	104.94(14)
O(3)-S(1)-Ni(1)	148.01(13)
O(1)-S(1)-Ni(1)	52.73(7)
O(2)-S(1)-Ni(1)	53.45(7)
C(32)-S(1)-Ni(1)	106.75(12)
S(1)-O(1)-Ni(1)	91.61(9)
S(1)-O(2)-Ni(1)	90.76(9)
C(1)-N(1)-C(4)	127.02(19)
C(1)-N(1)-C(2)	111.06(19)
C(4)-N(1)-C(2)	121.91(19)
C(1)-N(2)-C(16)	126.97(19)
C(1)-N(2)-C(3)	110.70(18)
C(16)-N(2)-C(3)	120.27(18)
N(1)-C(1)-N(2)	109.11(18)
N(1)-C(1)-Ni(1)	123.25(16)
N(2)-C(1)-Ni(1)	127.47(16)
N(1)-C(2)-C(3)	101.69(19)
N(2)-C(3)-C(2)	101.73(19)
C(9)-C(4)-C(5)	122.1(2)
C(9)-C(4)-N(1)	118.3(2)
C(5)-C(4)-N(1)	119.6(2)
C(6)-C(5)-C(4)	117.6(2)
C(6)-C(5)-C(10)	119.5(2)
C(4)-C(5)-C(10)	122.9(2)
C(7)-C(6)-C(5)	121.4(3)
C(6)-C(7)-C(8)	120.1(3)
C(7)-C(8)-C(9)	121.2(3)
C(8)-C(9)-C(4)	117.5(2)
C(8)-C(9)-C(13)	119.5(2)
C(4)-C(9)-C(13)	122.9(2)
C(11)-C(10)-C(5)	112.2(3)
C(11)-C(10)-C(12)	108.9(3)
C(5)-C(10)-C(12)	110.1(2)
C(9)-C(13)-C(14)	113.6(3)
C(9)-C(13)-C(15)	109.4(2)
C(14)-C(13)-C(15)	108.5(3)
C(21)-C(16)-C(17)	121.8(2)
C(21)-C(16)-N(2)	119.8(2)
C(17)-C(16)-N(2)	118.3(2)
C(16)-C(17)-C(18)	117.6(2)
C(16)-C(17)-C(22)	123.9(2)
C(18)-C(17)-C(22)	118.4(2)
C(19)-C(18)-C(17)	121.2(3)
C(18)-C(19)-C(20)	120.2(3)
C(19)-C(20)-C(21)	121.5(3)
C(20)-C(21)-C(16)	117.6(2)
C(20)-C(21)-C(25)	118.9(2)
C(16)-C(21)-C(25)	123.4(2)
C(17)-C(22)-C(23)	112.4(3)
C(17)-C(22)-C(24)	110.1(3)
C(23)-C(22)-C(24)	109.7(3)
C(21)-C(25)-C(26)	112.4(3)
C(21)-C(25)-C(27)	109.8(3)
C(26)-C(25)-C(27)	110.8(3)
F(1)-C(28)-C(31)	110.2(2)
F(1)-C(28)-C(29)	108.8(2)
C(31)-C(28)-C(29)	88.21(19)
F(1)-C(28)-Ni(1)	117.22(16)
C(31)-C(28)-Ni(1)	114.71(19)
C(29)-C(28)-Ni(1)	114.07(17)
F(3)-C(29)-F(2)	107.4(2)
F(3)-C(29)-C(30)	111.6(2)
F(2)-C(29)-C(30)	114.7(3)
F(3)-C(29)-C(28)	114.1(2)
F(2)-C(29)-C(28)	117.6(2)
C(30)-C(29)-C(28)	90.9(2)
F(5)-C(30)-F(4)	108.5(3)
F(5)-C(30)-C(31)	115.1(3)
F(4)-C(30)-C(31)	114.2(3)
F(5)-C(30)-C(29)	114.3(3)
F(4)-C(30)-C(29)	115.3(3)
C(31)-C(30)-C(29)	88.5(2)
F(7)-C(31)-F(6)	107.6(3)
F(7)-C(31)-C(30)	112.1(2)
F(6)-C(31)-C(30)	114.3(3)
F(7)-C(31)-C(28)	114.8(3)
F(6)-C(31)-C(28)	116.3(2)
C(30)-C(31)-C(28)	91.1(2)
F(10)-C(32)-F(9)	108.5(3)
F(10)-C(32)-F(8)	109.4(4)

F(9)-C(32)-F(8)	108.4(3)
F(10)-C(32)-S(1)	109.6(3)
F(9)-C(32)-S(1)	109.6(3)
F(8)-C(32)-S(1)	111.4(2)
C(35)-C(34)-C(33)	118.0(6)
C(34)-C(35)-C(35)#1	119.3(7)

Table S6. Bond lengths [Å] and angles [°] for complex **5c**.

Ni(1)-C(30)	1.895(7)
Ni(1)-C(32)	1.896(6)
Ni(1)-C(1)	1.928(6)
Ni(1)-O(1)	1.969(4)
F(1)-C(30)	1.418(8)
F(2)-C(32)	1.375(7)
F(3)-C(39)	1.355(8)
F(4)-C(31)	1.375(8)
F(5)-C(31)	1.343(7)
F(6)-C(39)	1.358(8)
F(7)-C(32)	1.386(7)
O(1)-C(28)	1.227(8)
O(2)-C(28)	1.320(8)
O(2)-C(30)	1.437(8)
N(1)-C(1)	1.343(7)
N(1)-C(4)	1.440(7)
N(1)-C(2)	1.474(7)
N(2)-C(1)	1.351(7)
N(2)-C(16)	1.439(7)
N(2)-C(3)	1.475(7)
C(2)-C(3)	1.521(8)
C(4)-C(9)	1.401(8)
C(4)-C(5)	1.402(9)
C(5)-C(6)	1.405(9)
C(5)-C(10)	1.507(9)
C(6)-C(7)	1.368(10)
C(7)-C(8)	1.369(10)
C(8)-C(9)	1.388(9)
C(9)-C(13)	1.514(9)
C(10)-C(12)	1.526(10)
C(10)-C(11)	1.533(11)
C(13)-C(14)	1.521(9)
C(13)-C(15)	1.537(9)
C(16)-C(17)	1.393(9)
C(16)-C(21)	1.405(9)
C(17)-C(18)	1.398(9)
C(17)-C(22)	1.523(9)
C(18)-C(19)	1.373(10)
C(19)-C(20)	1.367(10)
C(20)-C(21)	1.387(9)
C(21)-C(25)	1.510(9)
C(22)-C(23)	1.521(10)
C(22)-C(24)	1.533(10)
C(25)-C(26)	1.514(9)
C(25)-C(27)	1.527(9)
C(28)-C(29)	1.475(9)
C(30)-C(31)	1.492(10)
C(31)-C(39)	1.502(9)
C(32)-C(39)	1.542(9)

C(30)-Ni(1)-C(32)	85.8(3)
C(30)-Ni(1)-C(1)	170.9(3)
C(32)-Ni(1)-C(1)	97.8(3)
C(30)-Ni(1)-O(1)	81.5(2)
C(32)-Ni(1)-O(1)	161.1(2)
C(1)-Ni(1)-O(1)	96.9(2)
C(28)-O(1)-Ni(1)	111.3(4)
C(28)-O(2)-C(30)	111.6(5)
C(1)-N(1)-C(4)	127.4(5)
C(1)-N(1)-C(2)	112.3(4)
C(4)-N(1)-C(2)	116.3(4)
C(1)-N(2)-C(16)	124.8(5)
C(1)-N(2)-C(3)	112.9(4)

C(16)-N(2)-C(3)	122.3(5)	C(23)-C(22)-C(17)	114.0(6)
N(1)-C(1)-N(2)	107.3(5)	C(23)-C(22)-C(24)	110.1(6)
N(1)-C(1)-Ni(1)	134.1(4)	C(17)-C(22)-C(24)	110.3(6)
N(2)-C(1)-Ni(1)	118.6(4)	C(21)-C(25)-C(26)	114.1(6)
N(1)-C(2)-C(3)	102.1(4)	C(21)-C(25)-C(27)	108.9(5)
N(2)-C(3)-C(2)	101.1(4)	C(26)-C(25)-C(27)	110.2(6)
C(9)-C(4)-C(5)	122.6(6)	O(1)-C(28)-O(2)	122.2(6)
C(9)-C(4)-N(1)	118.0(5)	O(1)-C(28)-C(29)	123.2(7)
C(5)-C(4)-N(1)	119.0(5)	O(2)-C(28)-C(29)	114.6(6)
C(4)-C(5)-C(6)	116.8(6)	F(1)-C(30)-O(2)	104.5(5)
C(4)-C(5)-C(10)	124.5(6)	F(1)-C(30)-C(31)	103.4(5)
C(6)-C(5)-C(10)	118.7(6)	O(2)-C(30)-C(31)	112.5(6)
C(7)-C(6)-C(5)	120.9(7)	F(1)-C(30)-Ni(1)	113.5(5)
C(6)-C(7)-C(8)	121.1(6)	O(2)-C(30)-Ni(1)	110.3(5)
C(7)-C(8)-C(9)	121.1(6)	C(31)-C(30)-Ni(1)	112.3(5)
C(8)-C(9)-C(4)	117.5(6)	F(5)-C(31)-F(4)	107.0(6)
C(8)-C(9)-C(13)	120.2(6)	F(5)-C(31)-C(30)	116.0(6)
C(4)-C(9)-C(13)	122.3(5)	F(4)-C(31)-C(30)	106.0(5)
C(5)-C(10)-C(12)	111.6(6)	F(5)-C(31)-C(39)	113.2(6)
C(5)-C(10)-C(11)	111.2(6)	F(4)-C(31)-C(39)	108.9(6)
C(12)-C(10)-C(11)	111.5(7)	C(30)-C(31)-C(39)	105.4(6)
C(9)-C(13)-C(14)	111.8(5)	F(2)-C(32)-F(7)	104.0(5)
C(9)-C(13)-C(15)	110.5(5)	F(2)-C(32)-C(39)	108.4(5)
C(14)-C(13)-C(15)	110.4(6)	F(7)-C(32)-C(39)	104.7(5)
C(17)-C(16)-C(21)	123.1(5)	F(2)-C(32)-Ni(1)	118.3(4)
C(17)-C(16)-N(2)	118.1(5)	F(7)-C(32)-Ni(1)	108.1(4)
C(21)-C(16)-N(2)	118.8(6)	C(39)-C(32)-Ni(1)	112.1(4)
C(16)-C(17)-C(18)	117.2(6)	F(3)-C(39)-F(6)	105.1(5)
C(16)-C(17)-C(22)	123.8(6)	F(3)-C(39)-C(31)	109.5(5)
C(18)-C(17)-C(22)	118.9(6)	F(6)-C(39)-C(31)	110.9(6)
C(19)-C(18)-C(17)	120.3(7)	F(3)-C(39)-C(32)	109.1(5)
C(20)-C(19)-C(18)	121.3(6)	F(6)-C(39)-C(32)	113.6(5)
C(19)-C(20)-C(21)	121.4(7)	C(31)-C(39)-C(32)	108.5(5)
C(20)-C(21)-C(16)	116.6(6)		
C(20)-C(21)-C(25)	120.5(6)		
C(16)-C(21)-C(25)	122.7(5)		

Table S7. Optimized structure (Cartesian coordinates, Å) of **3** with an isopropyl-CH_3 agostic interaction. B3LYP/TZVP without dispersion correction.

Ni	-0.381956	0.794859	0.529500
C	3.789956	-2.386599	-2.887355
C	4.732575	-0.188091	-0.812193
C	3.136272	-0.001705	-3.380984
C	5.204272	0.173073	0.439927
C	3.015391	-1.157257	-2.373853
C	3.473593	-0.764873	-0.974427
C	4.423177	-0.048799	1.561865
C	2.688957	-0.971689	0.178064
C	3.159883	-0.633894	1.460880
C	1.345736	-3.098112	-0.064609
C	3.065800	-1.971850	3.603219
C	2.373681	-0.903694	2.737054
C	-0.155824	-3.363099	-0.230617
C	-2.510594	-3.194565	-3.279299
C	-2.537451	-0.677990	-3.517885
C	0.194845	-1.052719	0.104820
C	-2.182170	-1.854679	-2.594426
C	2.130146	0.380203	3.546680
C	-2.863479	-1.748045	-1.236859
C	-2.157250	-1.808027	-0.021598
C	-4.248561	-1.585026	-1.175986
C	-2.812007	-1.716507	1.222244
C	-2.038058	-1.758975	2.534128
C	-1.608250	-0.347210	2.961767
C	-4.908563	-1.479196	0.037196
C	-4.194515	-1.539550	1.224942
C	-2.803850	-2.443888	3.675974
H	4.850585	-2.154636	-3.008376
H	3.405311	-2.700722	-3.860709
H	5.350594	-0.009642	-1.682630
H	4.180137	0.263107	-3.563524
H	6.181799	0.628901	0.540817
H	3.720451	-3.236486	-2.204765
H	2.702810	-0.298224	-4.338979
H	2.613875	0.886489	-3.031972
H	1.958021	-1.418908	-2.318226
H	4.802868	0.232007	2.536165
H	1.932433	-3.450199	-0.910811
H	1.756189	-3.543499	0.844410
H	3.225048	-2.899230	3.048613
H	4.040964	-1.626708	3.953144
H	-1.954723	-3.289885	-4.215009
H	-1.961874	-0.745617	-4.443781
H	-0.407722	-3.744126	-1.221071
H	-1.104829	-1.811474	-2.430730
H	-2.263079	-4.050610	-2.647537
H	3.067705	0.807190	3.907883
H	2.459780	-2.201744	4.483098
H	1.398447	-1.300775	2.454587
H	-0.553923	-4.055413	0.512744
H	-2.310182	0.278880	-3.050560
H	-3.574697	-3.261949	-3.517247
H	1.627716	1.143918	2.951434
H	-3.595462	-0.685860	-3.788597
H	1.510223	0.167655	4.420832
H	-1.130336	-2.343095	2.365504
H	-0.817473	0.058960	2.305163
H	-4.816945	-1.528061	-2.095367
H	-1.157284	-0.349776	3.956170
H	-2.439854	0.355611	2.954902
H	-2.144191	-2.579818	4.535374
H	-3.174831	-3.424920	3.374306
H	-5.982872	-1.342690	0.059215
H	-4.723236	-1.450525	2.164205
H	-3.655303	-1.850519	4.014284
N	1.408695	-1.619266	0.036909
N	-0.732748	-2.014721	-0.036295
C	0.218514	1.666180	-1.047528
C	-0.553105	2.988793	-1.272224

C	-0.726022	3.651547	0.112557
C	-1.110190	2.507713	1.075246
F	1.556137	1.968413	-0.961254
F	0.085847	0.896808	-2.185555
F	0.057112	3.817296	-2.154870
F	0.470004	4.178748	0.486400
F	-1.786114	2.695084	-1.770545
F	-1.623891	4.666765	0.059090
F	-0.741959	2.868870	2.362460
F	-2.496075	2.428617	1.106100

Table S8. Optimized structure (Cartesian coordinates, Å) of **3** with an isopropyl-CH_3 agostic interaction. B3LYP/TZVP with the dispersion correction.

Ni	-0.391174	0.808147	0.452908
C	3.789903	-2.904621	-2.317653
C	4.696197	-0.385735	-0.615341
C	3.144436	-0.632997	-3.211219
C	5.113266	0.208497	0.566642
C	3.008014	-1.610101	-2.033143
C	3.443326	-0.986950	-0.715673
C	4.280147	0.210513	1.674134
C	2.620735	-0.985245	0.424107
C	3.022073	-0.391381	1.631113
C	1.262357	-3.119865	0.497021
C	2.790358	-1.144306	4.034125
C	2.145703	-0.370904	2.873074
C	-0.235944	-3.384601	0.291852
C	-2.317106	-3.504546	-2.900414
C	-2.259843	-1.027211	-3.414094
C	0.150851	-1.063846	0.314723
C	-2.010774	-2.103017	-2.345544
C	1.803885	1.069096	3.286176
C	-2.802131	-1.829016	-1.076894
C	-2.196200	-1.758634	0.186930
C	-4.179063	-1.613165	-1.147512
C	-2.921533	-1.442490	1.349053
C	-2.216599	-1.261256	2.685577
C	-1.686039	0.176906	2.812245
C	-4.915879	-1.313062	-0.012995
C	-4.290094	-1.215473	1.222697
C	-3.092911	-1.605159	3.896429
H	4.851791	-2.689474	-2.457197
H	3.422414	-3.381636	-3.229295
H	5.349164	-0.368060	-1.478459
H	4.192015	-0.412230	-3.427054
H	6.086793	0.680384	0.621056
H	3.710141	-3.623233	-1.498943
H	2.709725	-1.073501	-4.111429
H	2.630039	0.302745	-3.005412
H	1.948715	-1.857214	-1.950072
H	4.611164	0.687340	2.588021
H	1.887580	-3.619013	-0.239777
H	1.609405	-3.400734	1.494488
H	3.011640	-2.175588	3.750134
H	3.726573	-0.679041	4.348987
H	-1.700156	-3.711741	-3.777850
H	-1.584356	-1.179488	-4.258498
H	-0.449495	-3.866257	-0.663251
H	-0.949781	-2.055263	-2.097533
H	-2.133286	-4.287073	-2.160588
H	2.698777	1.614180	3.591895
H	2.121118	-1.162692	4.897750
H	1.208481	-0.874328	2.634963
H	-0.681517	-3.982322	1.087404
H	-2.082453	-0.029404	-3.017644
H	-3.364314	-3.580202	-3.202246
H	1.346461	1.623657	2.464827
H	-3.282041	-1.072809	-3.795979
H	1.108390	1.073564	4.127991
H	-1.355685	-1.934752	2.704126
H	-0.765448	0.318719	2.213234
H	-4.676511	-1.662754	-2.107508
H	-1.349586	0.398888	3.826352

H	-2.426896	0.917255	2.519622
H	-2.488459	-1.601884	4.805461
H	-3.546460	-2.591903	3.789765
H	-5.981760	-1.137448	-0.091817
H	-4.878011	-0.957176	2.092618
H	-3.894201	-0.877394	4.038241
N	1.351114	-1.648937	0.348529
N	-0.790083	-2.016453	0.306958
C	0.350001	1.361073	-1.204248
C	-0.356252	2.642037	-1.705522
C	-0.582085	3.544211	-0.471229
C	-1.092361	2.606119	0.642104
F	1.691060	1.638045	-1.079913
F	0.263159	0.409621	-2.204442
F	0.332465	3.285202	-2.680306
F	0.618380	4.068501	-0.104359
F	-1.570761	2.296314	-2.218669
F	-1.411372	4.576313	-0.766559
F	-0.822137	3.188036	1.872556
F	-2.480013	2.567774	0.559985

Table S9. Optimized structure (Cartesian coordinates, Å) of **3'.** B3LYP/TZVP without the dispersion correction.

Ni	0.716337	0.619532	-0.128477
C	2.380342	-3.856324	-2.632154
C	4.014733	-1.899747	-0.799134
C	2.332598	-1.420464	-3.323239
C	4.635239	-1.615874	0.406875
C	1.993035	-2.426788	-2.212105
C	2.631394	-2.061042	-0.878480
C	3.885001	-1.487694	1.565964
C	1.881939	-1.909079	0.308957
C	2.499294	-1.635936	1.549775
C	-0.239719	-3.359226	0.460329
C	2.050623	-2.677984	3.804689
C	1.715102	-1.517830	2.850059
C	-1.701900	-2.962338	0.210329
C	-3.082523	-1.998010	-3.485488
C	-1.971190	0.273643	-3.590764
C	-0.375798	-1.027060	0.096892
C	-2.361755	-0.901306	-2.679978
C	1.931351	-0.160549	3.538538
C	-3.199373	-0.461860	-1.485031
C	-2.841449	-0.739128	-0.152413
C	-4.396783	0.218135	-1.709397
C	-3.671779	-0.387513	0.928833
C	-3.336703	-0.737720	2.373430
C	-3.400935	0.477760	3.312142
C	-5.218900	0.591279	-0.658303
C	-4.859898	0.284988	0.645361
C	-4.252835	-1.860869	2.896344
H	3.454378	-3.935708	-2.813402
H	1.865224	-4.134374	-3.554554
H	4.614047	-1.995534	-1.695363
H	3.398035	-1.429748	-3.562140
H	5.709933	-1.486164	0.443186
H	2.121611	-4.588494	-1.864022
H	1.789431	-1.674995	-4.236223
H	2.069443	-0.401368	-3.039082
H	0.910674	-2.405567	-2.079304
H	4.384896	-1.260939	2.498733
H	0.122343	-4.113197	-0.239159
H	-0.068465	-3.722476	1.476528
H	1.875123	-3.650034	3.338058
H	3.097423	-2.645540	4.114450
H	-2.447388	-2.352181	-4.301226
H	-1.311580	-0.074478	-4.389174
H	-2.093174	-3.370727	-0.723661
H	-1.433938	-1.330542	-2.301474
H	-3.343527	-2.855712	-2.861143
H	2.966566	-0.035354	3.862500
H	1.435809	-2.617085	4.705651
H	0.653758	-1.587805	2.609439
H	-2.366853	-3.260489	1.018934

H	-1.455424	1.054023	-3.032996
H	-4.007750	-1.619825	-3.925726
H	1.689172	0.669291	2.874312
H	-2.847681	0.722319	-4.063225
H	1.296295	-0.085755	4.424053
H	-2.309022	-1.103687	2.394946
H	-2.761387	1.284916	2.960386
H	-4.691033	0.456811	-2.723682
H	-3.074041	0.191271	4.314709
H	-4.418903	0.863643	3.400604
H	-3.957073	-2.156782	3.905897
H	-4.222445	-2.748065	2.259953
H	-6.142452	1.122230	-0.855138
H	-5.513090	0.576765	1.457902
H	-5.292174	-1.527276	2.938679
N	0.453227	-2.073451	0.254768
N	-1.634693	-1.479943	0.112348
C	2.113402	1.923895	-0.409702
C	1.556062	3.351247	-0.555902
C	0.327503	3.405450	0.377597
C	-0.455901	2.082219	0.167922
F	3.012969	1.924669	0.643199
F	2.866990	1.616152	-1.532163
F	2.439853	4.338050	-0.266911
F	0.764992	3.456513	1.664829
F	1.130569	3.540133	-1.835271
F	-0.425390	4.509658	0.155660
F	-1.260211	1.882288	1.263039
F	-1.303658	2.258074	-0.897087

Table S10. Optimized structure (Cartesian coordinates, Å) of **3'.** B3LYP/TZVP with the dispersion correction.

Ni	0.635538	0.582751	-0.240352
C	2.835043	-3.653462	-2.645862
C	4.123693	-1.694342	-0.673952
C	2.053758	-1.271730	-3.023928
C	4.714874	-1.268198	0.506078
C	2.122962	-2.440381	-2.030016
C	2.764253	-2.001348	-0.723327
C	3.959247	-1.136178	1.662348
C	2.014991	-1.848527	0.458221
C	2.595481	-1.421477	1.666264
C	-0.039204	-3.389353	0.700202
C	2.283461	-2.083596	4.086277
C	1.772772	-1.215169	2.926930
C	-1.497644	-3.093538	0.314923
C	-2.376732	-1.922178	-3.717857
C	-1.275287	0.330804	-3.340893
C	-0.266403	-1.111670	0.150882
C	-1.819957	-0.941268	-2.673670
C	1.726787	0.271149	3.312798
C	-2.858149	-0.615391	-1.609545
C	-2.689536	-0.932105	-0.251670
C	-4.036982	0.030775	-1.981524
C	-3.663568	-0.630360	0.714089
C	-3.485538	-0.987255	2.181715
C	-3.728693	0.209570	3.113386
C	-5.013348	0.336683	-1.046617
C	-4.827614	0.005993	0.287892
C	-4.396876	-2.164219	2.573350
H	3.853721	-3.407986	-2.952242
H	2.297863	-3.993888	-3.533798
H	4.722827	-1.777018	-1.571538
H	3.051637	-0.910998	-3.279000
H	5.769449	-1.022181	0.521557
H	2.890136	-4.483817	-1.938848
H	1.554484	-1.580820	-3.944946
H	1.504006	-0.422788	-2.612838
H	1.096973	-2.741358	-1.813962
H	4.431586	-0.782997	2.569871
H	0.409727	-4.187440	0.108811
H	0.076243	-3.633402	1.759516
H	2.300816	-3.141822	3.815454
H	3.295788	-1.798905	4.380364

H	-1.597811	-2.195688	-4.433718
H	-0.515902	0.074805	-4.081732
H	-1.780501	-3.546489	-0.638748
H	-0.975267	-1.432047	-2.190588
H	-2.747515	-2.836300	-3.248383
H	2.721327	0.645131	3.563899
H	1.639429	-1.963649	4.960236
H	0.747306	-1.520048	2.714392
H	-2.210880	-3.407102	1.073393
H	-0.827893	1.000311	-2.606304
H	-3.202267	-1.479055	-4.278490
H	1.341740	0.879327	2.495159
H	-2.068347	0.882003	-3.849540
H	1.078765	0.418814	4.179237
H	-2.447871	-1.294974	2.322624
H	-3.111480	1.059912	2.830305
H	-4.190101	0.302227	-3.018278
H	-3.488794	-0.065342	4.143279
H	-4.774490	0.523661	3.095566
H	-4.216385	-2.463335	3.608723
H	-4.240152	-3.035268	1.933288
H	-5.919967	0.841521	-1.357436
H	-5.594377	0.255892	1.009912
H	-5.448412	-1.881801	2.484164
N	0.602752	-2.097336	0.408516
N	-1.501126	-1.617006	0.167292
C	1.821691	2.045501	-0.665664
C	1.106771	3.404983	-0.566932
C	0.081834	3.246041	0.577925
C	-0.610896	1.873823	0.369352
F	2.900523	2.063057	0.204625
F	2.375813	1.915843	-1.930989
F	1.923377	4.465905	-0.352721
F	0.753886	3.225057	1.761440
F	0.419652	3.633935	-1.720403
F	-0.791634	4.280882	0.619056
F	-1.195774	1.496012	1.556543
F	-1.639066	2.053177	-0.518351

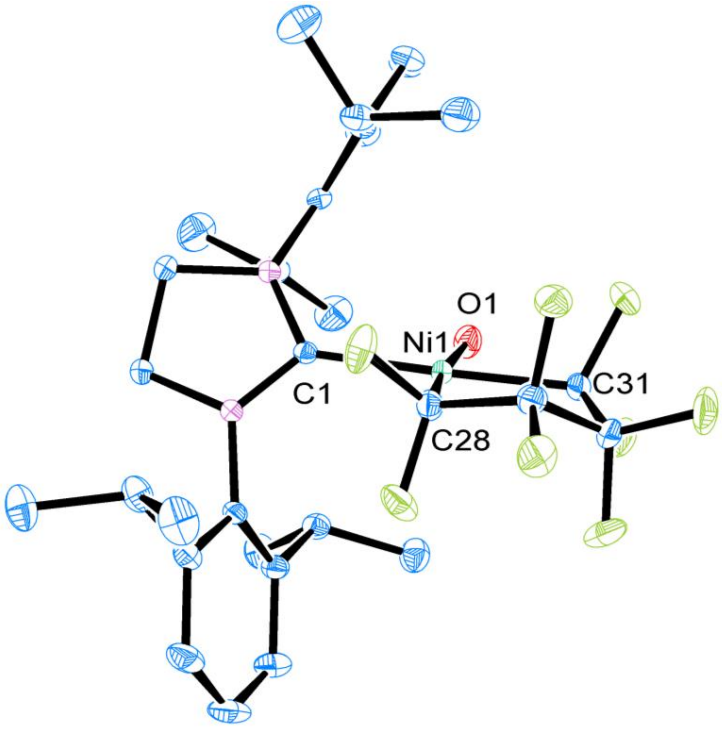

Figure S34. ORTEP representation of the molecular structure of **3**•H_2O with thermal ellipsoid probabilities set to 30 % and hydrogen atoms omitted for clarity.

Table S11. Crystal data and structure refinement for **3**•H_2O.

Complex	**3**•H_2O
ID code	tb069
Formula	$C_{37}H_{46}F_8N_2NiO$
Mw	667.35
Color	yellow
Temp (K)	200(2)
Crystal system Space group	Monoclinic P2(1)/c
a/Å	16.5255(8)
b/ Å	10.6186(5)
c/ Å	20.8839(9)
α/°	90.00
β/°	101.931(2)
γ/°	90.00
V/Å^3	3585.5(3)
Z	4
Dc/g cm^{-1}	1.381
μ/mm^{-1}	0.614
F(000)	1560
Crystal size/mm	0.22x0.19x0.18

2θ range/^{o}	1.99-28.36
Index range	-22<h<22 -14<k<14 -27<l<27
Indep. reflns collected/unique	50510/8894
Max. and min. transmission	0.8974 and 0.8767
(Rint)	0.0234
R1, wR2 (I>2θ(I))	0.0299, 0.0782
R1, wR2(all data)	0.0376, 0.0831
Goodness of fit, F^2	1.027
Data/restraints/params	8894/0/442
Largest diff. peak, hole/Å^3	0.360, -0.283

Table S12. Bond lengths [Å] and angles [°] for complex **3**•H_2O.

……....Ni(1)-C(28)	1.8868(13)	C(5)-C(6)	1.3941(19)
Ni(1)-C(31)	1.9257(14)	C(5)-C(10)	1.5232(19)
Ni(1)-C(1)	1.9580(12)	C(6)-C(7)	1.379(2)
Ni(1)-O(1)	1.9872(10)	C(7)-C(8)	1.379(2)
F(1)-C(28)	1.3766(15)	C(8)-C(9)	1.3984(18)
F(2)-C(28)	1.3825(16)	C(9)-C(13)	1.5126(18)
F(3)-C(29)	1.3560(15)	C(10)-C(12)	1.526(2)
F(4)-C(29)	1.3550(15)	C(10)-C(11)	1.525(2)
F(5)-C(30)	1.3472(16)	C(13)-C(15)	1.522(2)
F(6)-C(30)	1.3638(16)	C(13)-C(14)	1.531(2)
F(7)-C(31)	1.3937(15)	C(16)-C(21)	1.3989(17)
F(8)-C(31)	1.3926(15)	C(16)-C(17)	1.4039(16)
N(1)-C(1)	1.3513(15)	C(17)-C(18)	1.3912(19)
N(1)-C(4)	1.4356(15)	C(17)-C(22)	1.5170(18)
N(1)-C(2)	1.4742(16)	C(18)-C(19)	1.378(2)
N(2)-C(1)	1.3464(15)	C(19)-C(20)	1.378(2)
N(2)-C(16)	1.4384(14)	C(20)-C(21)	1.3965(18)
N(2)-C(3)	1.4787(15)	C(21)-C(25)	1.5173(17)
C(2)-C(3)	1.5166(17)	C(22)-C(23)	1.534(2)
C(4)-C(9)	1.3981(17)	C(22)-C(24)	1.533(2)
C(4)-C(5)	1.4080(18)	C(25)-C(26)	1.528(2)
		C(25)-C(27)	1.5313(19)
		C(28)-C(29)	1.5383(18)

C(29)-C(30)	1.523(2)
C(30)-C(31)	1.521(2)
C(32)-C(33)	1.358(3)
C(32)-C(37)	1.355(4)
C(33)-C(34)	1.321(4)
C(34)-C(35)	1.386(5)
C(35)-C(36)	1.392(4)
C(36)-C(37)	1.359(4)
C(28)-Ni(1)-C(31)	85.98(6)
C(28)-Ni(1)-C(1)	93.26(5)
C(31)-Ni(1)-C(1)	177.64(5)
C(28)-Ni(1)-O(1)	174.05(5)
C(31)-Ni(1)-O(1)	88.07(5)
C(1)-Ni(1)-O(1)	92.69(4)
C(1)-N(1)-C(4)	126.83(10)
C(1)-N(1)-C(2)	112.92(10)
C(4)-N(1)-C(2)	120.12(10)
C(1)-N(2)-C(16)	126.93(10)
C(1)-N(2)-C(3)	112.48(9)
C(16)-N(2)-C(3)	116.78(9)
N(2)-C(1)-N(1)	106.79(10)
N(2)-C(1)-Ni(1)	129.78(8)
N(1)-C(1)-Ni(1)	123.37(8)
N(1)-C(2)-C(3)	101.14(9)
N(2)-C(3)-C(2)	101.67(9)
C(9)-C(4)-C(5)	122.07(11)
C(9)-C(4)-N(1)	120.21(11)
C(5)-C(4)-N(1)	117.62(11)
C(6)-C(5)-C(4)	117.37(12)
C(6)-C(5)-C(10)	119.57(12)
C(4)-C(5)-C(10)	123.04(12)
C(7)-C(6)-C(5)	121.44(13)
C(8)-C(7)-C(6)	120.24(13)
C(7)-C(8)-C(9)	120.93(13)
C(4)-C(9)-C(8)	117.88(12)
C(4)-C(9)-C(13)	122.49(11)
C(8)-C(9)-C(13)	119.59(11)
C(5)-C(10)-C(12)	113.03(13)
C(5)-C(10)-C(11)	110.87(13)
C(12)-C(10)-C(11)	109.36(14)
C(9)-C(13)-C(15)	111.81(13)
C(9)-C(13)-C(14)	109.97(12)
C(15)-C(13)-C(14)	110.19(13)
C(21)-C(16)-C(17)	122.16(11)
C(21)-C(16)-N(2)	119.52(10)
C(17)-C(16)-N(2)	118.07(11)
C(18)-C(17)-C(16)	117.68(12)
C(18)-C(17)-C(22)	119.32(12)
C(16)-C(17)-C(22)	123.00(11)
C(19)-C(18)-C(17)	121.01(13)
C(18)-C(19)-C(20)	120.56(13)
C(19)-C(20)-C(21)	120.87(14)
C(20)-C(21)-C(16)	117.68(12)
C(20)-C(21)-C(25)	118.33(12)
C(16)-C(21)-C(25)	123.97(11)
C(17)-C(22)-C(23)	111.15(12)
C(17)-C(22)-C(24)	111.76(13)
C(23)-C(22)-C(24)	109.78(12)
C(21)-C(25)-C(26)	111.55(11)
C(21)-C(25)-C(27)	110.78(11)
C(26)-C(25)-C(27)	110.94(11)
F(1)-C(28)-F(2)	104.88(10)
F(1)-C(28)-C(29)	104.54(10)
F(2)-C(28)-C(29)	106.53(10)
F(1)-C(28)-Ni(1)	111.37(9)
F(2)-C(28)-Ni(1)	116.14(9)
C(29)-C(28)-Ni(1)	112.47(9)
F(4)-C(29)-F(3)	106.18(11)
F(4)-C(29)-C(30)	108.05(11)
F(3)-C(29)-C(30)	111.73(11)
F(4)-C(29)-C(28)	110.04(11)
F(3)-C(29)-C(28)	113.96(11)
C(30)-C(29)-C(28)	106.77(11)

F(5)-C(30)-F(6)	106.72(11)
F(5)-C(30)-C(31)	109.93(12)
F(6)-C(30)-C(31)	114.85(12)
F(5)-C(30)-C(29)	108.71(12)
F(6)-C(30)-C(29)	110.71(12)
C(31)-C(30)-C(29)	105.82(10)
F(8)-C(31)-F(7)	102.57(10)
F(8)-C(31)-C(30)	106.35(11)
F(7)-C(31)-C(30)	107.68(11)
F(8)-C(31)-Ni(1)	111.21(9)
F(7)-C(31)-Ni(1)	115.04(9)
C(30)-C(31)-Ni(1)	113.14(9)
C(33)-C(32)-C(37)	121.4(3)
C(34)-C(33)-C(32)	120.5(3)
C(33)-C(34)-C(35)	119.7(2)
C(34)-C(35)-C(36)	120.0(3)
C(37)-C(36)-C(35)	118.6(3)
C(36)-C(37)-C(32)	119.7(2)

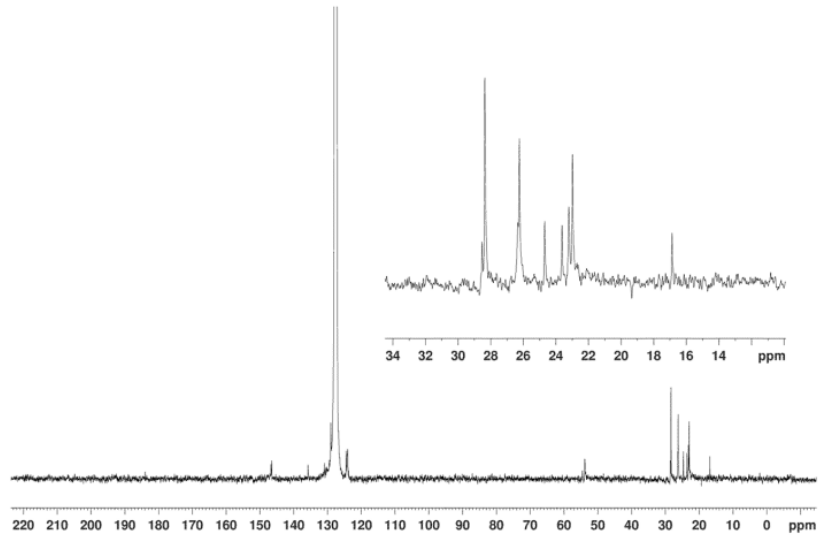

Figure S22. $^{13}C\{^{1}H\}$ NMR spectrum (75 MHz, C_6D_6) of **5c**. The inset shows the expanded (horizontal scale) signal.

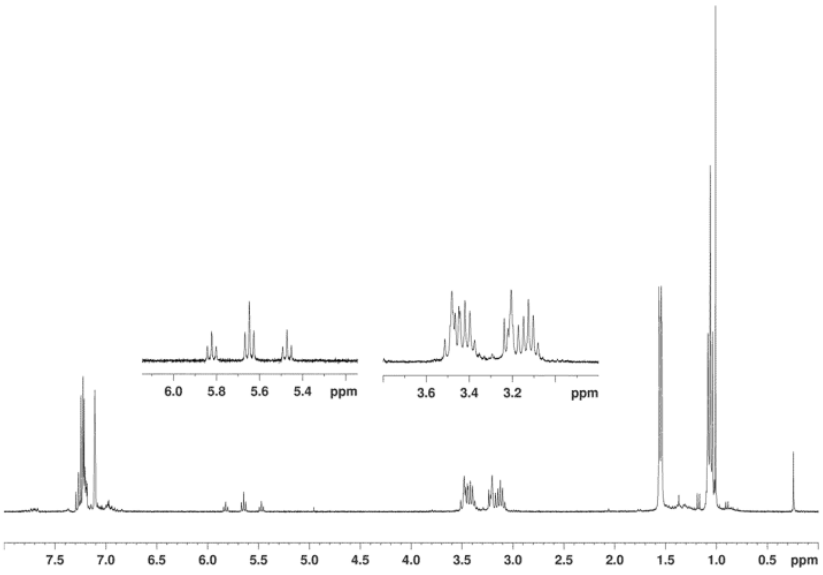

Figure S23. ^{1}H NMR spectrum (300 MHz, C_6D_6) of **6a**. The residual protio-solvent peak is labeled '*'. The inset shows the expanded (horizontal scale) signal.

Supplement B (Part 2)

Contents

Experimental

All phosphine and phosphite ligands were used as received from Strem, Sigma-Aldrich, Alfa Aesar, or Cytec Canada. Bis(1,5-cyclooctadiene)nickel(0) (Strem), vinylidene difluoride (Synquest), 1-adamantyl amine (Oakwood), trimethylsilyl trifluoromethanesulfonate (Fluka), tert-butylamine (Alfa), paraformaldehyde (Alfa), glyoxal (Sigma-Aldrich), and tetrafluoroboric acid (Fisher) were used as received. All reactions (except for the syntheses of the NHC salts) were performed in a N_2-filled

glovebox. The HFO-1132a gas was injected into the reaction medium using a bonded-septum vial outside the glovebox, while any workup steps were performed in the glovebox. All solvents used were dried by distillation from CaH_2 (acetonitrile, $CHCl_3$) or sodium (isooctane, xylenes, toluene. Deuterated benzene was dried by passing through a column packed with activated (Brockmann I) alumina. The remainder of solvents used were dried using an mBraun Solvent Purification System.

Preparation of 1,3-di(1-adamantyl)imidazolium tetrafluoroborate (**IAd-HBF$_4$**)

A 125 ml flask was charged with 1-adamantyl amine (5.00 gr, 33 mmol) and paraformaldehyde (993 mg, 33 mmol). The contents were suspended in 50 ml of chloroform and stirred at RT for 1 hour. Then, the solution was transferred to an ice bath and another 5.00 grams of 1-adamantyl amine were added, followed by dropwise addition of (in order) aqueous tetrafluoroboric acid 48% (4.3 ml, 33 mmol) and 40% aqueous glyoxal (3.8 ml, 33 mmol). The mixture was heated at 65ºC for 18 hours, following which the solution was diluted with 50 ml of methylene chloride and extracted with 50 ml of saturated aqueous sodium carbonate. Occasionally this produces some precipitate which must be filtered before the next step. The aqueous phase was extracted two more times with 20 ml of methylene chloride and dried over anhydrous $MgSO_4$. The solution was then concentrated under reduced pressure to about 25% of its original volume and petroleum ether (25 ml) was added. The product precipitated out of the red-orange solution as a white solid. The white solid was filtered, washed with another portion (10 ml) of petroleum ether, and redissolved in a minimum of boiling chloroform. As the solution cooled to room temperature, a few drops of petroleum ether was added, and the flask was cooled to –10ºC for several hours to produce the title compound as colorless crystals which were filtered, washed with petroleum ether (3 x 10 ml), and dried in vacuo at 50˚C for an hour – recovered 7.1 grams (51% yield). ^{1}H NMR shifts match those reported in the literature. **I^{t}Bu-HBF$_4$** was prepared similarly.

Preparation of 1,3-di(1-adamantyl)imidazol-2-ylidene (**IAd**)

A round-bottomed flask was charged with IAd-HBF_4 (1.00 gr, 2.36 mmol) and dissolved in THF (75 ml). Potassium *tert*-butylate (290 mg, 1 equiv.) was added and the mixture was stirred at RT for 4 hours. The reaction mixture clarified over the elapsed time. The volatiles were removed under reduced pressure, and the residue extracted into ethyl ether (3 x 5 ml). The extracts were combined, filtered through a pad of celite, and dried under reduced pressure to give the title compound as a free-flowing off-white powder – recovered 740 mg (93% yield).

I^{t}Bu was prepared similarly from 1.00 gr (3.73 mmol) of the analogous tetrafluoroborate salt – recovered 580 mg, (87% yield – some product likely lost to sublimation).

Synthesis of **(DPEphos)Ni(η^2-VDF)**

Bis(1,5-cyclooctadiene)nickel(0) (100 mg, 364 μmol) and DPEPhos (200 mg, 1 equiv.) were dissolved in ethyl ether (5 ml), giving a red-orange solution; VDF (45 ml) was then added in a single injection, and the reaction was stirred at room temperature for 45 minutes, giving a yellow precipitate. After the elapsed time the reaction was cooled to -35˚C, filtered through a medium porosity fritted funnel, washed with hexanes (3 x 5ml), and dried *in vacuo* to give the title compound as a bright yellow powder – recovered 274 mg (97% yield). ^{19}F NMR (292 MHz) –92.5 ppm (tt, J_{F-P} = 47 Hz, J_{F-H} = 13 Hz).

Formation of **(DPEphos)Ni(CF=CH$_2$)OTf** (not isolated)

(DPEphos)Ni(η^2-VDF) (20 mg, 30 μmol) was dissolved in benzene and trimethylsilyl triflate (7 mg, 1 equiv.) was added. The mixture was allowed to sit at room temperature for 30 minutes. 19F NMR (292 MHz) shows the presence of [Ni(DPEphos)(C(**F**)=CH$_2$)$^+$] : –30.6 ppm (tdd, J_{F-P} = 48 Hz, $J_{F-H(trans)}$ = 41 Hz, $J_{F-H(cis)}$ = 21 Hz).

Generalized method for ligand screening for 3-membered VDF-metallacycles

Bis(1,5-cyclooctadiene)nickel(0) (20 mg, 73 μmol) and ligand (1 equiv. if bidentate, 2 equiv. if monodentate) were added to a scintillation vial, dissolved in benzene and sealed with a bonded-septum screw-cap. VDF (20 ml) was added by syringe injection through the septum and the reaction was warmed at 45˚C for 30 minutes prior to analysis by NMR. The reader should note that these metallacycles are unstable under vacuum, and so they may be only isolated by precipitation from the reaction media. Since the trialkylphosphine ligand products do not precipitate even out of pentane, they could not be isolated in pure form, and were thus only characterized spectroscopically. **The results of the screening are in Tables 1 and 2** of Part 2.

Synthesis of **[Ni(IAd)($CF_2CH_2C(F)=CH_2$)(μ-F)]$_2$**

IAd (61 mg, 0.182 mmol) and bis(1,5-cyclooctadiene)nickel(0) (50 mg, 1 eq.) were added to a scintillation vial and suspended in anhydrous isooctane (5 ml). The vial was sealed with a septum-fitted screw cap and vinylidene difluoride (50 ml) was added via syringe injection to the solution while stirring. The solution was allowed to stir at 45˚C for 1 hour, after which time a tangerine-orange precipitate formed. The vial was then cooled to -35ºC and filtered through a medium porosity fritted funnel to give the product as a golden-yellow powder (75 mg, 79% yield).

Note: the solvent for this reaction is preferably isooctane (for highest yield) but methyl tert-butyl ether can also be used. The product is soluble in THF, and aromatic solvents, so if any of these are used in the preparation, the volatiles must be first removed under reduced pressure, and the residue triturated with hexanes to liberate the product. X-ray quality crystals can be obtained from a warm toluene liquor.

^{1}H NMR (400 MHz): 6.41 ppm (2H s, NHC backbone), 4.55 ppm (1H dd, 17, 2.2 Hz, =CH *cis*), 4.16 ppm (1H dd, 49, 2.2 Hz, =CH *trans*), 3.65 ppm (6H d(b), Ad CH_2), 3.30 ppm (6H d(b), Ad CH_2), 3.20 ppm (2H q, 20 Hz, $CF_2C\mathbf{H}_2$–CF=), 2.50 ppm (6H, s(b), Ad CH), 2.15 ppm (6H d(b), Ad CH_2), 1.90 ppm (6H, d(b), Ad CH_2). **^{19}F NMR** (376 MHz): -71.1 ppm (2F qt, 20, 12, 7 Hz, α-CF_2), -87.3 ppm (1F dq, 49, 17, 7 Hz, γ-CF), -426.7 ppm (Ni–F).

Synthesis of **[Ni(ItBu)($CF_2CH_2C(F)=CH_2$)(*μ*-F)]$_2$**

I^{t}Bu (66 mg, 0.364 mmol) and bis(1,5-cyclooctadiene)nickel(0) (100 mg, 1 eq.) were added to a scintillation vial and suspended in anhydrous isooctane (5 ml). The vial was sealed with a septum-fitted screw cap and vinylidene difluoride (50 ml) was added via syringe injection to the solution while stirring. The solution was allowed to stir at 45˚C for 1 hour, after which time a tangerine-orange precipitate formed. The vial was then cooled to -35ºC and filtered through a medium porosity fritted funnel to give the product as a golden-yellow powder (102 mg, 76% yield).

Note: the solvent for this reaction is preferably isooctane (for highest yield) but methyl tert-butyl ether can also be used. The product is soluble in THF, and aromatic solvents, so if any of these are used in the preparation, the volatiles must be first removed under reduced pressure, and the residue triturated with hexanes to liberate the product.

^{1}H NMR (400 MHz): 6.41 ppm (2H s, NHC backbone), 4.54 ppm (1H dd - 17, 2.2 Hz, =CH *cis*), 4.11 ppm (1H dd, 49, 2.2 Hz, =CH *trans*), 2.90 ppm (2H q, 19.8 Hz, β-H), 2.44-2.39 ppm (18H s, *tert*-butyls). **^{19}F NMR** (376 MHz): -73.3 ppm (2F, m), -88.8 ppm (1F, m), -427.1 ppm (Ni-F). MS (m/z 337.4, 393.3, 413.3, 421.3, 434.3, 503,5, 544.4)

Catalytic hydrodefluorodimerization reactions

1mg each of $Ni(COD)_2$ and ligand were weighed into a scintillation vial and suspended in 3ml of anhydrous benzene. Triethylsilane (50 μL) was added by syringe and the vial was sealed with a bonded-septum cap. Vinylidene difluoride (30 ml) was injected by syringe and the reaction was warmed at 40˚C for 45 minutes. ^{19}F NMR after the elapsed time shows only VDF (m, 82.8 ppm), **HFO** (-96 ppm (m, CF), -117 ppm (dtd 55 Hz (F–CH2), 16 Hz (F–H), 4 Hz (F–F)), Et_3SiF (–175 ppm, s) and a small signal for free fluoride (–150 ppm, s). The conversion was determined based on integration of the silyl fluoride peak. The results of the ligand screening are presented in **Table 4.**

Formation of **[Ni(IAd)($CF_2CH_2C(F)=CH_2$)(p-NO_2-C_6H_4COO)]** (not isolated)

[Ni(IAd)($CF_2CH_2C(F)=CH_2$)(μ-F)]$_2$ (5 mg, 9 μmol) and *p*-nitrobenzoic acid (2 mg, 1 equiv.) were dissolved in chloroform-d and stirred at RT for 1 hour. ^{19}F NMR (272 MHz) -70.1 ppm (td, CF_2, 20 Hz (F–H), 7 Hz (F–F)), -89 ppm (m, CF).

Reaction of **[Ni(IAd)($CF_2CH_2C(F)=CH_2$)(μ-F)]$_2$** with diphenylzinc with $P(OEt)_3$

[Ni(IAd)($CF_2CH_2C(F)=CH_2$)(μ-F)]$_2$ (20 mg) and diphenylzinc (16 mg) were dissolved in benzene-d_6 and two drops of triethylphosphite were added. The reaction was allowed to stir at room temperature for one hour. In addition to residual starting material, two isomers of a butadiene product were identified by NMR as well as the proposed intermediate [Ni(IAd)($CF_2CH_2C(F)=CH2$)($P(OEt)_3$)]. 1-phenyl-1,3-difluorobutadiene was produced in both cis and trans isomers in a ratio of 1:1.5 respectively. NMR data is shown below:

cis-1-phenyl-1,3-difluorobutadiene: ^{19}F NMR (282 MHz) -97.3 ppm (ddd, γ-F, 47 Hz, 23 Hz, 16 Hz), -111 ppm (d, α-F, 37 Hz)

trans-1-phenyl-1,3-difluorobutadiene: ^{19}F NMR (282 MHz) -98.5 ppm (ddt, γ-F, 49 Hz, 21 Hz, 18 Hz), -107 ppm (dd, α-F, 36 Hz, 22 Hz)

[Ni(IAd)($CF_2CH_2C(F)=CH_2$)($P(OEt)_3$)]: ^{19}F NMR (282 MHz) -72.6 ppm (dtd, α-F, 41 Hz (F–P), 21 Hz (F–H), 7 Hz (F–F)), -86 ppm (m, γ-F)

NMR Spectra

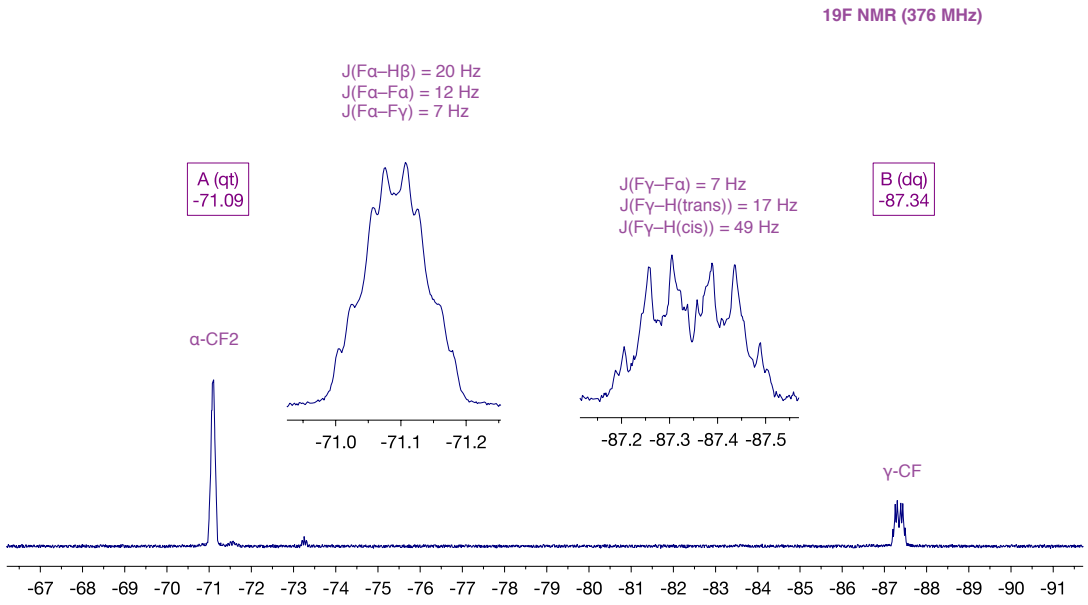

Figure S35: ^{19}F NMR (376 MHz. in C_6D_6) of $[Ni(IAd)(CF_2CH_2CF(=CH_2)(\mu–F)]_2$ (referenced externally to C_6F_6).

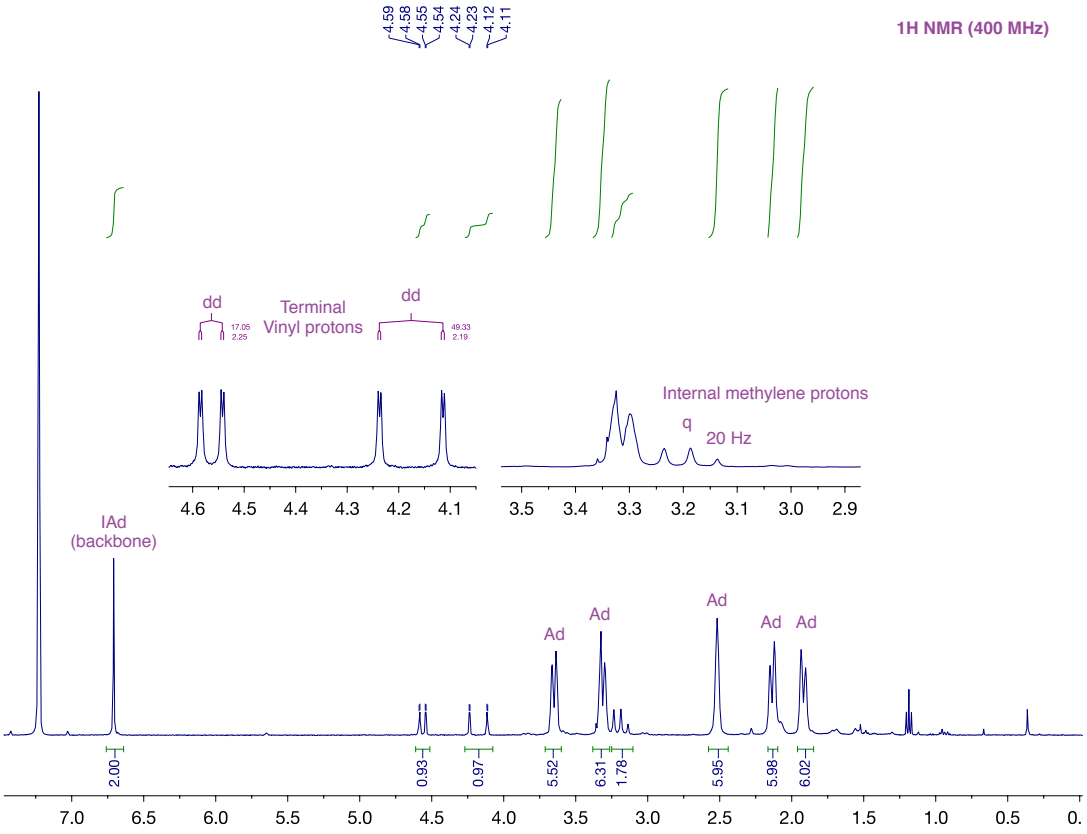

Figure S36: ^{1}H NMR (400 MHz. in C_6D_6) of $[Ni(IAd)(CF_2CH_2CF(=CH_2)(\mu–F)]_2$.

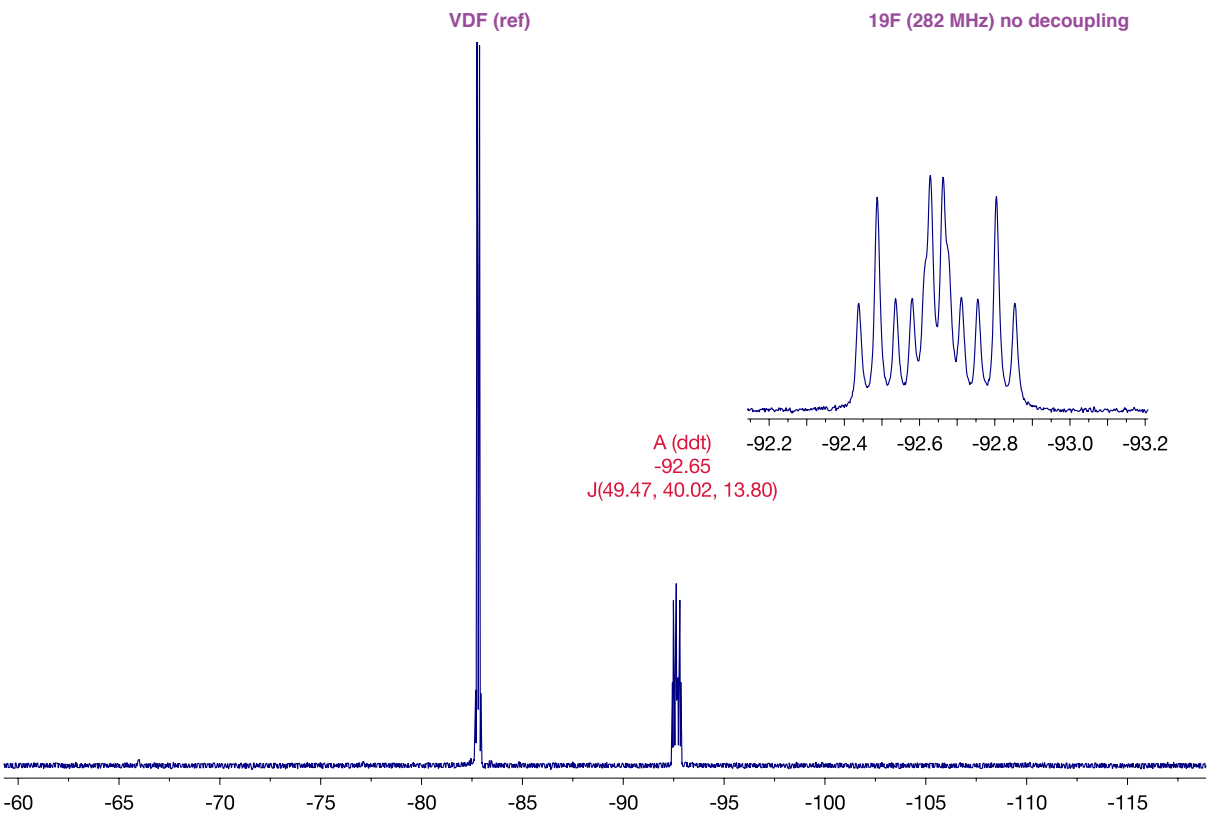

Figure S37: ^{19}F NMR (282 MHz. in C_6D_6) of [Ni(dibpe)(η^2-CF_2=CH_2)] (referenced to VDF)

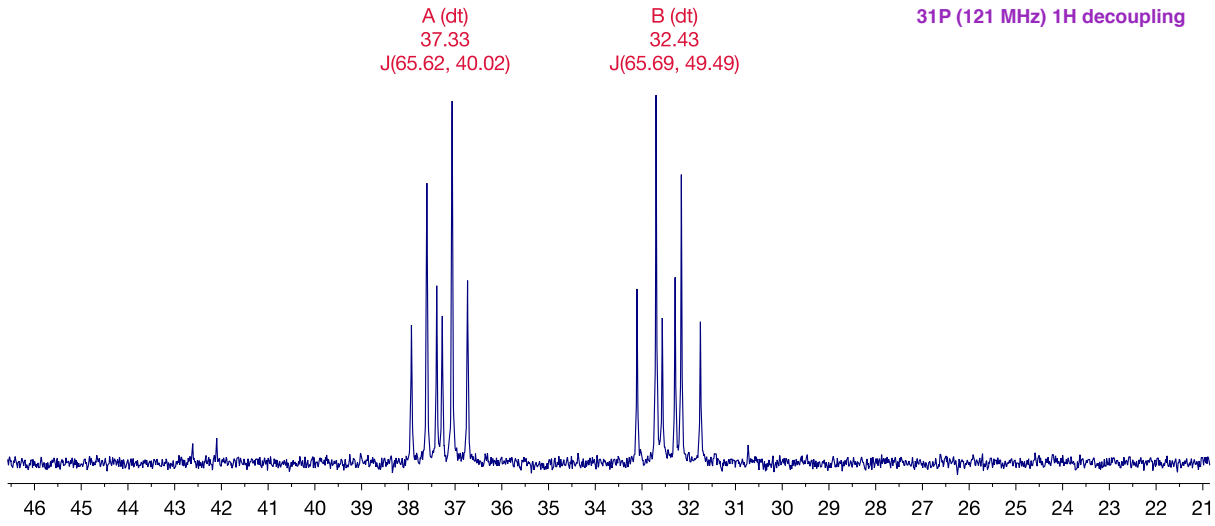

Figure S38: ^{31}P NMR (121 MHz. in C_6D_6) of [Ni(dibpe)(η^2-CF_2=CH_2)] (referenced externally to H_3PO_4)

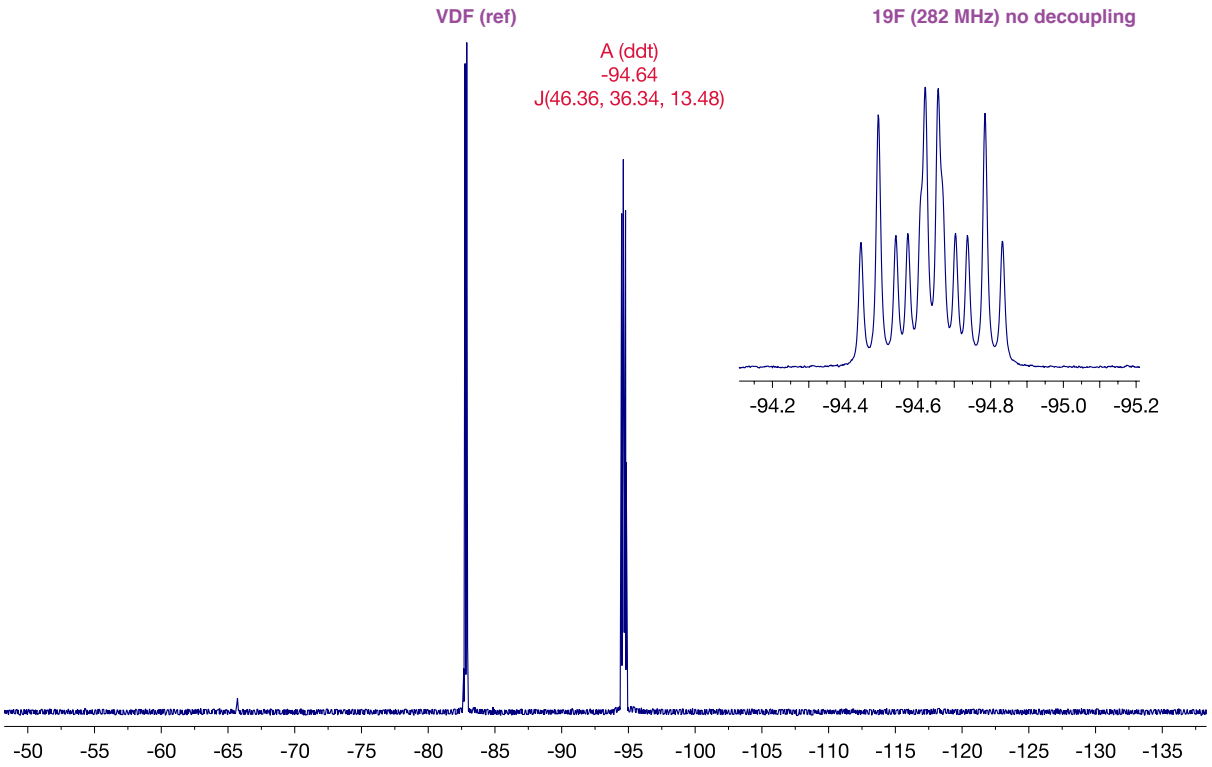

Figure S39: ^{19}F NMR (282 MHz. in C_6D_6) of [Ni(dibpp)(η^2-CF_2=CH_2)] (referenced to VDF)

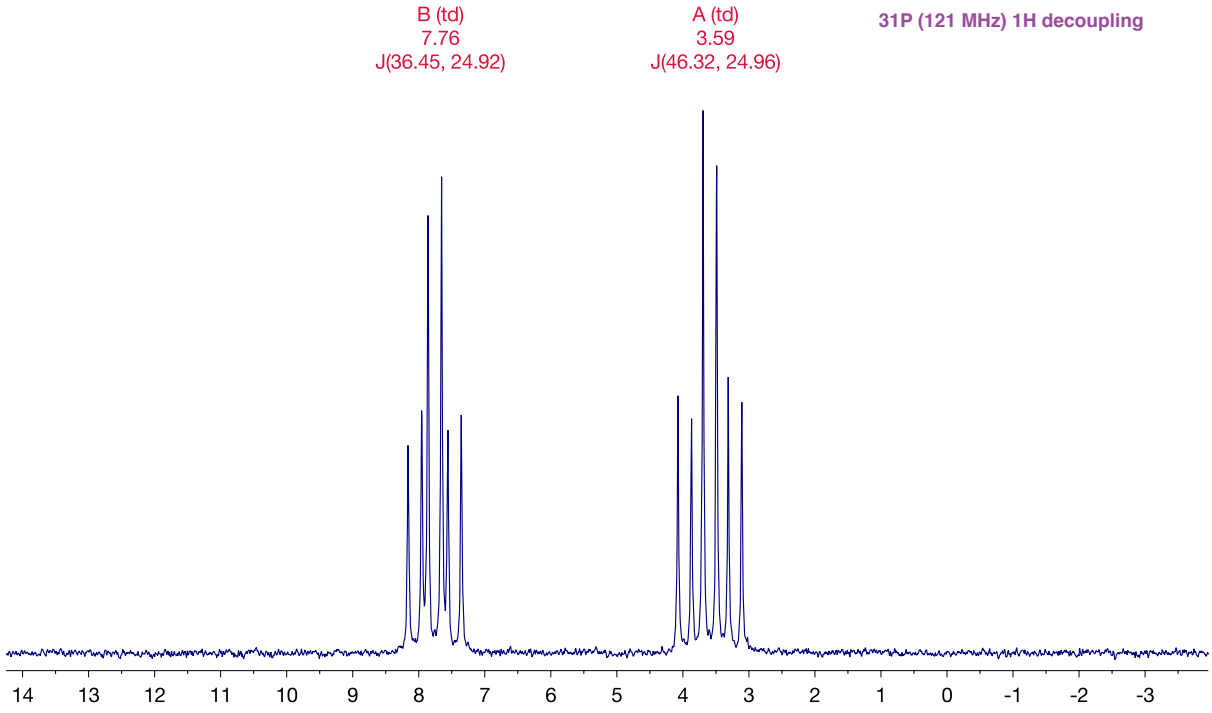

Figure S40: ^{31}P NMR (121 MHz. in C_6D_6) of [Ni(dibpp)(η^2-CF_2=CH_2)] (referenced externally to H_3PO_4)

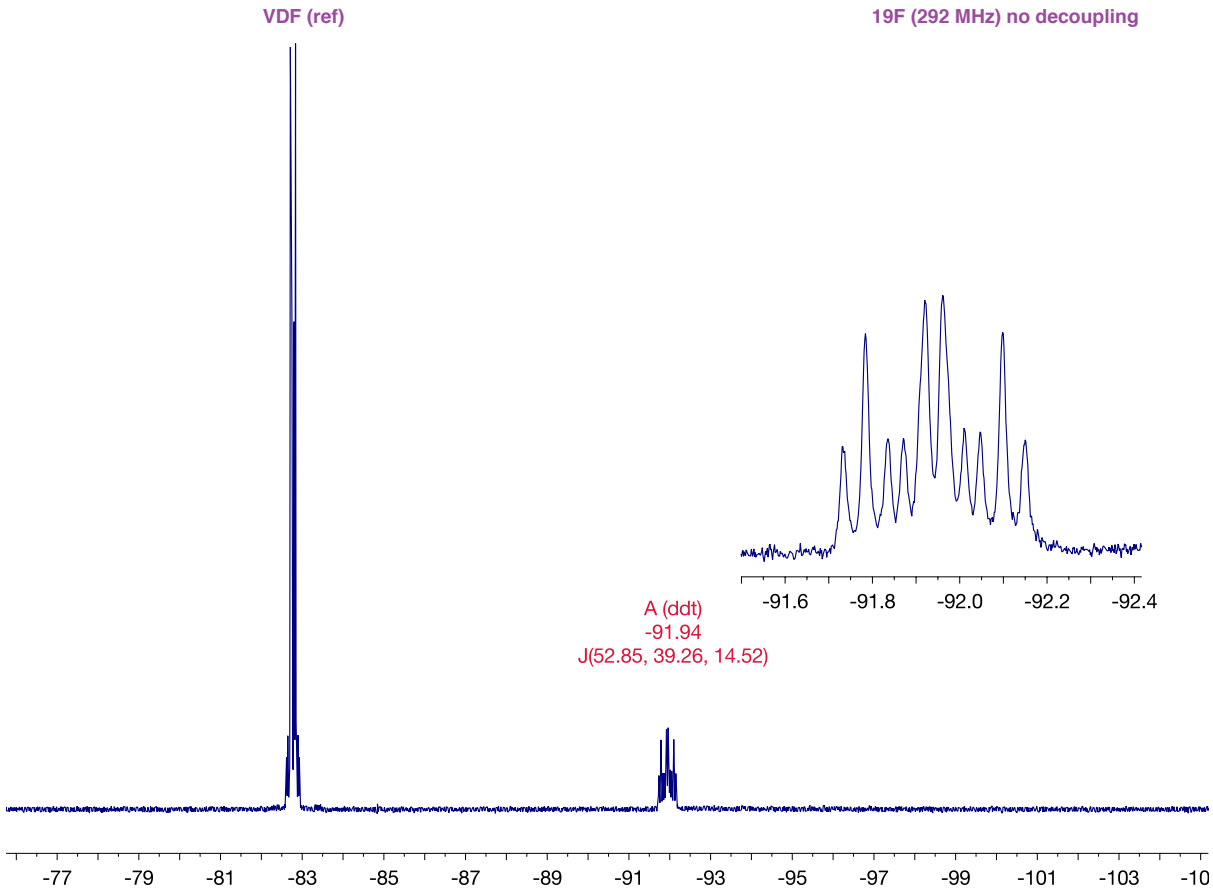

Figure S41: ^{19}F NMR (282 MHz. in C_6D_6) of [Ni(dcppe)(η^2-CF_2=CH_2)] (referenced to VDF)

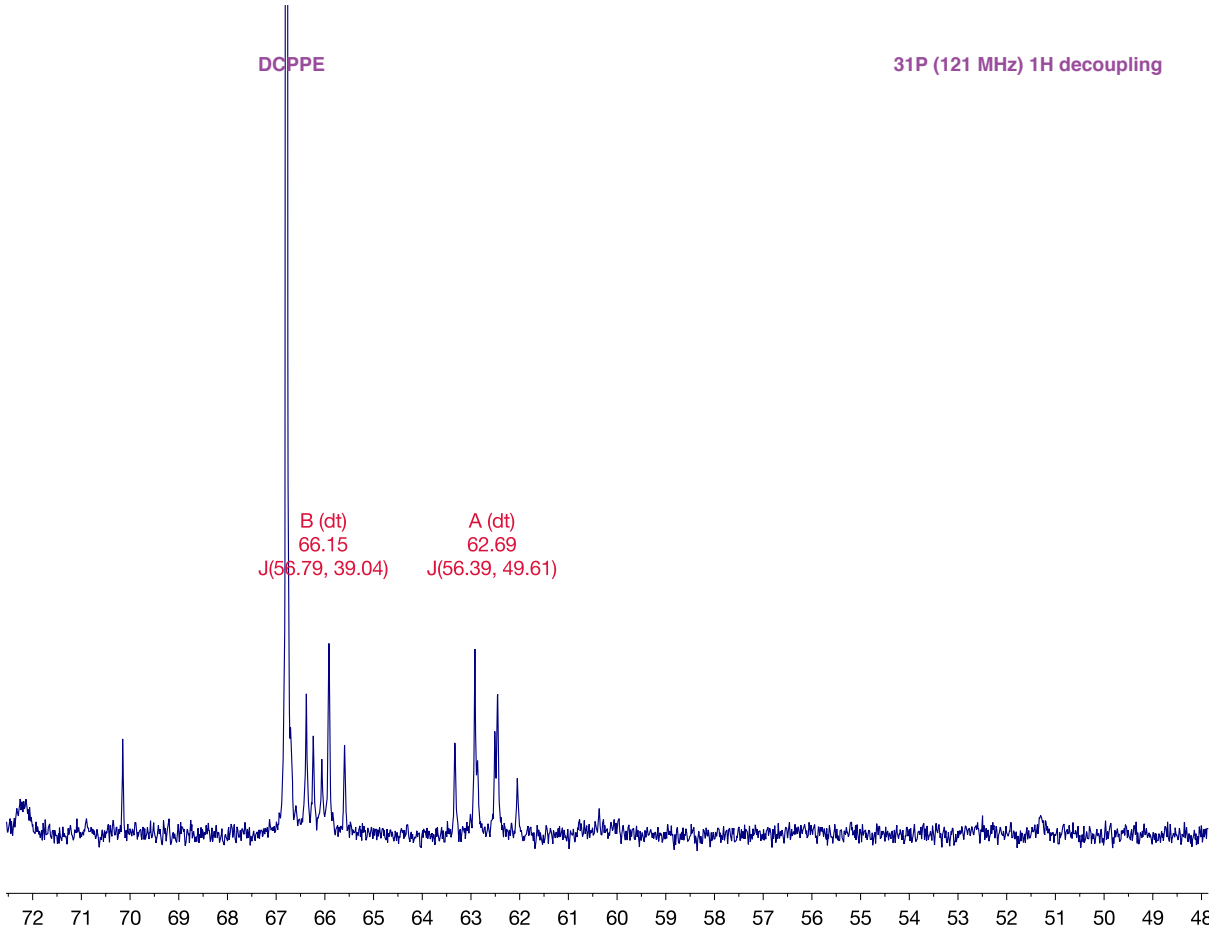

Figure S42: ^{31}P NMR (121 MHz. in C_6D_6) of [Ni(dcppe)(η^2-CF_2=CH_2)] (referenced externally to H_3PO_4)

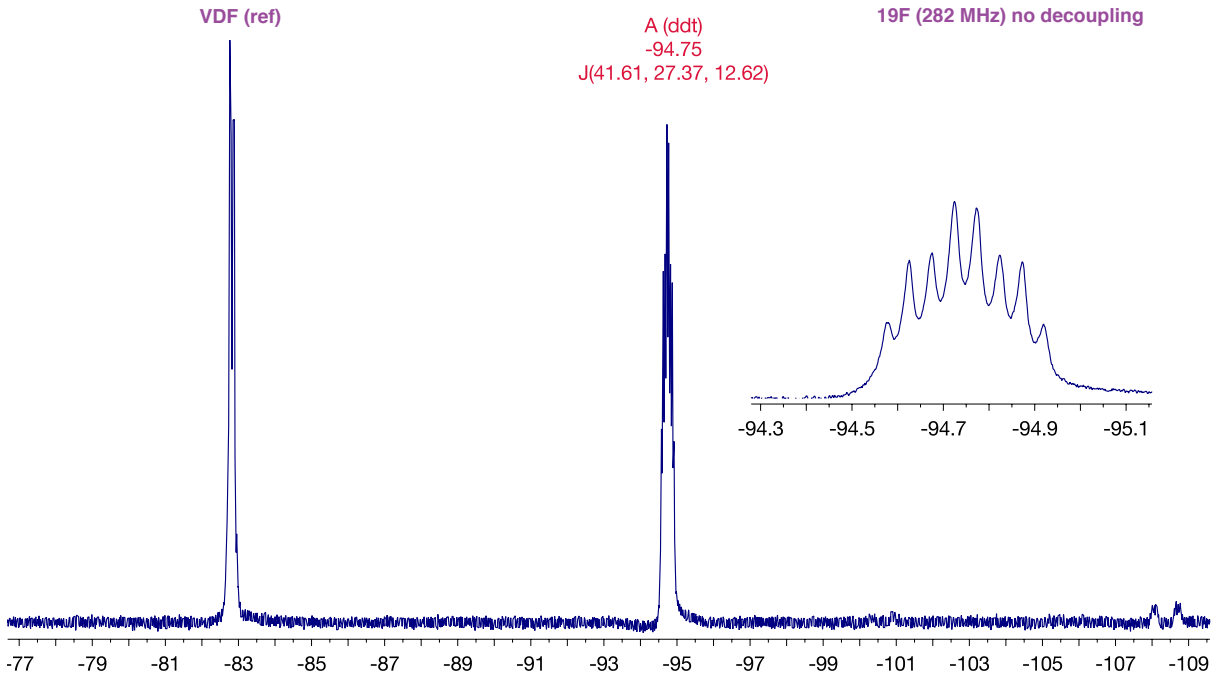

Figure S43: ^{19}F NMR (282 MHz. in C_6D_6) of [Ni(dppf)(η^2-CF_2=CH_2)] (referenced to VDF)

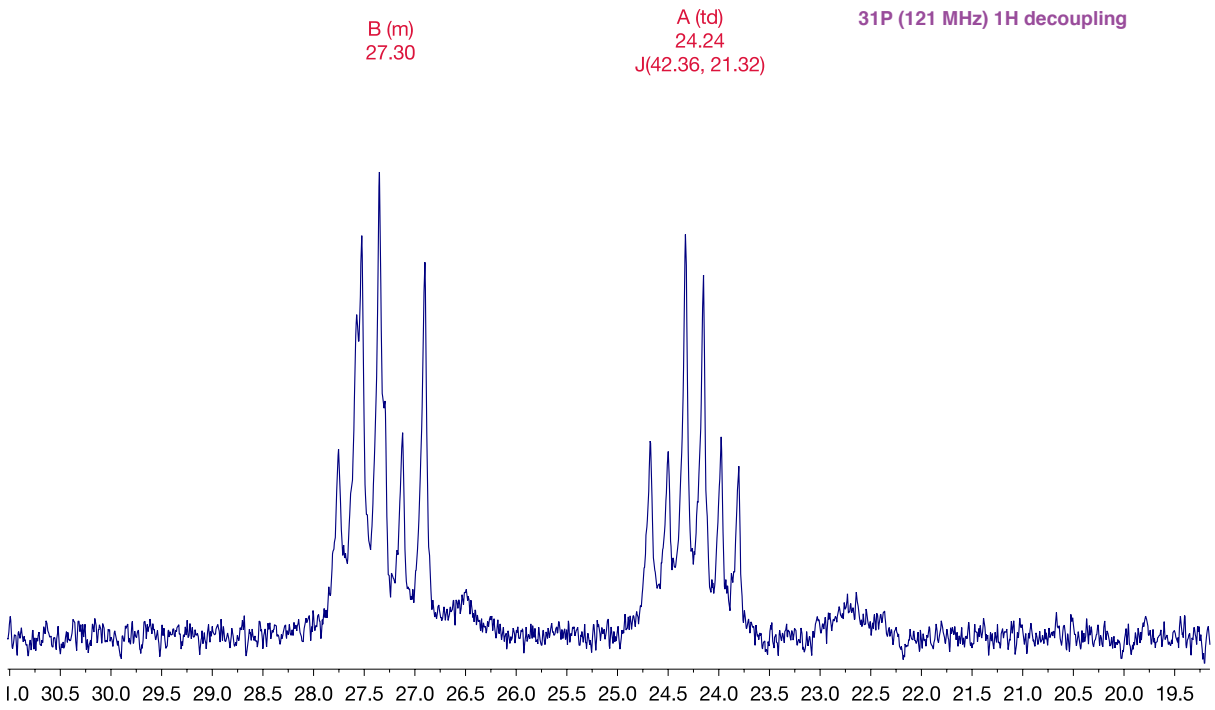

Figure S44: ^{31}P NMR (121 MHz. in C_6D_6) of [Ni(dppf)(η^2-CF_2=CH_2)] (referenced externally to H_3PO_4)

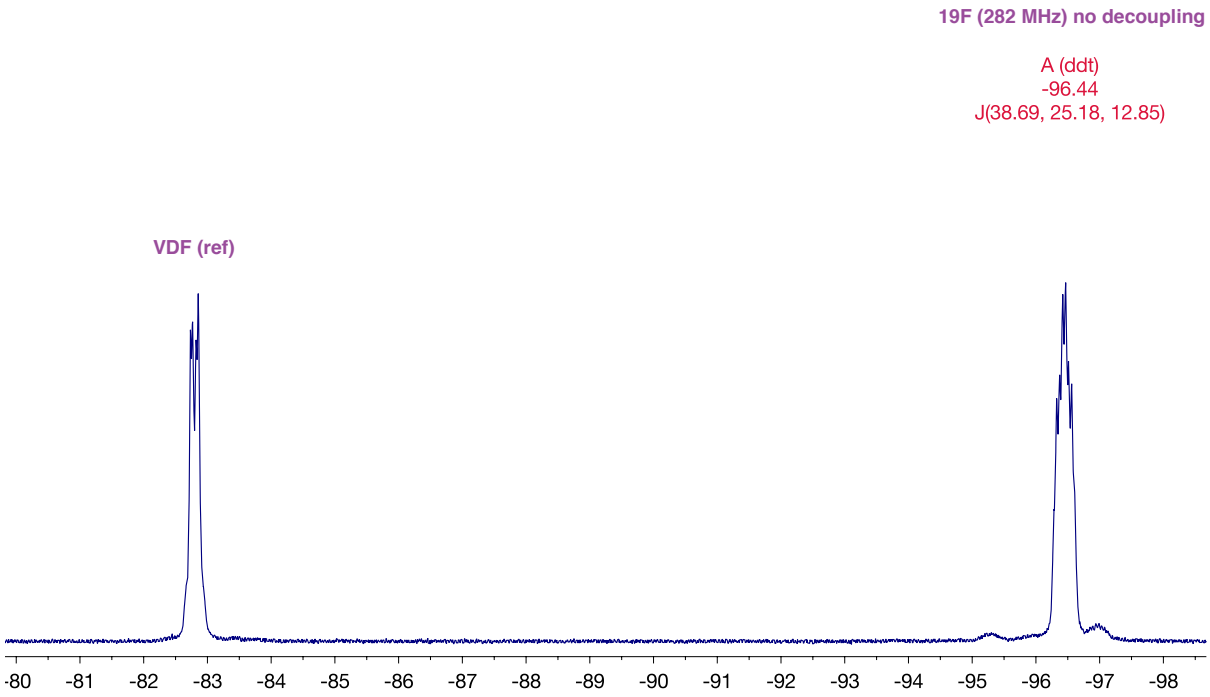

Figure S45: ^{19}F NMR (282 MHz. in C_6D_6) of $[Ni(PBu_3)_2(\eta^2\text{-}CF_2{=}CH_2)]$ (referenced to VDF)

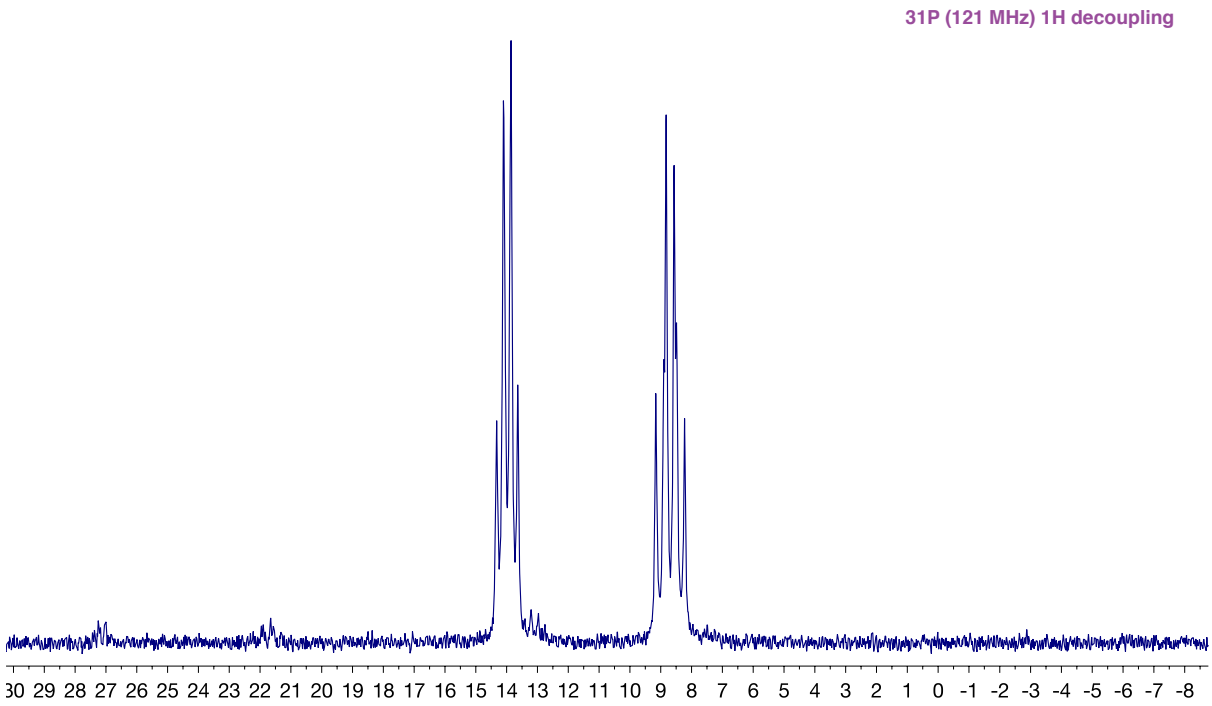

Figure S46: ^{31}P NMR (121 MHz. in C_6D_6) of $[Ni(PBu_3)_2(\eta^2\text{-}CF_2{=}CH_2)]$ (referenced externally to H_3PO_4)

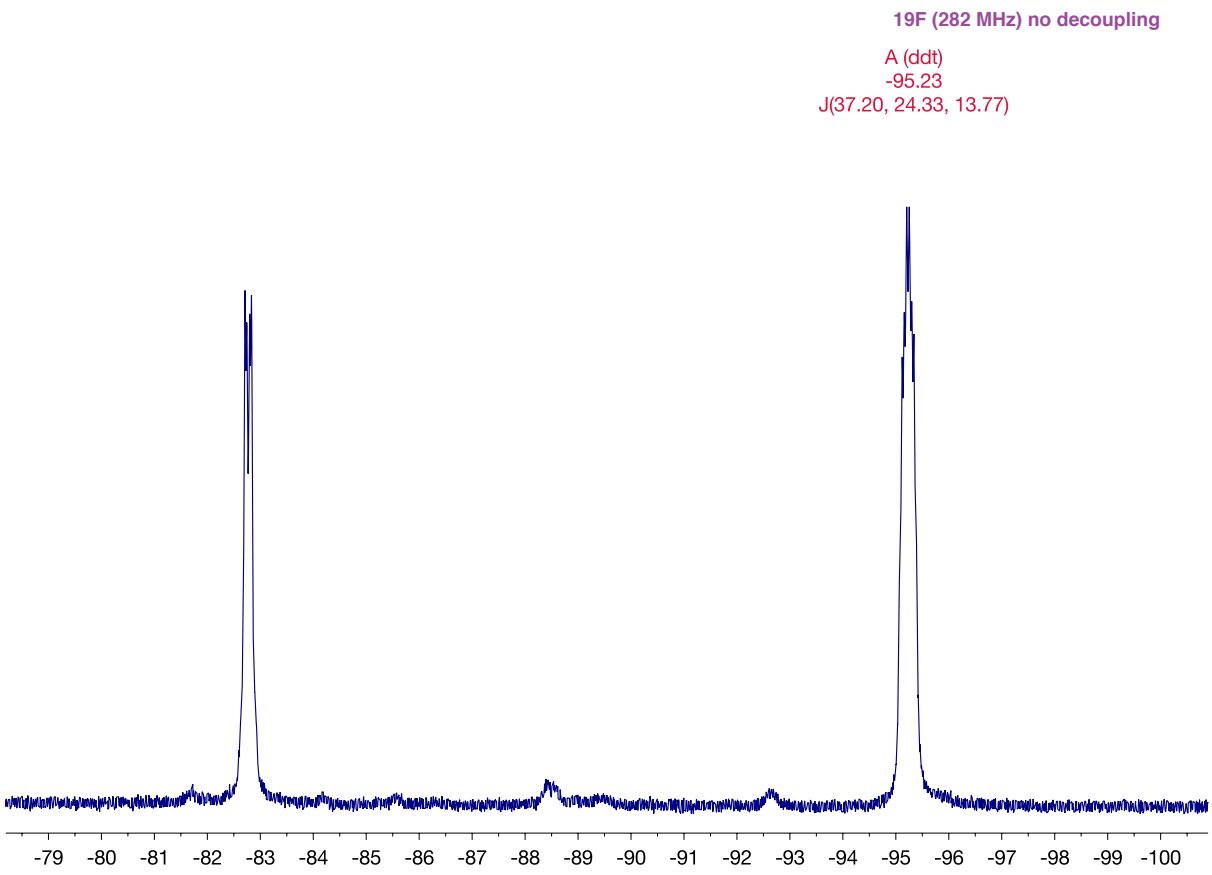

Figure S47: ^{19}F NMR (282 MHz. in C_6D_6) of [Ni(P(*i*-Bu)$_3$)$_2$(η^2-CF_2=CH_2)] (referenced to VDF)

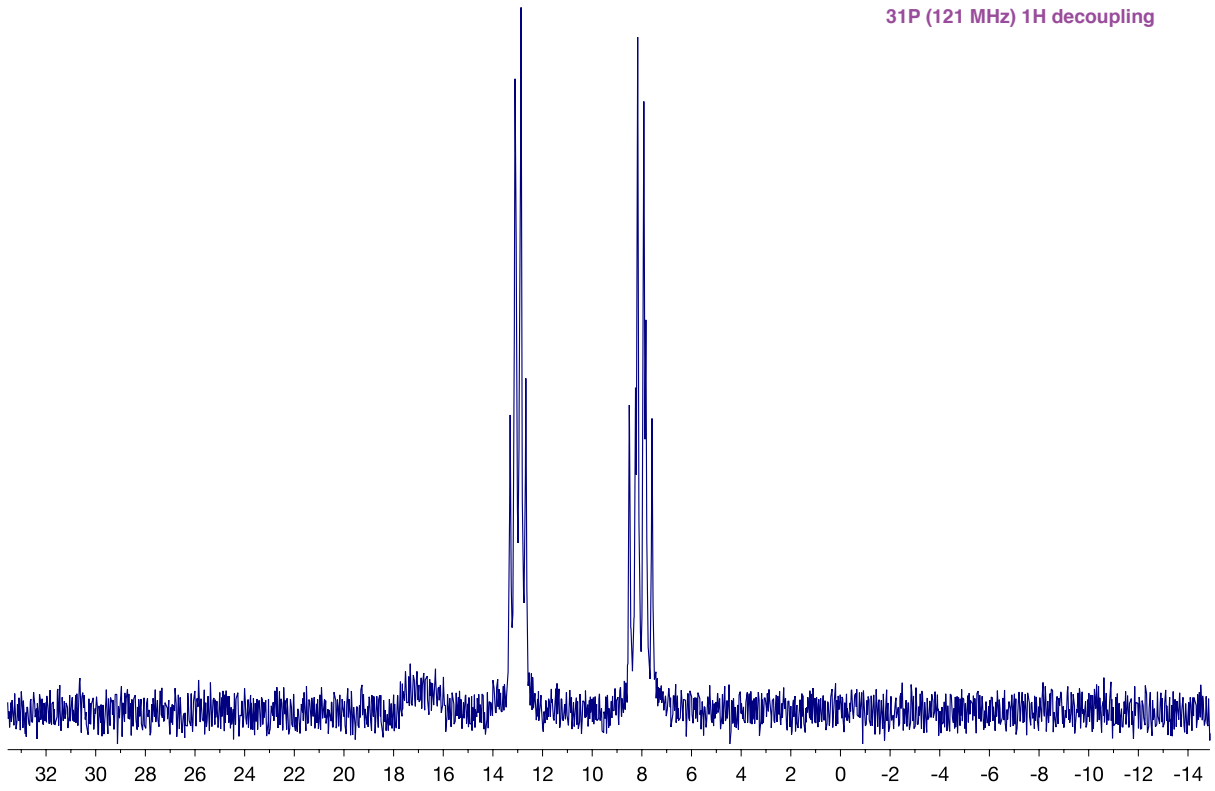

Figure S48: ^{31}P NMR (121 MHz. in C_6D_6) of [Ni(P(*i*-Bu)$_3$)$_2$(η^2-CF_2=CH_2)] (referenced externally to H_3PO_4)

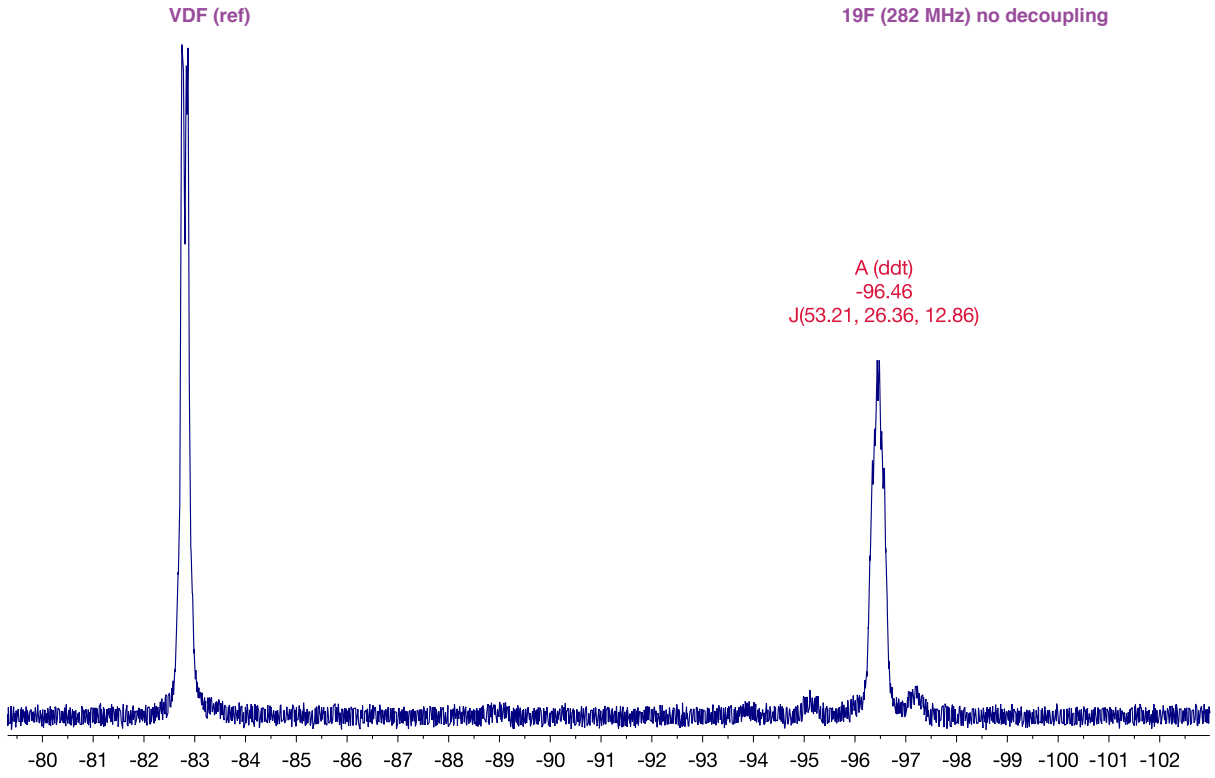

Figure S49: ^{19}F NMR (282 MHz. in C_6D_6) of [Ni(P(*n*-Pr)$_3$)$_2$(η^2-CF_2=CH_2)] (referenced to VDF)

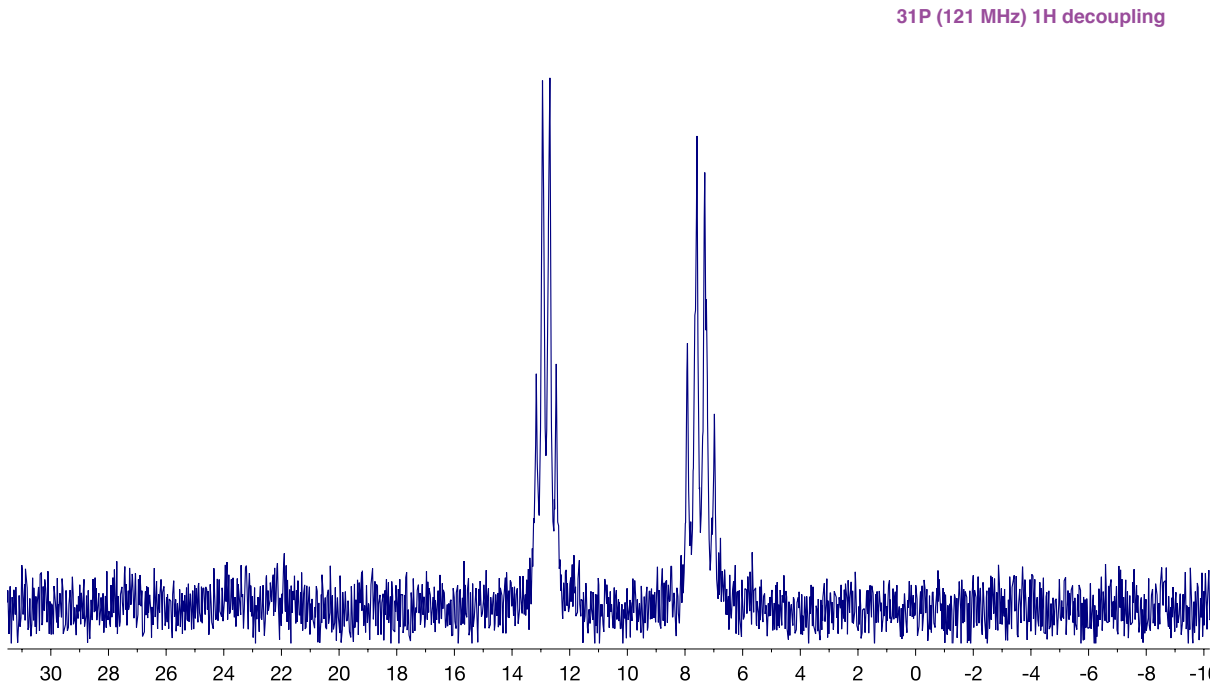

Figure S50: ^{31}P NMR (121 MHz. in C_6D_6) of [Ni(P(*n*-Pr)$_3$)$_2$(η^2-CF_2=CH_2)] (referenced externally to H_3PO_4)

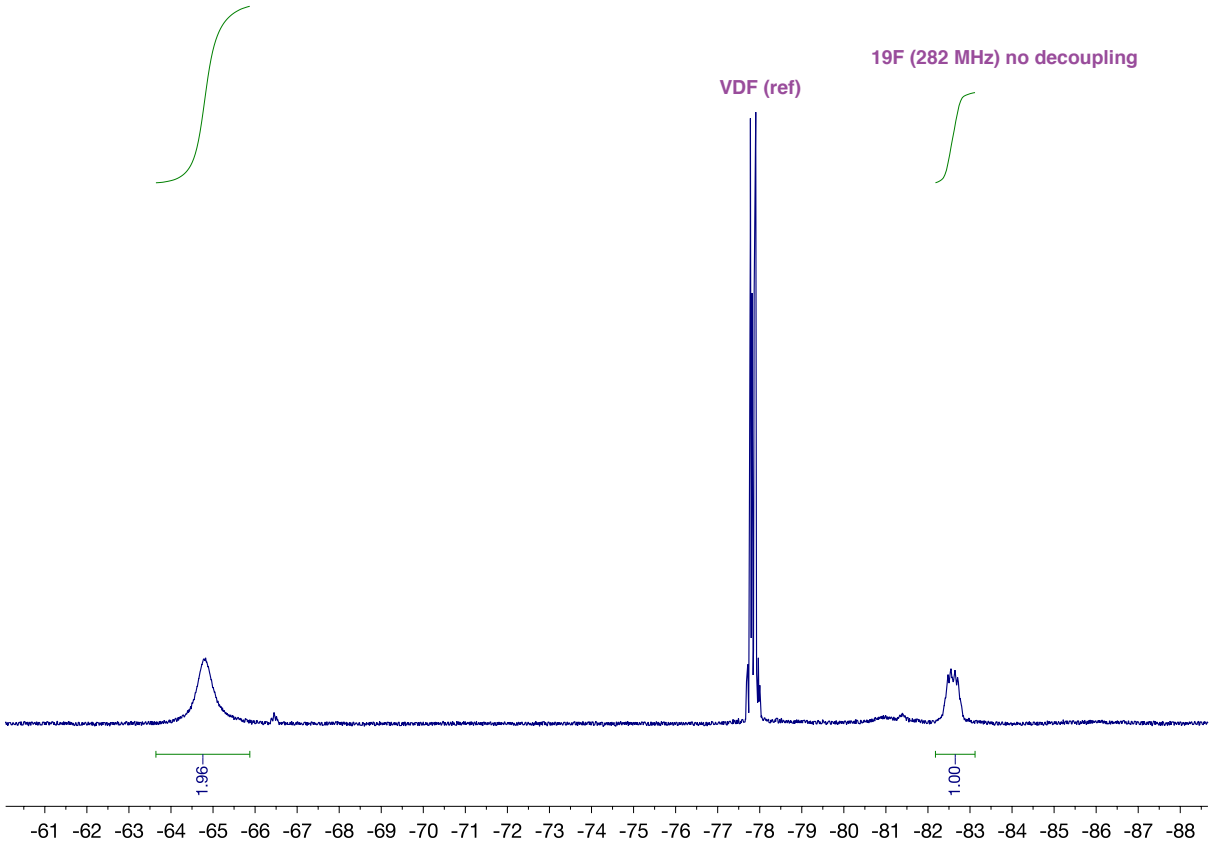

Figure S51: ^{19}F NMR (282 MHz. in C_6D_6) of [Ni(P(*t*-Bu)$_2$(*n*-Bu))($CF_2CH_2CF(=CH_2)$(μ–F)]$_2$ (referenced to VDF).

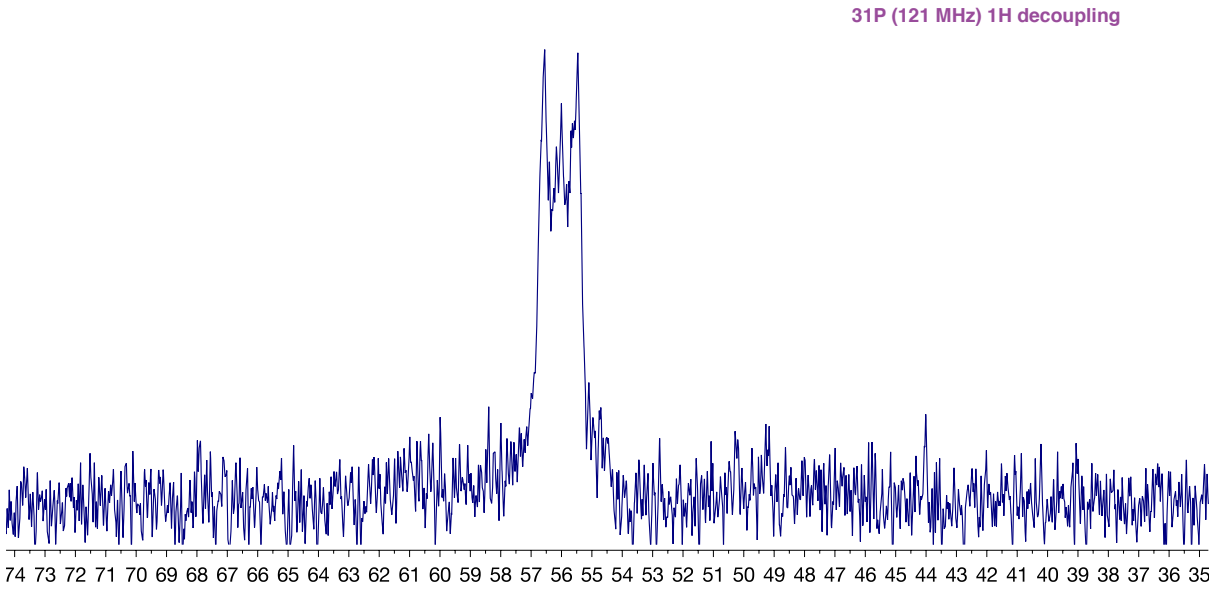

Figure S52: ^{31}P NMR (121 MHz. in C_6D_6) of [Ni(P(*t*-Bu)$_2$(*n*-Bu))($CF_2CH_2CF(=CH_2)$(μ–F)]$_2$ (referenced externally to H_3PO_4)

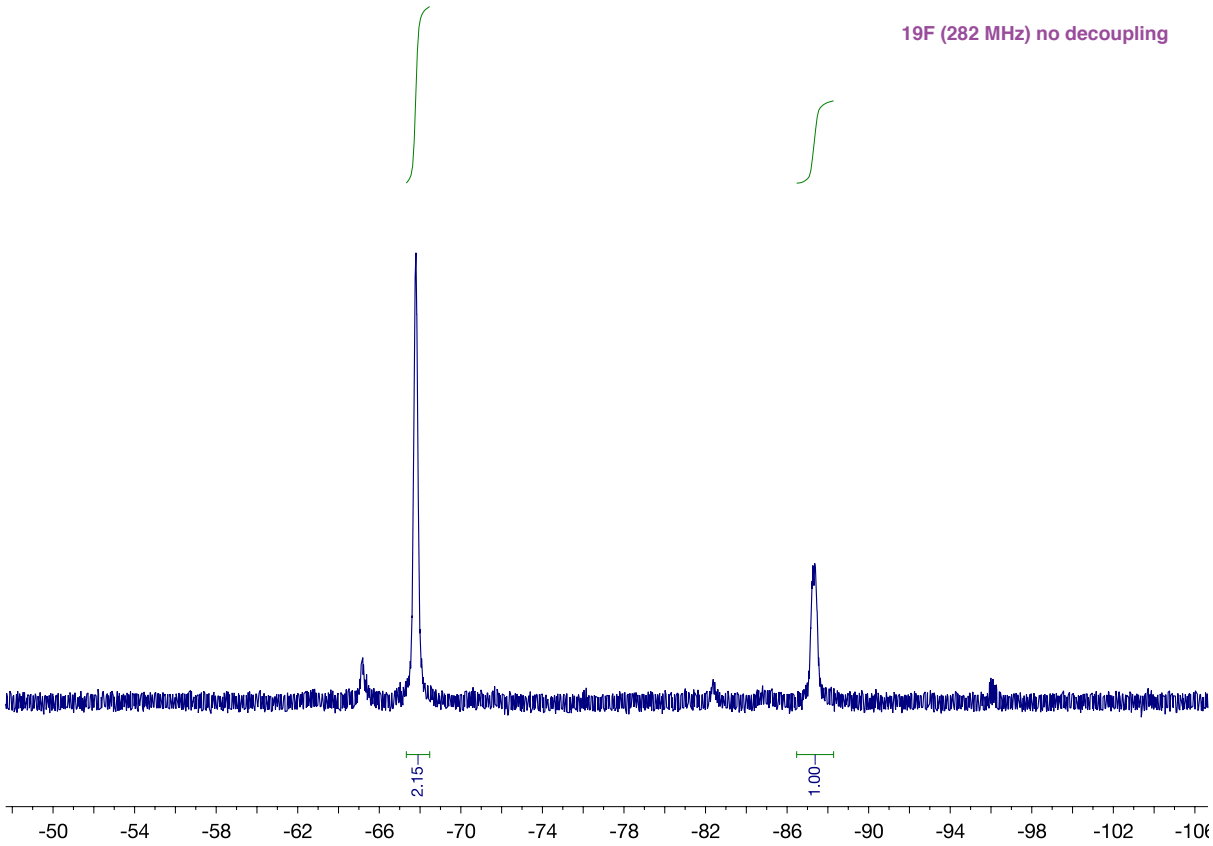

Figure S53: ^{19}F NMR (282 MHz. in C_6D_6) of $[Ni(PCp_3)(CF_2CH_2CF(=CH_2)(\mu–F)]_2$ (referenced to VDF).

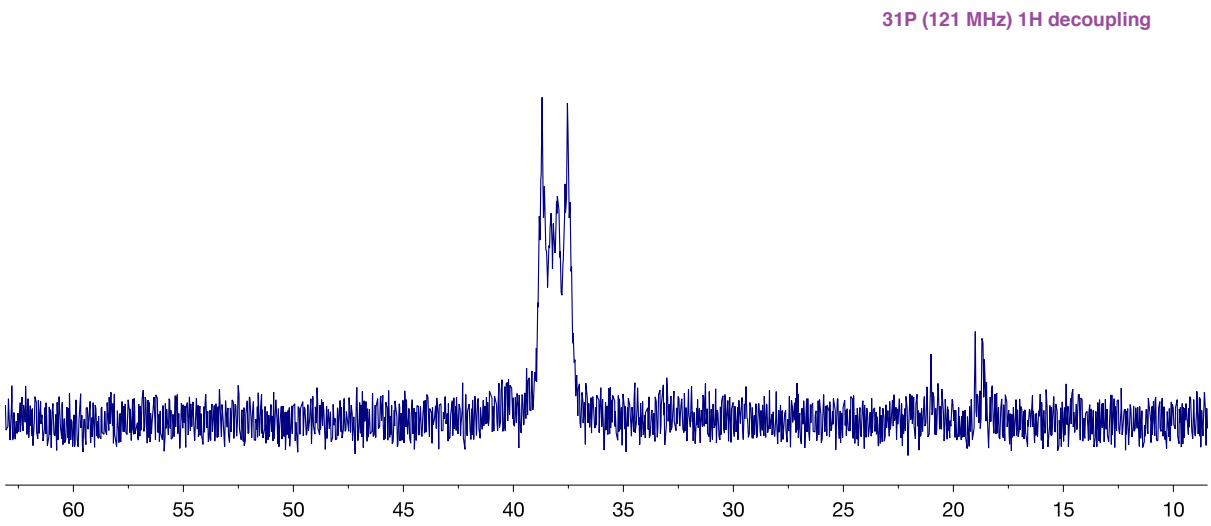

Figure S54: ^{31}P NMR (121 MHz. in C_6D_6) of $[Ni(PCp_3)(CF_2CH_2CF(=CH_2)(\mu–F)]_2$ (referenced externally to H_3PO_4)

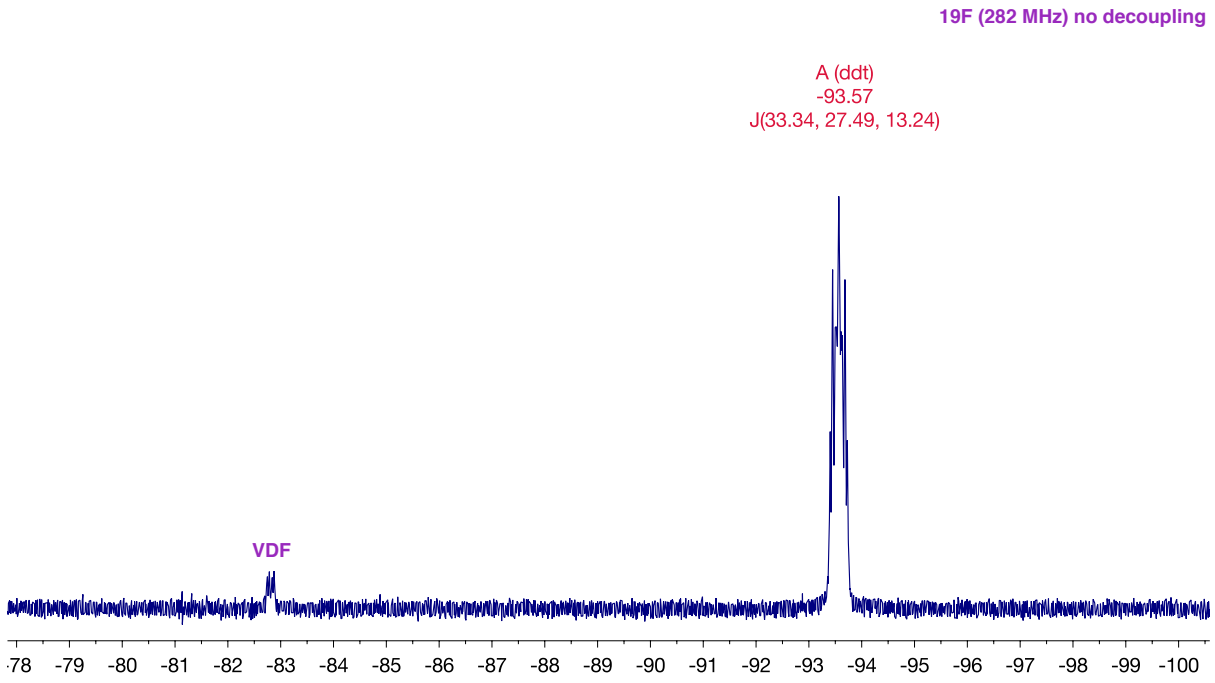

Figure S55: ^{19}F NMR (282 MHz. in C_6D_6) of [Ni(DPEphos)(η^2-CF_2=CH_2)] (referenced to VDF)

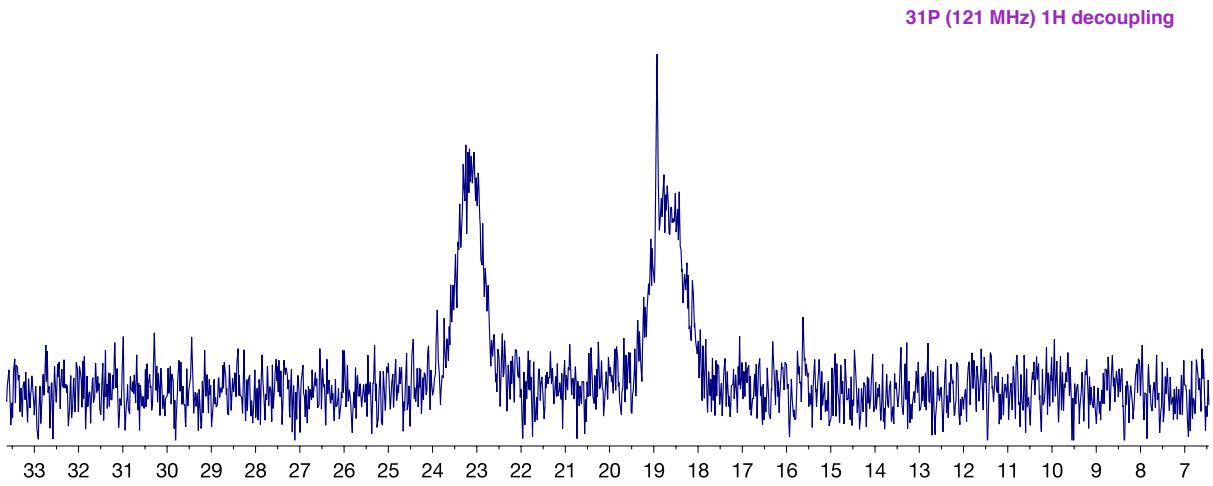

Figure S56: ^{31}P NMR (121 MHz. in C_6D_6) of [Ni(DPEphos)(η^2-CF_2=CH_2)] (referenced externally to H_3PO_4)

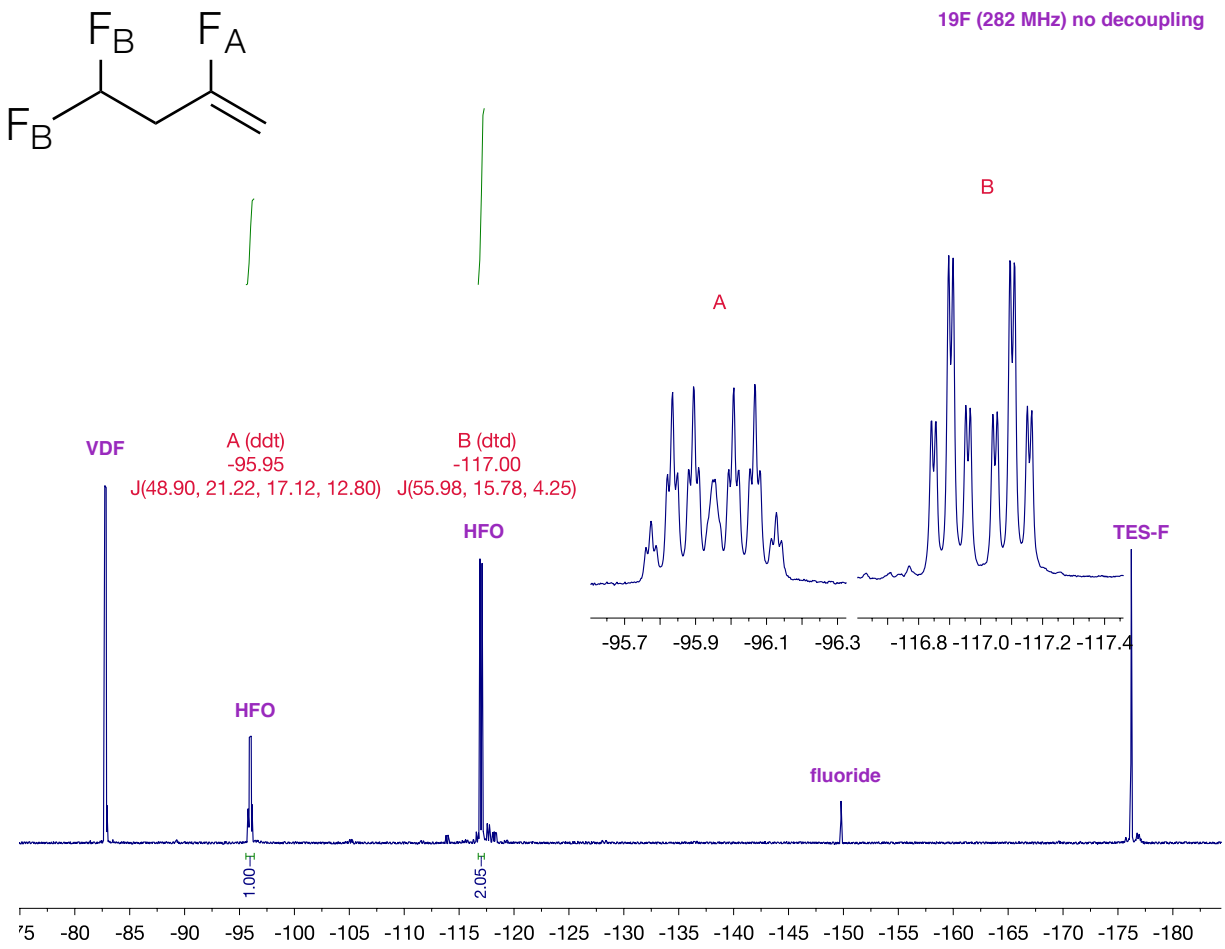

Figure S55: ^{19}F NMR (282 MHz. in C_6D_6) of catalytic hydrodefluorodimerization reaction (at 1 mol% of $Ni(cod)_2$/IAd) with TES-H after 45 minutes at 45˚C (referenced to VDF) showing HFO-1363pyf peaks.

Table S13: Crystal data and structure refinement for $[Ni(PCp_3)(CF_2CH_2CF{=}CH_2)(\mu\text{-}F)]_2$.

Identification Code	PCp_3-butenyl	
Empirical Formula	$C_{38}H_{62}F_8Ni_2P_2$	
Formula weight	850.23	
Temperature	200(2) K	
Wavelength	0.71073 Å	
Crystal system	Monoclinic	
Space group	P21/c	
Unit cell dimensions	a = 12.1460(4) Å	a = 90˚
	b = 11.7688(5) Å	b = 96.2710(10)º
	c = 14.0712(5) Å	g = 90º
Volume	1999.36(13) $Å^3$	
Z	2	
Density (calculated)	1.412 Mg/m^3	
Absorption coefficient	1.085 mm^{-1}	
F(000)	896	
Crystal size	0.392 x 0.227 x 0.110 mm^3	
Theta range for data collection	2.262 to 27.916˚	
Index ranges	-15 ≦ h ≦ 9, -15 ≦ k ≦ 12, -18 ≦ l ≦ 17	
Reflections collected	11308	
Completeness to theta = 25.242˚	99.5%	
Refinement method	Full-matrix least squares on F^2	
Data / restraints / parameters	4661 / 51 / 245	
Goodness-of-fit on F^2	1.034	
Final R indices [I>2sigma(I)]	R1 = 0.0413, wR2 = 0.0831	
R indices (all data)	R1 = 0.0663, wR2 = 0.0927	
Extinction coefficient	n/a	
Largest diff. peak and hole	0.593 and -0.285e $Å^{-3}$	

Table S14: Atomic coordinates (x 104) and equivalent isotropic displacement parameters ($Å^2$x 103) for PCp_3-butenyl. U(eq) is defined as one third of the trace of the orthogonalized Uij tensor.

	x	y	z	U(eq)
Ni(1)	6197(1)	4787(1)	4984(1)	25(1)
P(1)	7247(1)	4064(1)	3986(1)	25(1)
F(1)	5177(1)	5328(1)	5818(1)	37(1)
F(3)	8433(1)	4743(2)	5830(1)	48(1)
F(2)	7147(1)	4204(2)	6699(1)	49(1)
F(4)	8669(2)	7156(2)	5668(2)	82(1)
C(1)	6482(2)	3655(2)	2839(2)	32(1)
C(2)	5589(2)	2740(3)	2887(2)	40(1)
C(3)	4903(2)	2837(3)	1920(2)	53(1)
C(4)	4895(3)	4088(3)	1674(2)	59(1)
C(5)	5879(2)	4643(3)	2285(2)	41(1)
C(6)	8406(2)	4950(2)	3681(2)	30(1)
C(7)	9100(2)	4498(3)	2905(2)	44(1)
C(8)	9563(2)	5561(3)	2452(2)	49(1)
C(9)	9218(2)	6562(3)	3026(2)	48(1)
C(10)	8138(2)	6170(3)	3379(2)	42(1)
C(11)	7944(2)	2775(3)	4496(2)	37(1)
C(12)	7210(3)	2054(3)	5094(2)	55(1)
C(13')	7536(18)	877(17)	5042(17)	63(5)
C(14')	8305(18)	775(13)	4281(12)	70(4)
C(15)	8423(3)	1922(3)	3839(2)	48(1)
C(16)	7343(2)	4983(3)	5989(2)	38(1)
C(17)	7362(2)	6142(3)	6462(2)	38(1)
C(18)	7576(3)	7096(3)	5828(2)	48(1)
C(19)	6896(4)	7815(3)	5402(3)	74(1)

Table S15: Bond lengths / angles

Bond	Length [Å]
Ni(1)–C(16)	1.887(2)
Ni(1)–F(1)	1.9066(13)
Ni(1)–F(1)#1	1.9142(14)
Ni(1)–P(1)	2.1717(7)
Ni(1)–Ni(1)#1	2.9555(6)
P(1)–C(1)	1.836(3)
P(1)–C(6)	1.836(3)
P(1)–C(11)	1.845(3)
F(1)–Ni(1)#1	1.9143(14)
F(3)–C(16)	1.395(3)
F(2)–C(16)	1.395(3)
F(4)–C(18)	1.372(3)
C(1)–C(5)	1.535(4)
C(1)–H(1)	1.0000
C(2)–C(3)	1.520(4)
C(2)–H(2A)	0.9900
C(2)–H(2B)	0.9900
C(3)–C(4)	1.512(5)
C(3)–H(3A)	0.9900
C(3)–H(3B)	0.9900
C(4)–C(5)	1.539(4)
C(4)–H(4A)	0.9900
C(4)–H(4B)	0.9900
C(5)–H(5A)	0.9900
C(5)–H(5B)	0.9900
C(6)–C(10)	1.522(4)
C(6)–C(7)	1.544(3)
C(6)–H(6)	1.0000
C(7)–C(8)	1.538(4)
C(7)–H(7A)	0.9900
C(7)–H(7B)	0.9900
C(8)–C(9)	1.513(4)
C(8)–H(8A)	0.9900
C(8)–H(8B)	0.9900
C(9)–C(10)	1.524(4)
C(9)–H(9A)	0.9900
C(9)–H(9B)	0.9900
C(10)–H(10A)	0.9900
C(10)–H(10B)	0.9900
C(11)–C(15)	1.522(4)
C(11)–H(11)	1.0000
C(12)–C(13)	1.44(2)
C(12)–C(13')	1.554(15)
C(12)–H(12A)	0.9900
C(12)–H(12B)	0.9900
C(12)–H(12C)	0.9900
C(12)–H(12D)	0.9900
C(13)–C(14)	1.56(3)
C(13)–H(13A)	0.9900
C(13)–H(13B)	0.9900
C(14)–C(14A)	0.9900
C(14)–H(14B)	0.9900

C(13')–C(14')	1.44(2)
C(13')–H(13C)	0.9900
C(13')–H(13D)	0.9900
C(14')–H(14C)	0.9900
C(14')–H(14D)	0.9900
C(15)–H(15A)	0.9900
C(15)–H(15B)	0.9900
C(15)–H(15C)	0.9900
C(15)–H(15D)	0.9900
C(16)–C(17)	1.517(4)
C(17)–C(18)	1.475(4)
C(17)–H(17A)	0.9900
C(17)–H(17B)	0.9900
C(18)–C(19)	1.284(5)
C(19)–H(19A)	0.9500
C(19)–H(19B)	0.9500

Bonds	Angle [°]
C(16)-Ni(1)-F(1)	88.49(9)
C(16)-Ni(1)-F(1)#1	167.05(9)
F(1)-Ni(1)-F(1)#1	78.66(6)
C(16)-Ni(1)-P(1)	95.45(8)
F(1)-Ni(1)-P(1)	174.94(5)
F(1)#1-Ni(1)-P(1)	97.29(4)
C(16)-Ni(1)-Ni(1)#1	127.90(8)
F(1)-Ni(1)-Ni(1)#1	39.42(4)
F(1)#1-Ni(1)-Ni(1)#1	39.23(4)
P(1)-Ni(1)-Ni(1)#1	136.45(2)
C(1)-P(1)-C(6)	105.68(12)
C(1)-P(1)-C(11)	107.05(13)
C(6)-P(1)-C(11)	103.13(12)
C(1)-P(1)-Ni(1)	113.21(8)
C(6)-P(1)-Ni(1)	116.56(9)
C(11)-P(1)-Ni(1)	110.36(8)
Ni(1)-F(1)-Ni(1)#1	101.34(6)
C(2)-C(1)-C(5)	104.6(2)
C(2)-C(1)-P(1)	115.96(18)
C(5)-C(1)-P(1)	114.45(19)
C(2)-C(1)-H(1)	107.1
C(5)-C(1)-H(1)	107.1
P(1)-C(1)-H(1)	107.1
C(3)-C(2)-C(1)	103.3(2)
C(3)-C(2)-H(2A)	111.1
C(1)-C(2)-H(2A)	111.1
C(3)-C(2)-H(2B)	111.1
C(1)-C(2)-H(2B)	111.1
H(2A)-C(2)-H(2B)	109.1
C(4)-C(3)-C(2)	105.5(3)
C(4)-C(3)-H(3A)	110.6
C(2)-C(3)-H(3A)	110.6
C(4)-C(3)-H(3B)	110.6
C(2)-C(3)-H(3B)	110.6
H(3A)-C(3)-H(3B)	108.8
C(3)-C(4)-C(5)	107.5(3)
C(3)-C(4)-H(4A)	110.2
C(5)-C(4)-H(4A)	110.2

C(3)-C(4)-H(4B)	110.2	C(10)-C(9)-H(9A)	111.0
C(5)-C(4)-H(4B)	110.2	C(8)-C(9)-H(9B)	111.0
H(4A)-C(4)-H(4B)	108.5	C(10)-C(9)-H(9B)	111.0
C(4)-C(5)-C(1)	105.0(3)	H(9A)-C(9)-H(9B)	109.0
C(4)-C(5)-H(5A)	110.7	C(6)-C(10)-C(9)	102.2(2)
C(1)-C(5)-H(5A)	110.7	C(6)-C(10)-H(10A)	111.3
C(4)-C(5)-H(5B)	110.7	C(9)-C(10)-H(10A)	111.3
C(1)-C(5)-H(5B)	110.7	C(6)-C(10)-H(10B)	111.3
H(5A)-C(5)-H(5B)	108.8	C(9)-C(10)-H(10B)	111.3
C(10)-C(6)-C(7)	104.2(2)	H(10A)-C(10)-H(10B)	109.2
C(10)-C(6)-P(1)	117.01(17)	C(15)-C(11)-C(12)	104.5(2)
C(7)-C(6)-P(1)	117.4(2)	C(15)-C(11)-P(1)	119.7(2)
C(10)-C(6)-H(6)	105.7	C(12)-C(11)-P(1)	113.33(19)
C(7)-C(6)-H(6)	105.7	C(15)-C(11)-H(11)	106.1
P(1)-C(6)-H(6)	105.7	C(12)-C(11)-H(11)	106.1
C(8)-C(7)-C(6)	105.4(2)	P(1)-C(11)-H(11)	106.1
C(8)-C(7)-H(7A)	110.7	C(13)-C(12)-C(11)	108.7(8)
C(6)-C(7)-H(7A)	110.7	C(11)-C(12)-C(13')	100.2(6)
C(8)-C(7)-H(7B)	110.7	C(13)-C(12)-H(12A)	109.9
C(6)-C(7)-H(7B)	110.7	C(11)-C(12)-H(12A)	109.9
H(7A)-C(7)-H(7B)	108.8	C(13)-C(12)-H(12B)	109.9
C(9)-C(8)-C(7)	106.0(2)	C(11)-C(12)-H(12B)	109.9
C(9)-C(8)-H(8A)	110.5	H(12A)-C(12)-H(12B)	108.3
C(7)-C(8)-H(8A)	110.5	C(11)-C(12)-H(12C)	111.7
C(9)-C(8)-H(8B)	110.5	C(13')-C(12)-H(12C)	111.7
C(7)-C(8)-H(8B)	110.5	C(11)-C(12)-H(12D)	111.7
H(8A)-C(8)-H(8B)	108.7	C(13')-C(12)-H(12D)	111.7
C(8)-C(9)-C(10)	103.7(2)	H(12C)-C(12)-H(12D)	109.5
C(8)-C(9)-H(9A)	111.0	C(12)-C(13)-C(14)	105.8(15)

C(12)-C(13)-H(13A)	110.6	C(14)-C(15)-H(15B)	111.8
C(14)-C(13)-H(13A)	110.6	H(15A)-C(15)-H(15B)	109.5
C(12)-C(13)-H(13B)	110.6	C(14')-C(15)-H(15C)	110.5
C(14)-C(13)-H(13B)	110.6	C(11)-C(15)-H(15C)	110.5
H(13A)-C(13)-H(13B)	108.7	C(14')-C(15)-H(15D)	110.5
C(13)-C(14)-C(15)	102.0(15)	C(11)-C(15)-H(15D)	110.5
C(13)-C(14)-H(14A)	111.4	H(15C)-C(15)-H(15D)	108.7
C(15)-C(14)-H(14A)	111.4	F(3)-C(16)-F(2)	102.7(2)
C(13)-C(14)-H(14B)	111.4	F(3)-C(16)-C(17)	106.4(2)
C(15)-C(14)-H(14B)	111.4	F(2)-C(16)-C(17)	105.8(2)
H(14A)-C(14)-H(14B)	109.2	F(3)-C(16)-Ni(1)	119.36(17)
C(14')-C(13')-C(12)	105.4(12)	F(2)-C(16)-Ni(1)	106.65(17)
C(14')-C(13')-H(13C)	110.7	C(17)-C(16)-Ni(1)	114.41(18)
C(12)-C(13')-H(13C)	110.7	C(18)-C(17)-C(16)	114.5(2)
C(14')-C(13')-H(13D)	110.7	C(18)-C(17)-H(17A)	108.6
C(12)-C(13')-H(13D)	110.7	C(16)-C(17)-H(17A)	108.6
H(13C)-C(13')-H(13D)	108.8	C(18)-C(17)-H(17B)	108.6
C(13')-C(14')-C(15)	107.9(11)	C(16)-C(17)-H(17B)	108.6
C(13')-C(14')-H(14C)	110.1	H(17A)-C(17)-H(17B)	107.6
C(15)-C(14')-H(14C)	110.1	C(19)-C(18)-F(4)	118.3(3)
C(13')-C(14')-H(14D)	110.1	C(19)-C(18)-C(17)	129.6(3)
C(15)-C(14')-H(14D)	110.1	F(4)-C(18)-C(17)	112.1(3)
H(14C)-C(14')-H(14D)	108.4	C(18)-C(19)-H(19A)	120.0
C(14')-C(15)-C(11)	106.3(6)	C(18)-C(19)-H(19B)	120.0
C(11)-C(15)-C(14)	100.0(9)	H(19A)-C(19)-H(19B)	120.0
C(11)-C(15)-H(15A)	111.8		
C(14)-C(15)-H(15A)	111.8		
C(11)-C(15)-H(15B)	111.8		

Table S16: Anisotropic displacement parameters (Å2x 103)for PCp_3-adduct. The anisotropic displacement factor exponent takes the form: -2p2[h2a*2U11 + ... + 2 h k a* b* U12]

	U^{11}	U^{22}	U^{33}	U^{21}	U^{13}	U^{12}
Ni(1)	19(1)	32(1)	24(1)	-4(1)	5(1)	2(1)
P(1)	22(1)	28(1)	27(1)	0(1)	9(1)	2(1)
F(1)	22(1)	59(1)	30(1)	-17(1)	5(1)	4(1)
F(3)	25(1)	76(1)	43(1)	-14(1)	-4(1)	15(1)
F(2)	63(1)	52(1)	32(1)	10(1)	0(1)	2(1)
F(4)	55(1)	109(2)	83(2)	11(1)	6(1)	-35(1)
C(1)	29(1)	40(2)	31(1)	-11(1)	11(1)	-2(1)
C(2)	34(1)	39(2)	48(2)	-13(1)	11(1)	-1(1)
C(3)	39(2)	65(3)	54(2)	-23(2)	7(1)	-11(2)
C(4)	43(2)	76(3)	55(2)	-1(2)	-8(2)	-8(2)
C(5)	40(2)	52(2)	31(1)	-1(1)	5(1)	-7(1)
C(6)	23(1)	36(2)	31(1)	5(1)	5(1)	-1(1)
C(7)	33(1)	50(2)	51(2)	7(2)	22(1)	-1(1)
C(8)	38(2)	66(2)	44(2)	16(2)	11(1)	-7(2)
C(9)	40(2)	47(2)	56(2)	19(2)	1(1)	-11(2)
C(10)	38(2)	35(2)	52(2)	3(1)	7(1)	-2(1)
C(11)	41(2)	32(2)	41(2)	4(1)	12(1)	7(1)
C(12)	69(2)	46(2)	56(2)	14(2)	32(2)	10(2)
C(13)	78(9)	41(5)	75(9)	13(4)	28(7)	3(5)
C(14)	104(11)	63(8)	130(14)	42(9)	58(10)	41(8)
C(13')	89(10)	44(5)	58(6)	26(4)	36(6)	27(6)
C(14')	113(12)	33(4)	74(6)	5(4)	50(7)	18(5)
C(15)	51(2)	41(2)	55(2)	-1(1)	21(1)	9(2)
C(16)	25(1)	47(2)	28(1)	1(1)	2(1)	3(1)
C(17)	30(1)	49(2)	34(2)	-10(1)	1(1)	-3(1)
C(18)	45(2)	53(2)	44(2)	-12(2)	1(1)	-12(2)
C(18)	45(2)	53(2)	44(2)	-12(2)	1(1)	-12(2)
C(19)	95(3)	50(3)	78(3)	7(2)	16(2)	10(2)

Table S17: Hydrogen coordinates (x 104) and isotropic displacement parameters (Å2x 103) for PCp_3-adduct

	x	y	z	U(eq)
H(1)	7035	3347	2429	39
H(2A)	5924	1976	2977	48
H(2B)	5133	2895	3414	48
H(3A)	5241	2389	1432	63
H(3B)	4140	2558	1958	63
H(4A)	4191	4440	1815	70
H(4B)	4969	4192	986	70
H(5A)	5615	5207	2731	49
H(5B)	6376	5028	1875	49
H(6)	8929	5005	4279	36
H(7A)	9710	4008	3194	52
H(7B)	8632	4053	2420	52
H(8A)	10380	5518	2483	59
H(8B)	9254	5632	1774	59
H(9A)	9100	7248	2621	57
H(9B)	9783	6730	3569	57
H(10A)	7952	6634	3926	50
H(10B)	7516	6202	2863	50
H(11)	8581	3044	4951	45
H(12A)	7301	2313	5768	66
H(12B)	6421	2141	4842	66
H(12C)	6464	1926	4752	66
H(12D)	7138	2405	5724	66
H(13A)	6950	430	4667	76
H(13B)	7674	544	5690	76
H(14A)	8700	161	4186	114
H(14B)	9280	991	5007	114
H(13C)	8521	1013	5707	74
H(13D)	7428	291	5348	74

H(14C)	7779	303	3863	85
H(14D)	9030	383	4364	85
H(15A)	9125	2197	3623	57
H(15B)	7892	1739	3275	57
H(15C)	8013	1950	3191	57
H(15D)	9213	2092	3787	57
H(17A)	6640	6270	6710	45
H(17B)	7940	6141	7015	45
H(19A)	7155	8370	4989	89
H(19B)	6135	7793	5500	89

Table S18: Torsion angles

Bonds	Angle (º)	Bonds	Angle (º)
C(6)-P(1)-C(1)-C(2)	169.74(19)	C(11)-P(1)-C(6)-C(10)	-170.8(2)
C(11)-P(1)-C(1)-C(2)	60.3(2)	Ni(1)-P(1)-C(6)-C(10)	-49.7(2)
Ni(1)-P(1)-C(1)-C(2)	-61.5(2)	C(1)-P(1)-C(6)-C(7)	-48.0(2)
C(6)-P(1)-C(1)-C(5)	-68.3(2)	C(11)-P(1)-C(6)-C(7)	64.2(2)
C(11)-P(1)-C(1)-C(5)	-177.72(18)	Ni(1)-P(1)-C(6)-C(7)	-174.70(17)
Ni(1)-P(1)-C(1)-C(5)	60.45(19)	C(10)-C(6)-C(7)-C(8)	21.3(3)
C(5)-C(1)-C(2)-C(3)	37.1(3)	P(1)-C(6)-C(7)-C(8)	152.51(19)
P(1)-C(1)-C(2)-C(3)	164.2(2)	C(6)-C(7)-C(8)-C(9)	5.0(3)
C(1)-C(2)-C(3)-C(4)	-35.1(3)	C(7)-C(8)-C(9)-C(10)	-29.4(3)
C(2)-C(3)-C(4)-C(5)	19.9(3)	C(7)-C(6)-C(10)-C(9)	-39.3(3)
C(3)-C(4)-C(5)-C(1)	3.3(3)	P(1)-C(6)-C(10)-C(9)	-170.71(19)
C(2)-C(1)-C(5)-C(4)	-24.9(3)	C(8)-C(9)-C(10)-C(6)	42.7(3)
P(1)-C(1)-C(5)-C(4)	-152.9(2)	C(1)-P(1)-C(11)-C(15)	37.2(3)
C(1)-P(1)-C(6)-C(10)	77.0(2)	C(6)-P(1)-C(11)-C(15)	-74.0(3)
		C(13)-C(14)-C(15)-C(11)	43(2)
		F(1)-Ni(1)-C(16)-F(3)	-178.2(2)

C(6)-P(1)-C(11)-C(15)	-74.0(3)
Ni(1)-P(1)-C(11)-C(15)	160.8(2)
C(1)-P(1)-C(11)-C(12)	-86.8(2)
C(6)-P(1)-C(11)-C(12)	162.0(2)
Ni(1)-P(1)-C(11)-C(12)	36.8(2)
C(15)-C(11)-C(12)-C(13)	18.8(11)
P(1)-C(11)-C(12)-C(13)	150.7(11)
C(15)-C(11)-C(12)-C(13')	34.8(9)
P(1)-C(11)-C(12)-C(13')	166.7(9)
C(11)-C(12)-C(13)-C(14)	9(2)
C(12)-C(13)-C(14)-C(15)	-32(3)
C(11)-C(12)-C(13')-C(14')	-39.3(19)
C(12)-C(13')-C(14')-C(15)	29(2)
C(13')-C(14')-C(15)-C(11)	-6(2)
C(12)-C(11)-C(15)-C(14')	-19.1(10)
P(1)-C(11)-C(15)-C(14')	-147.3(10)
C(12)-C(11)-C(15)-C(14)	-37.5(12)
P(1)-C(11)-C(15)-C(14)	-165.7(12)
F(1)#1-Ni(1)-C(16)-F(3)	174.8(3)
P(1)-Ni(1)-C(16)-F(3)	5.0(2)
Ni(1)#1-Ni(1)-C(16)-F(3)	-179.47(15)
F(1)-Ni(1)-C(16)-F(2)	66.19(17)
F(1)#1-Ni(1)-C(16)-F(2)	59.1(6)
P(1)-Ni(1)-C(16)-F(2)	-110.64(16)
Ni(1)#1-Ni(1)-C(16)-F(2)	64.9(2)
F(1)-Ni(1)-C(16)-C(17)	-50.44(19)
F(1)#1-Ni(1)-C(16)-C(17)	-57.5(6)
P(1)-Ni(1)-C(16)-C(17)	132.73(18)
Ni(1)#1-Ni(1)-C(16)-C(17)	-51.7(2)
F(3)-C(16)-C(17)-C(18)	70.4(3)
F(2)-C(16)-C(17)-C(18)	179.2(2)
Ni(1)-C(16)-C(17)-C(18)	-63.7(3)
C(16)-C(17)-C(18)-C(19)	102.0(4)
C(16)-C(17)-C(18)-F(4)	-75.4(3)

Symmetry transformations used to generate equivalent atoms:

#1 -x+1,-y+1,-z+1

Table S19: Hydrogen bonds for PCp_3-adduct (Å and °)

DH—A	d(D—H)	D(H—A)	d(D—A)	<(DHA)
C(2)-H(2B)...F(1)#1	0.99	2.40	3.118(3)	128.7
C(5)-H(5A)...F(1)#1	0.99	2.43	3.085(3)	122.9
C(6)-H(6)...F(3)	1.00	2.35	3.031(3)	124.8
C(10)-H(10A)...F(4)	0.99	2.58	3.417(4)	141.9
C(11)-H(11)...F(3)	1.00	2.37	3.000(3)	120.3
C(12)-H(12D)...F(2)	0.99	2.52	3.397(4)	147.3
C(15)-H(15B)...F(2)#2	0.99	2.56	3.494(4)	158.1
C(17)-H(17A)...F(1)	0.99	2.34	2.873(3)	112.9
C(2)-H(2B)...F(1)#1	0.99	2.40	3.118(3)	128.7
C(5)-H(5A)...F(1)#1	0.99	2.43	3.085(3)	122.9
C(6)-H(6)...F(3)	1.00	2.35	3.031(3)	124.8
C(10)-H(10A)...F(4)	0.99	2.58	3.417(4)	141.9
C(11)-H(11)...F(3)	1.00	2.37	3.000(3)	120.3
C(12)-H(12D)...F(2)	0.99	2.52	3.397(4)	147.3
C(15)-H(15B)...F(2)#2	0.99	2.56	3.494(4)	158.1
C(17)-H(17A)...F(1)	0.99	2.34	2.873(3)	112.9

Symmetry transformations used to generate equivalent atoms:

#1 -x+1,-y+1,-z+1 #2 x,-y+1/2,z-1/2

References Cited

[1] P. H. Carnell, R. S. Hovey, US Patent 2,439,299 *(Phillips Petroleum Co.)*, Apr 6, 1948

[2] C. B. Miller, F. H. Bratton, US Patent 2,478,201 *(Allied Chem. Dye Corp),* Aug. 9, 1949

[3] J. D. Calfee, L. B. Smith, US Patent 2,417,059 *(Gen. Chemical Corp.)*, Mar. 11, 1947

[4] J. D. Calfee, L. B. Smith, US Patent 2,459,767 *(Allied Chem. Dye Corp),* Jan. 18, 1949

[5] A. F. Benning, US Patent 2,450,415 *(Kinetic Chemicals Inc.),* Oct. 5, 1948

[6] N. Fine, US Patent 2,908,650 *(Colgate Palmolive Co.)*, Oct. 13, 1959

[7] A. L. Edelstein, US Patent 2,764,454, Sep. 25, 1956

[8] A. L. La Via, US Patent 2,853,423 *(Olin Mathieson Chemical. Co.),* Sep. 23, 1958

[9] R. J. Kerr, US Patent 2,659,704 *(Protective Coatings Corp.)*, Nov. 17, 1953

[10] Jr. C. L. Mills, US Patent 2,957,838 *(Monsanto Chemicals)*, Oct. 25, 1960

[11] R. P. Cox, L. A. Fish, US Patent 3,705,669 *(Wham-O Mfg. Co.)*, Dec. 12, 1972

[12] H. W. Daudt, M. A. Youker, US Patent 2,024,095 *(Kinetic Chemicals Inc.*), Dec. 10, 1935

[13] R. P. Ruh, R. A. Davis, US Patent 2,639,300 *(Dow Chemical Co.)*, May 19, 1953

[14] E. L. Muetterties, US Patent 2,709,184 *(E. I. DuPont de Nemours & Co.)*, May 24, 1955

[15] E. J. Prill, US Patent 2,894,044 *(Monsanto Chemicals)*, July 7, 1959

[16] I. Morioka, R. Ukaji, US Patent 3,833,676 *(Daikin Kogyo Co.)*, September 3, 1974

[17] O. Scherer, US Patent 2,146,354 *(I. G. Farbenindustrie)*, February 7, 1939

[18] J. Harmon, US Patent 2,399,024 *(E. I. DuPont de Nemours & Co.)*, April 23, 1946

[19] A. F. Benning, F. B. Downing, J. D. Park *(Kinetic Chemicals Inc.)*, September 3, 1946

[20] R. J. Plunkett, US Patent 2,230,654 *(Kinetic Chemicals Inc.)*, February 4, 1941

[21] R. P. Ruh, R. A. Davis, M. R. Broadworth, US Patent 2,885,427 *(Dow Chemical).* May 5, 1959

[22] W. H. Gumprecht, US Patent 4,311,863 *(E. I. DuPont de Nemours & Co.)*, January 19, 1982

[23] R. E. Burk, D. D. Coffman, G. H. Kalb, US Patent 2,425,991 (*E. I. DuPont de Nemours & Co.)*, August 19, 1947

[24] S. P. von Halasz, CA Patent 1,196,345 *(Hoechst Aktiengesellschaft)*, November 5, 1985

[25] S. P. von Halasz, US Patent 4,158,023 *(Hoechst Aktiengesellschaft)*, June 12, 1979

[26] H. W. Daudt, M. A. Youker, US Patent 2,062,743 *(Kinetic Chemicals Inc.)*, December 1, 1936

[27] F. B. Downing, A. F. Benning, R. C. McHarness, US Patent 2,413,695 *(Kinetic Chemicals Inc.)*, January 7, 1947

[28] H. S. Tung, M. Van Der Puy, US Patent 6,518,467 *(Honeywell International Inc.)*, February 11, 2003

[29] D. M. Marquis, US Patent 2,931,840 *(E. I. du Pont de Nemours & Co.)*, April 5, 1960

[30] A. Pigamo, M. Devic, L. Wendlinger, US Application 14,978,789 *(Arkema France)*, March 21, 2016

[31] M. Y. Elsheikh, P. Bonnet, O. C. N. Keeley, B. Bin Chen, US Application 13,695,807 *(Arkema Inc.)*, March 7, 2013

[32] A. Pigamo, L. Wendlinger, P. Bonnet, US Application 13,642,589 *(Arkema France)*, July 15, 2014

[33] D. Deur-Bert, A. Pigamo, N. Doucet, & L. Wendlinger, US Patent 9,278,895 *(Arkema France)*, March 8, 2016

[34] A. Pigamo, L. Wendlinger, N. Doucet, US Patent 9,302,961 *(Arkema France)*, April 5, 2016

[35] G. B. Fozzard, US Patent 4,086,407 *(Phillips Petroleum Company)*, April 25, 1978

[36] M. Van Der Puy, US Patent 5,986,151 *(AlliedSignal Inc.)*, November 16, 1999

[37] H. Sung Tung, D. C. Merkel, Z. J. Dziadyk, C. H. Carson, H. T. Pham, US Patent 5,763,706 *(AlliedSignal Inc.)*, June 9, 1998

[38] Elsheikh *et al. (op. cit.)*

[39] A. Yamamoto, N. Shibata, T. Nakada, T. Shibanuma, US Patent 6,472,573 *(Daikin Industries Ltd.)*, February 5, 1999

[40] D. C. Merkel, R. R. Singh, H. S. Tung, US Patent 7,230,145 *(Honeywell International Inc.)*, June 12, 2007

[41] S. Mukhopadhyay, H. K. Nair, H. S. Tung, M. Van Der Puy, US Patent 7,345,209 *(Honeywell International Inc.)*, March 18, 2008

[42] S. Mukhopadhyay, H. K. Nair, H. S. Tung, M. Van Der Puy, US Patent 7,189,884 *(Honeywell International Inc.)*, March 13, 2007

[43] The Chemours Company. (2015). *Chemours breaks ground for world's first full-scale production of HFO-1336mzz.* [Press release]. Retrieved from https://investors.chemours.com/investor-relations/investor-news/press-release-details/2015/Chemours-Breaks-Ground-for-Worlds-First-Full-Scale-Production-of-HFO-1336mzz/default.aspx

[44] M. J. Nappa, E. N. Swearingen, US Patent 7,795,482 *(E. I. DuPont de Nemours & Co.)*, September 14, 2010

[45] A. C. Alty, R. A. Du Boisson, US Patent 7,482,499 *(Central Glass Co. Ltd.)*, January 27, 2009

[46] K. F. Watterson, & G. Wilkinson, *Chem. Ind. (London)* **1959**, 991

[47] C. S. Cundy, M. Green, & F. G. A. Stone, *J. Chem. Soc. A.* **1970**, 1647-1653

[48] G. W. Parshall & F. N. Jones, *J. Am. Chem. Soc.* **1965**, *87*, 5356

[49]L. J. Guggenberger & R. Cramer, *J. Am. Chem. Soc.* **1972,** *94*(11), pp 3779-3786

[50] R. B. King, P. M. Treichel, & F. G. A. Stone, *Proc. Chem. Soc.* **1961**, p. 69

[51] A. K. Burrell & W. R. Roper, *Organometallics* **1990**, *9*(6), 1905-1910

[52] M. C. Baird, J. T. Mague, & G. Wilkinson, *J. Chem. Soc. A.* **1967**, 1347-1360

[53]S. Monsaert, N. Ledoux, R. Drozdzak, P. Van Der Voort, & F. Verpoort. V. Dragutan *et al.* (eds.), *Green Metathesis Chemistry: Great Challenges in Synthesis, Catalysis and Nanotechnology*, **2010**, pp. 17–29

[54] Monsaert *et al.*, **2010**, *(op cit.)* pp. 31–38

[55] C. A. Tolman, *Chem. Rev.* **1977**, *77*(3), pp 313–348

[56] J. Huang, H.-J. Schanz, E. D. Stevens, & S. P. Nolan, *Organometallics* **1999**, *18*, 2370–2375.

[57] A. C. Hillier, W. J. Sommer, B. S. Yong, J. L. Petersen, L. Cavallo, & S. P. Nolan, *Organometallics* **2003**, *22*, 4322–4326.

[58] H. Clavier & S. P. Nolan, *Chem. Commun.* **2010**, *46*, 841–861

[59] T. Schaub, P. Fischer, A. Steffen, T. Braun, U. Radius, & A. Mix, *J. Am. Chem. Soc.* **2008**, *130*(29), pp. 9304-9317

[60] T. Schaub, M. Backes, & U. Radius, *Organometallics* **2006**, *25*(17), pp. 4196-4206

[61] K. Matsubara, S. Miyazaki, Y. Koga, Y. Nibu, T. Hashimura, & T. Matsumoto, *Organometallics* **2008**, *27*(22), pp. 6060-6024

[62] S. Kuhl, R. Schneider, & Y. Fort, *Organometallics* **2003**, *22*(21), pp. 4184-4186

[63] S. G. Rull, J. F. Blandez, M. R Fructos, T. R. Belderrain, & M. C. Nicasio, *Adv. Synth. Catal.*, **2015**, *357*(5), pp. 907-911

[64] X. Hu, I. Castro-Rodriguez, & K. Meyer, *Chem. Commun.* **2004**, 2164-2165

[65] Y. Hoshimoto, Y. Hayashi, H. Suzuki, M. Ohashi, & S. Ogoshi, *Organometallics*, **2014**, *33*(5), pp. 1276-1282

[66] N. D. Clement, K. J. Cavell, & L. Ooi, *Organometallics*, **2006**, *25*(17), pp. 4155-4165

[67] J. Wu, N. Hazari, & C. D. Incarvito, *Organometallics*, **2011**, *30*(11), pp. 3142-3150

[68] K. C. Mondal, P. P. Samuel, Y. Li, H. W. Roesky, S. Roy, L. Ackermann, N. S. Sidhu, G. M. Sheldrick, E. Carl, S. Demeshko, S. De, P. Parameswaran, L. Ungur, L. F. Chibotaru, & D. M. Andrada, *Eur. J. Inorg. Chem.*, **2014**, *2014*(5*)*, pp. 818-823

[69] C. A. Laskowski, A. J. M. Miller, G. L. Hillhouse, & T. R. Cundari, *J. Am. Chem. Soc.* **2011**, *133*(4), pp. 771-773

[70] A. Leleu, Y. Fort, & R. Schneider, *Adv. Synth. Catal.* **2006***, 348*(9), pp. 1086-1092

[71] Z. Xi, B. Liu, & W. Chen, *J. Org. Chem.* **2008***, 73*(10), pp. 3954-3957

[72] M. G. Organ, S. Çalimsiz, M. Sayah, K. H. Hoi, & A. J. Lough, *Angew. Chem.* **2009**, *121*, pp. 2419-2423

[73] N. O. Andrella, A. J. Sicard, S. I. Gorelsky, I. Korobkov, & R. Tom Baker, *Chem. Sci.*, **2015**, *6*, 6392

[74] (a) R. D. Chambers, *Fluorine in Organic Chemistry*, Blackwell, Oxford, **2004**; (b) P. Kirsch, *Modern Fluoroorganic Chemistry: Synthesis, Reactivity, Applications*, Wiley-VCH, Weinheim, 2 edn, **2013**; (c) S. Purser, P. R. Moore, S. Swallow and V. Gouverneur, *Chem. Soc. Rev.*, **2008**, *37*, 320; (d) I. Ojima, *Fluorine in Medicinal Chemistry and Chemical Biology*, John Wiley & Sons, Ltd, Chichester, **2009**.

[75] Stoichiometric [Cu]–CF_3 reagents for trifluoromethylation of organic substrates, particularly aryl halides: (a) H. Morimoto, T. Tsubogo, N. D. Litvinas and J. F. Hartwig, *Angew. Chem., Int. Ed.*, **2011**, *50*, 3793; (b) G. G. Dubinina, H. Furutachi and D. A. Vicic, *J. Am. Chem. Soc.*, **2008**, *130*, 8600; (c) D. M. Wiemers and D. J. Burton, *J. Am. Chem. Soc.*, **1986**, *108*, 832.

[76] Metal-catalyzed C–F and C–CF_3 bond formation: (a) T. Furuya, A. S. Kamlet and T. Ritter, *Nature*, **2011**, *473*, 470; (b) E. J. Cho, T. D. Senecal, T. Kinzel, Y. Zhang, D. A. Watson and S. L. Buchwald, *Science*, **2010**, *328*, 1678; (c) V. V. Grushin, *Acc. Chem. Res.*, **2010**, *43*, 160; (d) J. M. Brown and V. Gouverneur, *Angew. Chem., Int. Ed.*, **2009**, *48*, 8610; (e) K. L. Hull, W. Q. Anani and M. S. Sanford, *J. Am. Chem. Soc.*, **2006**, *128*, 7134.

[77] Non-metal based approaches to introducing fluorocarbon fragments to organic substrates: (a) F. Wang, T. Luo, J.-B. Hu, Y. Wang, H. S. Krishnan, P. V. Jog, S. K. Ganesh, G. K. S. Prakash and G. A. Olah, *Angew. Chem., Int. Ed.*, **2011**, *50*, 7153 (CF_2 addition to alkenes); (b) R. P. Singh, G. Cao, R. L. Kirchmeier and J. M. Shreeve, *J. Org. Chem.*, **1999**, *64*, 2873. (Me_3Si–CF_3 addition to carbonyl groups).

[78] (a) H.-J. Arpe, *Industrial Organic Chemistry*, Wiley-VCH, Weinheim, 5th edn, **2010**; (b) *Applied Homogeneous Catalysis with Organometallic Compounds*, ed. B. Cornils and W. A. Herrmann, Wiley-VCH, New York, **1996**

[79] (a) F. L. Taw, A. E. Clark, A. H. Mueller, M. T. Janicke, T. Cantat, B. L. Scott, P. J. Hay, R. P. Hughes and J. L. Kiplinger, *Organometallics*, **2012**, *31*, 1484; (b) R. P. Hughes, *Adv. Organomet. Chem.*, **1990**, *31*, 183; (c) J. A. Morrison, *Advances in Organometallic Chemistry: Trifluoromethyl-Containing Transition Metal Complexes*, Academic Press, **1993**, vol. 35; (d) P. J. Brothers and W. R. Roper, *Chem. Rev.*, **1988**, *88*, 1293.

[80] [Mn]–CF_3 inert to CO migratory-insertion: S. K. Shin and J. L. Beauchamps, *J. Am. Chem. Soc.*, **1990**, *112*, 2057.

[81] (a) M. Ohashi, M. Shibata, H. Saijo, T. Kambara and S. Ogoshi, *Organometallics*, **2013**, *32*, 3631; (b) W. Gasafi-Martin, G. Oberendfellner and K. von Werner, *Can. J. Chem.*, **1996**, *74*, 1922; (c) M. Green, A. Laguna, J. L. Spencer and F. G. A. Stone, *J. Chem. Soc., Dalton Trans.*, **1977**, 1010; (d) J. Browning, H. D. Empsall, M. Green and F. G. A. Stone, *J. Chem. Soc., Dalton Trans.*, **1973**, 381; (e) C. S. Cundy, M. Green and F. G. A. Stone, *J. Chem. Soc. A*, **1970**, 1647; (f) M. Green, R. B. L. Osborn, A. J. Rest and F. G. A Stone, *J. Chem. Soc. A*, **1968**, 2525; (g) P. M. Treichel and F. G. A. Stone, *Adv. Organomet. Chem.*, **1964**, *1*, 143.

[82] R. R. Burch, J. C. Calabrese and S. D. Ittel, *Organometallics*, **1988**, *7*, 1642.

[83] K. A. Giffin, D. J. Harrison, I. Korobkov and R. T. Baker, *Organometallics*, **2013**, *32*, 7424.

[84] (a) R. T. Baker, R. P. Beatty, W. B. Farnham and R. L. Wallace Jr, US Patent, 5,670,679, **1997**; (b) Generation of perfluorocyclobutylene or perfluorocyclobutane from an iron perfluorometallacyclopentane complex, under thermal or thermal/oxidizing (Br_2) conditions, respectively, T. A. Manuel, S. L. Stafford and F. G. A. Stone, *J. Am. Chem. Soc.*, **1961**, 83, 249.

[85] M. Ohashi and S. Ogoshi, Catalytic Transformations of Fluorinated Olefins. in *Topics in Organometallic Chemistry*, Springer, Switzerland, **2014**.

[86] Activation of C–F bonds in [M]–R^F complexes: (a) R. P. Hughes, *J. Fluorine Chem.*, **2010**, *131*, 1059; (b) J. Goodman, V. V. Grushin, R. B. Larichev, S. A. Macgregor, W. J. Marshall and D. C. Roe, *J. Am. Chem. Soc.*, **2009**, *131*, 4236; (c) S. A. Garratt, R. P. Hughes, I. Kovacik, A. J. Ward, S. Willemsen and D. Zhang, *J. Am. Chem. Soc.*, **2005**, *127*, 15585; (d) H. Torrens, *Coord. Chem. Rev.*, **2005**, *249*, 1957; (e) D. Huang, P. R. Koren, K. Folting, E. R. Davidson and K. G. Caulton, *J. Am. Chem. Soc.*, **2000**, *122*, 8916; (f) T. G. Richmond and D. F. Shriver, *Organometallics*, **1984**, *3*, 314; (g) T. G. Richmond and D. F. Shriver, *Organometallics*, **1983**, *2*, 1061, see also ref. 80a.

[87] (a) R. H. Crabtree, *J. Organomet. Chem.*, **2005**, *690*, 5451; (b) D. J. D. Wilson, S. A. Couchman and J. L. Dutton, *Inorg. Chem.*, **2012**, *51*, 7657

[88] D. J. Nelson and S. P. Nolan, *Chem. Soc. Rev.*, **2013**, *42*, 6723.

[89] Hillhouse & Cundari, **2011** (op. cit.)

[90] S. Miyazaki, Y. Koga, T. Matsumoto and K. Matsubara, *Chem. Commun.*, **2010**, *46*, 1932.

[91] P. S. Hanley, S. L. Marquard, T. R. Cundari and J. F. Hartwig, *J. Am. Chem. Soc.*, **2012**, *134*, 15281.

[92] Burch *et al.*, **1988** (op. cit.)

[93] Burch *et al.*, **1988** (op. cit.)

[94] Giffin, Baker *et al.*, **2013** (op. cit.)

[95] Ni–R^F bond lengths for structure **2** (see ESI): 1.956(1) Å (trans to P); 1.945(1) Å (trans to C). Ni–C(NHC) bond length for **2**: 1.945(1) Å.

[96] See ESI page S14 for low temperature NMR spectra.

[97] S. Grimme, *J. Comput. Chem.*, **2006**, *27*, 1787.

[98] See ESI page S29.

[99] N. Islam and D. C. Gosh, *Theoretical and Computational Research in the 21st century*, ed. N. Islam, CRC Press, Boca Raton, **2014**, ch. 1, pp. 1–58.

[100] To the best of our knowledge, the only previously reported metal perfluorocyclobutyl complexes are: (a) B. L. Dyatkin, B. I. Martynov, L. G. Martynova, N. G. Kizim, S. R. Sterlin, Z. A. Stumbrevichute and L. A. Federov, *J. Organomet. Chem.*, **1973**, *57*, 423; (b) B. L. Dyatkin, S. R. Sterlin, B. I. Martynov, E. I. Mysov and I. L. Knunyants, *Tetrahedron*, **1971**, *27*, 2843.

[101] (a) The leaving group ability of OTf, R. K. Crossland, W. E. Wells and V. J. Shiner, *J. Am. Chem. Soc.*, **1971**, *93*, 4217.

[102] (a) T. Miura, Y. Ito and M. Murakami, *Chem. Lett.*, **2008**, *37*, 1006; (b) C. J. Bourgeois, R. P. Hughes, J. Yuan, A. G. DiPasquale and A. L. Rheingold, *Organometallics*, **2006**, *25*, 2908.

[103] For NMR spectra of compound **4a** see pages S21–S22.

[104] (a) M. H. Haindl, M. B. Schmid, K. Zeitler and R. M. Gschwind, *RSC Adv.*, **2012**, *2*, 5941; (b) T. Cohen, D. A. Bennett and A. J. Mura Jr, *J. Org. Chem.*, **1976**, *41*, 2507; (c) J. Jover, R. Bosque and J. Sales, *QSAR Comb. Sci.*, **2008**, *27*, 563.

[105] Gschwind *et al.*, **2012** (*op. cit.*)

[106] Mura *et al.,* **1976** (*op. cit.*)

[107] Sales *et al.*, **2008** (*op. cit.*)

[108] W. Riemenschneider and H. M. Bolt, Esters, Organic, in *Ullman's Encyclopedia of Industrial Chemistry*, Wiley-VCH, Weinheim, **2005**.

[109] Previous work showed protonation of C–F bond instead of Ir–CH_3 using a strong acid: R. P. Hughes, D. Zhang, L. N. Zakharov and A. L. Rheingold, *Organometallics*, **2002**, *21*, 4902.

[110] E. W. Kalberer, J. F. Houlis and D. M. Roddick, *Organometallics*, **2004**, *23*, 4112–4115.

[111] Similar reactivity was previously observed for 3-membered perfluorinated metallacycles: W. Xu, H. Sun, Z. Xiong and X. Li, *Organometallics*, **2013**, *32*, 7122.

[112] Baker *et al.*, **1997** (*op. cit.*)

[113] R. P. Hughes and J. M. Smith, *J. Am. Chem. Soc.*, **1999**, *121*, 6084.

[114] Kennedy, E. M. & Dlugogorski, B. Z., US Patent 8088959 B2, **2012**

[115] Schultz, N., Martens, P., & Vahlensieck, H. J., US Patent 4148831 A, **1979**

[116] Asahi Glass Company Limited: Furuta, S., Takeuchi, Y. Patent EP2826766 A1, **2015**

[117] Allied Chem. and Dye Corp. US Patent 2606937, **1949**

[118] Allied Chem. and Dye Corp. US Patent 2723297, **1954**

[119] Farbw, Hoechst, Patent DE1007771, **1954**

[120] Tarrant, P., Lovelace, A. M., & Lilyquist, M. R., *J. Am. Chem. Soc.* **1955**, *77*, 2783–2787

[121] Hauptschein, M., Braid, M., & Lawlor, F. E., *J. Am. Chem. Soc.* **1958**, *80*, 846–847

[122] Haran, G. & Sharp, D. W. A., *J. Chem. Soc. Perkin Trans. 1* **1972**, 34–38

[123] Keim, W. & Fischer, W., *J. Organomet. Chem.* **1991**, *417*(1/2), C20–C23

[124] Ferrando-Miguel, G., Gerard, H, Eisenstein, O., & Caulton, K. G., *Inorg. Chem.* **2002**, *41*(24), 6440–6449

[125] Kraft, B. M. & Jones, W. D., *J. Am. Chem. Soc.* **2002**, *124*(29), 8681-8689

[126] Huang, D., Renkema, K. B., & Caulton, K. G., *Polyhedron*, **2006**, *25*(2), 459–468

[127] Anderson, D. J., McDonald, R., & Cowie, M., *Angew. Chem. Int. Ed.*, **2007**, *26*(20), 3741–3744

[128] Mukhopadhyay, S., Nair, H. K., Tung, H. S., Van Der Puy, M., & Ma, J. J., Honeywell International Inc., US Patent 245774 A1, **2005**

[129] Giffin, K., **2015** (unreported work)

[130] M. Leclerc, S. I. Gorelsky, B. M. Gabidullin, I. Korobkov, & R. T. Baker, *Chem. Eur. J.*, **2016**, *22*(24), pp. 8063-8067

[131] Aizenberg, M., Milstein, D., *Science* **1994**, *265*(5170), pp. 359–361

[132] R. J. hunadi & K. Baum, *Synthesis*, **1982**, *39*, 454

[133] (a) R. D. Chambers; D. J. Burton;, F. G. Drakesmith; J. Hutchinson; T. Kitazume; L. Lu; J. M. Percy; G. Sandford; T. Yamazaki, *Organofluorine Chemistry Techniques and Synthons*, Vol. 193; Springer: New York, **1997**. (b) Baker, R. T. *et al.* **1996** (*op. cit.*)

[134] see 133

[135] APEX Software Suite v.2012; Bruker AXS: Madison, WI, **2005**.

[136] R. Blessing, *Acta Cryst.* **1995**, *A51*, 33

[137] G. Sheldrick Cell_Now, Bruker-AXS: Madison, WI, **2004**.

[138] G. M. Sheldrick,*Acta Cryst.* **2008**, *A64*, 112.